
Theses and Dissertations

Spring 2011

Computational fluid dynamics applications for the Lake Washington Ship Canal

Adam C. Nielsen
University of Iowa

Copyright 2011 Adam Nielsen

This thesis is available at Iowa Research Online: <https://ir.uiowa.edu/etd/1043>

Recommended Citation

Nielsen, Adam C.. "Computational fluid dynamics applications for the Lake Washington Ship Canal." MS (Master of Science) thesis, University of Iowa, 2011.
<https://ir.uiowa.edu/etd/1043>. <https://doi.org/10.17077/etd.wyo8m0jl>

Follow this and additional works at: <https://ir.uiowa.edu/etd>



Part of the [Civil and Environmental Engineering Commons](#)

COMPUTATIONAL FLUID DYNAMICS APPLICATIONS FOR
THE LAKE WASHINGTON SHIP CANAL

by

Adam C. Nielsen

A thesis submitted in partial fulfillment
of the requirements for the Master of
Science degree in Civil and Environmental Engineering
in the Graduate College of
The University of Iowa

May 2011

Thesis Supervisor: Professor Larry J. Weber
Thesis Co-Supervisor: Justin W. Garvin

Graduate College
The University of Iowa
Iowa City, Iowa

CERTIFICATE OF APPROVAL

MASTER'S THESIS

This is to certify that the Master's thesis of

Adam C. Nielsen

has been approved by the Examining Committee
for the thesis requirement for the Master of Science
degree in Civil and Environmental Engineering at the May 2011 graduation.

Thesis Committee: _____
Larry J. Weber, Thesis Supervisor

Justin W. Garvin, Thesis Co-Supervisor

Jacob Odgaard

Dedicated to Amanda, Austin, and Bentley who are my love, life, and motivation.

O that thou mightest be like unto this river, continually running into the fountain
of all righteousness!

-1 Nephi 2:9

ACKNOWLEDGMENTS

I would like to acknowledge the many people that have come together to help make this project and thesis possible. My advisors Larry Weber and Justin Garvin sought after and received the work from the USACE Seattle District before I arrived. They then worked hard over the past 18 months to help me understand, organize, execute and summarize the CFD work requested by the Seattle District. Larry and Justin's council has greatly helped me focus my time and effort throughout this project. I would also like to thank Jacob Odgaard for his time and effort in contributing on my thesis committee.

I would like to thank Marcela Politano and Antonio Arenas Amado for their extensive knowledge of CFD modeling. Without their help, this project would never have been possible.

I would also like to thank the entire Seattle team that has worked so hard to improve fish passage and overall water quality in the LWSC. Lynne Melder, Fred Goetz, Andy Goodwin, Curtis DeGasperi and the rest of the team that helped fund this project and allow for the detailed research to take place. It has been a great pleasure to work with everyone on the "Ballard Locks" team.

I would like to specifically acknowledge my parents, Becky and Kevin Nielsen, who have spent over 27 years helping me get to where I am today. They truly have led me, guided me, and walked beside me to show me the way.

Finally, I want to especially thank my wonderful wife Amanda for her patience and dedication to my success; as well as my children, Austin and Bentley, who have become excellent sources of motivation to continue to the end.

TABLE OF CONTENTS

LIST OF TABLES	vii
LIST OF FIGURES	viii
LIST OF NOMENCLATURE	xi
CHAPTER 1: INTRODUCTION	1
1.1 Background	1
1.2 Motivation	3
1.3 Objectives	4
1.4 Overview	6
CHAPTER 2: REVIEW OF EXISTING LITERATURE (NUMERICAL MODELING OF FISH MIGRATION, AND WATER QUALITY)	8
2.1 Anadromous Fish Migration	9
2.1.1 Juvenile salmon migration	9
2.1.2 Adult salmon migration	10
2.1.3 How water quality affects salmon migration	11
2.2 Numerical simulation of fish migration	13
2.2.1 Two-Dimensional Models	13
2.2.2 Three-Dimensional Models	14
2.3 Numerical simulation of salt water intrusion	14
2.3.1 Salt Water Intrusion	15
2.3.2 One-Dimensional Models	16
2.3.3 Two-Dimensional Models	16
2.3.4 Three-Dimensional Models	17
2.3.5 Summary	19
CHAPTER 3: NUMERICAL METHODS	22
3.1 Reynolds-Averaged Navier-Stokes (RANS) Model	23
3.2 k- ϵ turbulence model	24
3.3 The Energy Equation	25
3.4 Species Fate and Transport	25
3.5 Volume-weighted-mixing-law	26
3.6 Solution Methods	26
3.6.1 Summary	26
CHAPTER 4: CFD MODEL SIMULATION SETUP	27
4.1 Physical Description	27
4.1.1 General Layout	27
4.1.2 Lake Washington Ship Canal (LWSC)	27
4.1.3 Lock and Dam	28
4.1.4 Water quality collection stations	30
4.2 Numerical Description	41
4.2.1 Mesh Generation	41
4.2.2 Boundary Conditions	42
4.3 Methods, and Controls	49
4.3.2 Summary	52
CHAPTER 5: RESULTS AND DISCUSSION	54
5.1 Project Development and Evolution	54

5.1.1	Preliminary Model Geometry Development.....	54
5.1.2	Development of the Initial Condition	55
5.2	Salt Water Intrusion and Temperature Analysis For Final Four Scenarios	60
5.2.1	Scenario 1 – August 2000	60
5.2.2	Scenario 2 – August 2000 (x2)	67
5.2.3	Scenario 3 – June 2007	73
5.2.4	Scenario 4 – June 2007 (Fish wall).....	79
5.2.5	Comparison and Summary of Scenarios 1 through 4.....	85
CHAPTER 6:	SUMMARY AND FUTURE WORK	88
6.1	Summary	88
6.2	Future Work	88
6.2.1	Model Improvement.....	89
6.2.2	Expanding Model Scale	90
REFERENCES	91
APPENDIX	94

LIST OF TABLES

Table 4.1 Mesh density vs. iteration time	50
Table 4.2 Computational speed.....	52
Table 5.1 Salt Flux over 24 hours.....	87
Table A.1 – Dissolved Oxygen (mg O ₂ l ⁻¹) at Saturation in Freshwater, Brackish Water, and Seawater at Different Temperatures.	95
Table A.2 – DO (mg/l) based on varying salinity concentrations (ppt) and water temperature (°C).	97
Table A.3 – Scenario 1 Boundary Conditions in 15 min increments	100
Table A.4 – Scenario 2 Boundary Conditions in 15 min increments	102
Table A.5 – Scenario 3 and 4 Boundary Conditions in 15 min increments.....	104

LIST OF FIGURES

Figure 1.1 – Map of Seattle.....	7
Figure 2.1 Illustration of the volume modeled by Ooi’s computational fluid dynamics (CFD) model and Goodwin’s ELAM NFS model.	20
Figure 2.2 Lake Roosevelt model area	21
Figure 4.1 General Map of Seattle	32
Figure 4.2 Features of the LWSC	33
Figure 4.3 Major Physical Features of the Locks	34
Figure 4.4 Major physical features of the Locks.	35
Figure 4.5 Saltwater drain, showing outlet to Puget Sound and pipe to fish ladder.....	36
Figure 4.6 Plan view of Ballard Locks spillway and fishladder , courtesy of Lynne Melder, Seattle District	37
Figure 4.7 Plan view of Ballard Locks, courtesy of Lynne Melder, Seattle District.....	38
Figure 4.8 Isometric view of SWD, courtesy of Lynne Melder, Seattle District	39
Figure 4.9 Water quality data collection stations. ACOE (Pink), King County (Green)	40
Figure 4.10 Combined bathymetry and topography of Seattle Washington area, University of Washington	45
Figure 4.11 ArcGIS cut bathymetry.....	45
Figure 4.12 Bathymetry used to create mesh river bed	46
Figure 4.13 Mesh of LWSC Model	46
Figure 4.14 Water surface elevation in the LWSC.....	47
Figure 4.15 Mesh of LWSC Model – Close up of Ballard Locks	47
Figure 4.16 Model overlayed on GoogleEarth	48
Figure 4.17 Top Left: 1000, Top Right: 1250, Bottom Left: 1500, Bottom Right: 2000.....	49
Figure 4.18 Mesh density vs. iteration time.....	50
Figure 4.19 Computational speed	52
Figure 5.1 Preliminary Model Mesh.....	57

Figure 5.2 June 2007 salt plume after 10 weeks of simulation.....	58
Figure 5.3 Lake Union patch, using August 2000 data.....	58
Figure 5.4 Lake Union patch, Solution after 6 days of simulation.....	59
Figure 5.5 Salt Concentrations in the LWSC for 2010.....	59
Figure 5.6 Scenario 1 - Lock and Dam salt monitor 3.....	62
Figure 5.7 Scenario 1 - Fremont Bridge salt monitor 3.....	62
Figure 5.8 Scenario 1 - Gas Works salt monitor 4.....	63
Figure 5.9 Scenario 1 - Lake Union salt monitor 4.....	63
Figure 5.10 Scenario 1 - University Bridge salt monitor 2.....	64
Figure 5.11 Scenario 1 - Lock and Dam temperature monitor 1.....	64
Figure 5.12 Scenario 1 - Fremont Bridge temperature monitor 1.....	65
Figure 5.13 Scenario 1 - Gas Works temperature monitor 1.....	65
Figure 5.14 Scenario 1 - Lake Union temperature monitor 1.....	66
Figure 5.15 Scenario 1 - University Bridge temperature monitor 1.....	66
Figure 5.16 Scenario 2 - Lock and Dam salt monitor 3.....	68
Figure 5.17 Scenario 2 - Fremont Bridge salt monitor 3.....	68
Figure 5.18 Scenario 2 - Gas Works salt monitor 4.....	69
Figure 5.19 Scenario 2 - Lake Union salt monitor 4.....	69
Figure 5.20 Scenario 2 - University Bridge salt monitor 2.....	70
Figure 5.21 Scenario 2 - Lock and Dam temperature monitor 1.....	70
Figure 5.22 Scenario 2 - Fremont Bridge temperature monitor 1.....	71
Figure 5.23 Scenario 2 - Gas Works temperature monitor 1.....	71
Figure 5.24 Scenario 2 - Lake Union temperature monitor 1.....	72
Figure 5.25 Scenario 2 - University Bridge temperature monitor 1.....	72
Figure 5.26 Scenario 3 - Lock and Dam salt monitor 3.....	74
Figure 5.27 Scenario 3 - Fremont Bridge salt monitor 3.....	74
Figure 5.28 Scenario 3 - Gas Works salt monitor 3.....	75

Figure 5.29 Scenario 3 - Lake Union salt monitor 4.....	75
Figure 5.30 Scenario 3 - University Bridge salt monitor 2.....	76
Figure 5.31 Scenario 3 - Lock and Dam temperature monitor 1	76
Figure 5.32 Scenario 3 - Fremont Bridge temperature monitor 1.....	77
Figure 5.33 Scenario 3 - Gas Works temperature monitor 1	77
Figure 5.34 Scenario 3 - Lake Union temperature monitor 1	78
Figure 5.35 Scenario 3 - University Bridge temperature monitor 1	78
Figure 5.36 Scenario 4 - Lock and Dam salt monitor 3.....	80
Figure 5.37 Scenario 4 - Fremont Bridge salt monitor 3	80
Figure 5.38 Scenario 4 - Gas Works salt monitor 3.....	81
Figure 5.39 Scenario 4 - Lake Union salt monitor 4.....	81
Figure 5.40 Scenario 4 - University Bridge salt monitor 2.....	82
Figure 5.41 Scenario 4 - Lock and Dam temperature monitor 1	82
Figure 5.42 Scenario 4 - Fremont Bridge temperature monitor 1.....	83
Figure 5.43 Scenario 4 - Gas Works temperature monitor 1	83
Figure 5.44 Scenario 4 - Lake Union temperature monitor 1	84
Figure 5.45 Scenario 4 - University Bridge temperature monitor 1	84
Figure 5.46 Salt Flux over 24 hours	87
Figure A.1 Datum planes in the vicinity of Lake Washington	99

LIST OF NOMENCLATURE

Acronyms and Abbreviations

1D	One-Dimensional
2D	Two-Dimensional
3D	Three Dimensional
Ballard Locks	Hiram M. Chittenden Locks and Dam
CFD	Computational Fluid Dynamics
DO	Dissolved Oxygen
DNR	Department of Natural Resources
ELAM	Eulerian Lagrangian Agent Model
FB	Freemont Bridge
FLUENT	ANSYS FLUENT 12.0
I-5	Interstate 5
IIHR	IIHR- Hydroscience & Engineering
KC	King County
LW	Lake Washington
LWSC	Lake Washington Ship Canal
PS	Puget Sound
SOW	Statement of Work
SWD	Salt Water Drain
UB	University Bridge
Seattle District	United States Army Corps of Engineers, Seattle District
USGS	United States Geological Survey

Equation Variables

Computational Variables

ρ	Density
u, v, w	Velocity components (x, y, and z)
p	Pressure
e	Total Energy
T	Temperature
$\tau_{(x,y,z), (x,y,z)}$	Viscous stresses
μ	Fluid viscosity
μ_t	Eddy viscosity
δ_{if}	Kronecker Delta
k	Turbulent kinetic energy
ε	Turbulent dissipation rate
G_k	Generation of turbulent kinetic energy due to mean velocity gradients
G_b	Generation of turbulent kinetic energy due to buoyancy
Pr_t	Prandtl number for energy
β	Coefficient of thermal expansion
$C_{1\varepsilon}$	k- ε equation constant
$C_{2\varepsilon}$	k- ε equation constant
C_μ	k- ε equation constant
σ_k	k- ε equation constant
σ_ε	k- ε equation constant
g	Gravitational acceleration
k_{eff}	Effective conductivity
J	Turbulent dispersion
D_m	Molecular Diffusivity
D_t	Turbulent Diffusivity

Sc_t	Schmidt number
E	Total Energy
h	Sensible enthalpy
Y	Species mass fraction
R	Change in mass due to reaction

CHAPTER 1: INTRODUCTION

1.1 Background

In the early 1900's Seattle looked very different than it does today. The major water bodies haven't moved, but the way they are all connected has been drastically altered (see Figure 1.1.A and B). Historically, Puget Sound (Figure 1.1.A.a) was connected to Salmon Bay (Figure 1.1.A.b) which was the outlet of a small stream that connected to Lake Union (Figure 1.1.A.c). Moving upstream, salty water from Elliot Bay (Figure 1.1.A.d) slowly turned fresh as it mixed with the fresh waters of the Duwamish River (Figure 1.1.A.e). The Duwamish was largely impacted by the Black River (Figure 1.1.A.f), whose confluence was at the far Southern end of Seattle. The Black River was a short connector between Lake Washington (Figure 1.1.B.g), the Cedar River (Figure 1.1.B.h), and the rest of the fresh Lake Washington water watershed. Salmon moved through the Lake Washington watershed by finding their way up the Duwamish River into the Cedar River and Lake Washington to reach their natal spawning grounds (US Army Corps of Engineers 2008).

For shipping purposes, in 1916 the USACE constructed the Hiram M. Chittenden Lock and Dam system (Ballard Locks) (Figure 1.1.B.k) and excavated out the Lake Washington Ship Canal (LWSC) to allow safe boat travel between Lake Washington and Puget Sound. During the excavation process two main cuts were made; the Montlake Cut (Figure 1.1.B.i) and the Fremont Cut (Figure 1.1.B.j). These two canals connected Lake Washington to Lake Union, and Lake Union to Salmon Bay respectively (US Army Corps of Engineers, 2008).

Historically, the Lake Washington water elevation fluctuated with seasonal changes, peaking around 32 feet above sea level in the winter and dropping off in the summer. The construction of the Ballard Locks and LWSC created a way to control lake levels between 20 and 22 feet above sea level. The dam also helped control salt water

intrusion from Puget Sound into Lake Washington. The locks (boat lifts) allowed boats to travel between the two sides of the dam. Due to lake levels falling from 32 to 22 feet, Lake Washington's shorelines receded, disconnecting Lake Washington from the Black River. In 1912 the entire Cedar River was diverted up into Lake Washington. The Duwamish River was severed completely from the Lake Washington and Cedar River watersheds, completely disconnecting migrating salmon from their original spawning grounds. Salmon either spawned in the Duwamish River and its tributaries or they had to migrate through the Ballard Locks to spawn in their natal streams. A fish ladder was installed at the Ballard Locks in the early 1970's to help facilitate migration past the locks and dam (US Army Corps of Engineers 2008).

Switching the salmon's main migratory path from the Duwamish River to the LWSC had drastic effects on the anadromous fish populations. After the construction of the fish ladder, and making other changes to the Ballard Locks operations, fish populations have rebounded, but are still well below escapement goals (US Army Corps of Engineers 2008). In the current study, the Seattle District is reviewing current management practices to see what changes could help migrating fish move upstream with as little interference as possible.

The Ballard Locks helps reduce the amount of salt water that flows upstream; however, it doesn't completely stop salt water from intruding into the system. Every time the locks have an up-lock (ships heading upstream), a wave of salt water spills into the fresh water canal. In an attempt to regulate the salt water, a salt water barrier was built inside the large lock. The barrier holds back the forward flow of salt water into Salmon Bay. A drain has also been placed near the upstream side of the locks allowing the denser salt water that does enter Salmon Bay to flow into the drain and be rerouted back over to Puget Sound. To avoid letting salt water alter the fresh water habitat of Lake Washington, regulations have been put in place limiting the salt water concentration past University Bridge to 1 part-per-thousand (ppt) (US Army Corps of Engineers 2008).

Differences in water temperature between Puget Sound and the LWSC have also been shown to affect salmon migration (US Army Corps of Engineers 2008). Coupled in the current models are both salinity and temperature affects due to current management practices. Dissolved Oxygen (DO) is also greatly affected by temperature and salinity concentrations. Therefore, the interaction between salinity, temperature, and DO in the LWSC will hopefully be better understood through this research.

1.2 Motivation

The Seattle District wants to better manage the Ballard Locks and structures along the LWSC in a way that will maintain the environmental sustainability and biodiversity in the area. Due to strict salt water intrusion regulations in the LWSC, the Seattle District is working on upgrading their management practices such that they will resolve two inter-related problems. First, to improve the fish passage conditions for migrating salmon; and second, to learn how to better manage the salt wedge that forms and intrudes upstream. Based on the hydrodynamic and water quality results that are produced by this research, the Engineer Research and Development Center (ERDC) Portland Office will use their Eulerian-Lagrangian-Agent-Model (ELAM) to analyze fish patterns, looking for the most beneficial management schemes that assist salmon in migrating upstream.

Understanding the management practices that affect the migration of an intrusive salt wedge will help the Seattle District develop guidelines for locking operations that will move the wedge up or downstream. The salt wedge not only affects the water quality of the LWSC for migrating salmon, if it is allowed to reach Lake Washington it can also drastically change the fresh water ecosystem.

CFD has made it possible for the Seattle District to more accurately analyze the LWSC to determine the biological and hydrodynamic parameters that affect salmon migration and salt water intrusion. Instead of making expensive or damaging physical changes to the Ballard Locks or changing the current management practices in a way that

could drastically affect the system; CFD allows the Seattle District to estimate the changes that would occur in each given hypothetical scenario. This will result in better understanding the LWSC system as a whole, as well as optimize the current management practices in a way that will hopefully improve both the salmon migration and salt water intrusion.

In the past, S.K. Ooi studied in detail the salt intrusion directly around the Ballard Locks (Ooi, 2006) (Goodwin, 2007). This current project is enlarging that study to look at the salt water intrusion and water quality in the entire LWSC.

1.3 Objectives

Locks, dams, canals, and other hydraulic structures have been created for the ease and safe passage of ships between Puget Sound and Lake Washington. A fish ladder, salt water barrier, salt water drain, and other structures have been created in an attempt to improve the water quality and ease of passage for migrating salmon. The effectiveness of these various structures is not completely known. The goals of this research are to implement CFD engineering techniques to help better understand the effectiveness of hydraulic structures in the area, as well as come up with management practices that both mitigate the salt water intrusion from Puget Sound, and improve the migrating passages for salmon. Understanding the affects different management practices have on water quality and salmon migration will help produce guidelines for addressing future water quality challenges.

The specific project objectives that have been outlined by the Seattle District are:

- Create 2 scenarios representing historical environmental conditions associated with upstream (1 scenario) and downstream (1 scenario) migrant observations between Ballard Locks and Montlake Cut that will be described using a 3-D time-variant CFD and water quality (temperature, dissolved oxygen, salinity) model.

- CFD and water quality modeled data will be provided to ERDC and the Northwest Division – Seattle District of the USACE (NWS) in Tecplot format, with the entire 3-D mesh stored as a single Tecplot zone and each Tecplot zone representing a separate time step.
- This project will build off and extend previous CFD, water quality, and ELAM modeling at the Locks, which demonstrated proof-of-concept ability to replicate/describe the 3-D movement trajectories of upstream migrating adult salmon measured through acoustic-tag telemetry.
- Once the ability to describe historical observations in upstream and downstream movement behavior and passage between Ballard Locks and Montlake Cut has been achieved, the technology will be used to assess 2 additional hypothetical scenarios representing the possible benefits associated with management alternatives in the structural and/or operational design of Ballard Locks.

The following are the 4 scenarios that will be modeled:

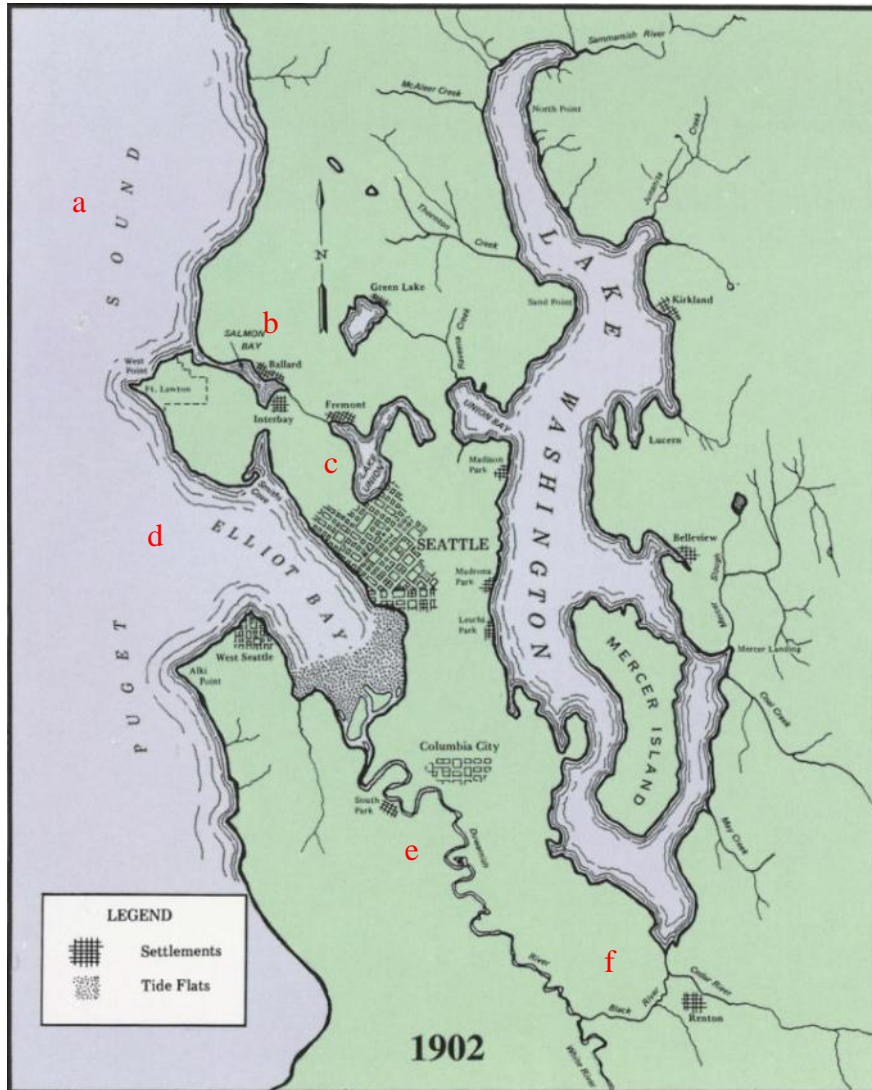
- 1) Beginning of June (10-25) Juvenile historical assessment #1
- 2) Beginning of June (10-25) Juvenile future hypothetical assessment #1
- 3) End of August (15-30) Adult historical assessment #1
- 4) End of August (15-30) Adult future hypothetical assessment #1

The historical assessments will be based on average lock operations during June 2007 and August 2000. The June hypothetical scenario will be identical to the historical scenario, except a floating wall will be placed parallel to the spillway, located in the forebay between the fish ladder and the small lock pier (see Figure 4.14). The August hypothetical scenario will be identical to the historical scenario, except that the number of lockings will be doubled in both the large and small locks. The increase in lockings will ideally demonstrate what false lockings (an up-locking with no boats) would do to benefit fish migration. Specific details for each scenario will be outlined in chapter 4 and in the appendix.

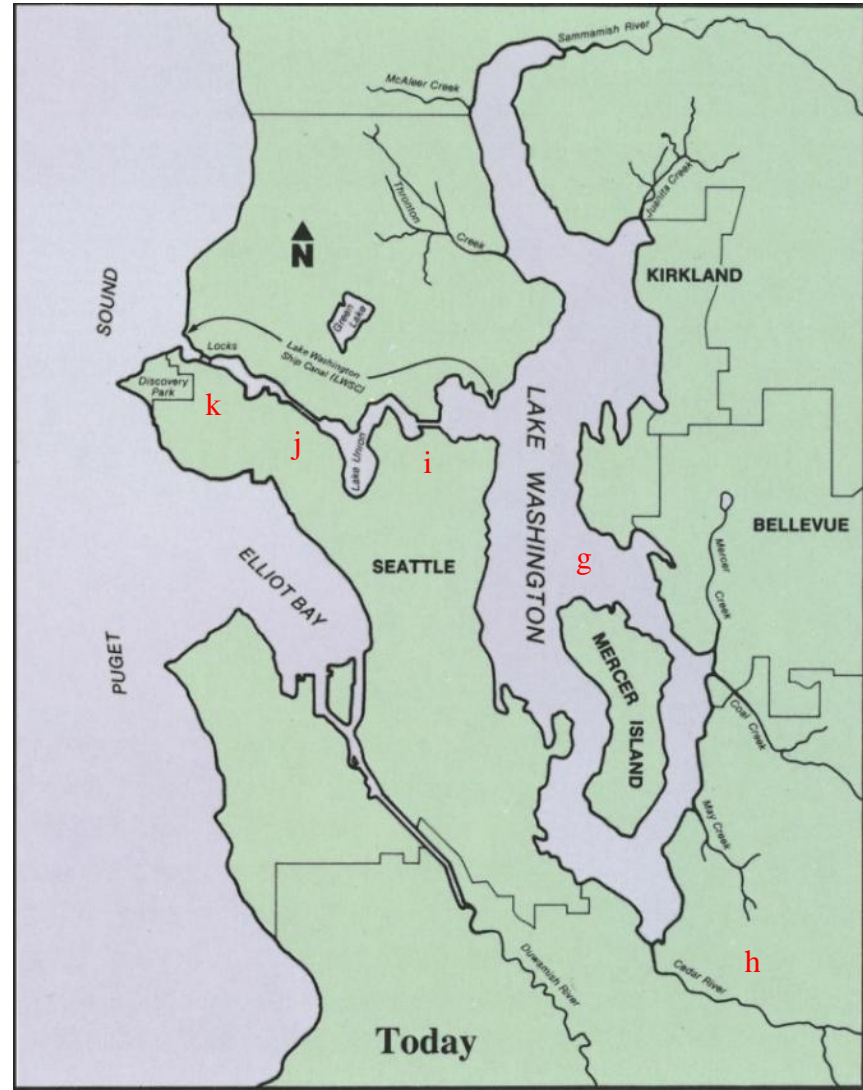
1.4 Overview

This thesis details the work completed to develop a hydrodynamic and water quality (species transport) model of the LWSC in Seattle Washington. This work began by studying the fundamentals of salt water intrusion and the affects of water quality parameters on migrating salmon. A previous Ballard Locks model (Ooi, 2006) was used as a reference to develop a completely new model of the LWSC. Bathymetric data supplied by the USACE was processed in ArcGIS to develop an accurate replica of the river bed. A CFD commercial software package known as Ansys FLUENT (FLUENT) was used to test the integrity of the mesh. Model boundary conditions were determined based on previous work (Ooi, 2006) as well as new conditions determined by the Seattle District. FLUENT was then used to predict the hydrodynamics (velocity, pressure, density) and species transport (salt wedge formation) of the system. Historic water quality data was used to initialize the model. The results demonstrated FLUENT's ability to accurately predict the LWSC hydrodynamics and water quality. These results were then used to justify creating the hypothetical scenarios that simulated a change in management practice.

The outline of the thesis is as follows. Chapter 2 describes the fundamentals of salt water intrusion and the affects of water quality parameters on migrating salmon, as well as a review of published hydrodynamic and salt water intrusion models. Chapter 3 discusses the discretized equations and computational methods used to simulate the LWSC. Chapter 4 addresses the process used to create the model. Both the mesh and boundary conditions used are discussed. Chapter 5 presents the results and a discussion of the findings. Chapter 6 summarizes the project and puts forth suggestions for future work.



(A) Seattle in 1902 (US Gov't, 1999)



(B) Seattle Today (US Gov't, 1999)

Figure 1.1 Map of Seattle

CHAPTER 2: REVIEW OF EXISTING LITERATURE (NUMERICAL MODELING OF FISH MIGRATION, AND WATER QUALITY)

Managing a dynamic, natural and man-influenced, system can be extremely challenging. The Ballard Locks controls numerous things, among which include; the elevation of the water on Lake Washington, the amount of salt water that intrudes upriver threatening the freshwater environment, the efficiency in which migrating salmon move up or downstream past the dam, the structural integrity of the floating highway bridges I-90 and Highway 520 as they cross Lake Washington, as well as controlling the boat traffic that moves between Puget Sound and Lake Washington (Personal Communication with Lynne Melder, 2010). To understand ways to better manage salmon migration, one must look at how management changes will affect the various dominos that come into play.

Due to the wide variety of elements affecting each other on this project, this chapter is dedicated to reviewing the literature of these various topics, and showing how they are all inter-related. The overarching goal of the project is to help improve the migration of anadromous fish through the LWSC. To achieve this goal a numerical model of the water quality and hydrodynamics of the LWSC has been created. Modeling the salt-water density-current that is created will help allow the Seattle District see changes that can be made to the management practices at the lock and dam. The results from the 3D model will be used in an ELAM model to help determine which conditions help salmon migrate through the LWSC more efficiently.

2.1 Anadromous Fish Migration

Anadromous fish are unique in that they spend their lives traveling great distances all with the purpose of sustaining the existence of their species. Juvenile salmon, or smolts, are pushed downstream out to sea while they swim facing upstream (Berggren, 1993). Adult salmon swim upstream to reach their natal spawning grounds to spawn and die. A review of the contributing factors that affect juvenile and adult salmon migration will help one better understand the parameters that are being modeled in this project.

2.1.1 Juvenile salmon migration

Juvenile salmon are pushed downstream out to sea while they swim facing upstream (Berggren, 1993). Through this journey juvenile salmon must avoid natural predators, such as cutthroat trout, rainbow trout, smallmouth bass, prickly sculpin, pike minnow, and piscivorous birds (Celedonia, 2008) (Seattle Division, 2008). If the salmon are successful in avoiding natural enemies, they must then traverse through the perilous exits of dams. Smolt flumes, turbines, spillways, locks, lock filling culverts, and fish ladders are some of the many outlets fish can attempt to use to bypass a dam.

Work done by Celedonia et al (Celedonia, 2008) showed that juvenile salmon traveling downstream through the LWSC move through the major sections of the canal in less than 24 hours. The smolts tend to spend a long time (more than 24 hours) in the southern end of Lake Union and in the forebay of the Ballard Locks in Salmon Bay before leaving the system (Celedonia, 2008). Previous to the work done by Celedonia it was assumed that salmon would prefer to only use the northern part of Lake Union (Celedonia, 2008), modeling the hydrodynamics and water quality in the southern end of Lake Union was therefore deemed as an important area to monitor. The results by Celedonia agree with similar results found in the executive summary put out by Seattle Public Utility (SPU) and the Seattle District (USACE) in 2008 (Seattle Division, 2008).

Juvenile salmon migrate past the Ballard Locks in the late spring to early summer, peaking in late June. Based on the 2007-2008 study by Celedonia et al (Celedonia, 2009), juveniles preferred using the smolt flume (52-89% of tagged fish) when the water temperature was below 18°C. This switched to as low as 17% using the smolt flumes when the water temperature increased to 20°C or greater. This pattern of having an aversion to higher temperatures was reproduced in both years of the study. When water temperatures rose, salmon used the small and large locks to migrate downstream (Celedonia, 2009). The 2008 report by SPU and the Seattle District (Seattle Division, 2008) agreed that an increasing number fish passed through the locks as water temperatures rose. Accurately modeling canal water temperatures will help determine if any specific management practices will greatly influence the migration paths salmon take near the Ballard Locks. For example, if the floating wall in the hypothetical June scenario is able to help pull cooler water up from the depths of the forebay into the area directly behind the smolt flumes, it is possible that fish will use this exit alternative further into the hot summer months.

In a typical estuary the cold ocean water and warm fresh water would have a much larger area to mix and thus make transition into the ocean smoother. The Ballard Locks induce a cold-salty versus warm-fresh water barrier. The impact that high salinity and cold water immediately downstream of the dam have on juvenile salmon is unknown. However, it is known that smolt migration out of Shilshole Bay typically happens within an hour of leaving the LWSC (Seattle Division, 2008).

2.1.2 Adult salmon migration

Adult migrating salmon are affected by many of the same physical hazards as juvenile salmon, only in reverse (Seattle Division, 2008). If an adult salmon survives in the predator filled world of the ocean, they eventually work their way back to their natal spawning grounds to repeat the life cycle. Adult Chinook salmon migrate past the

Ballard Locks between the end of July and mid-September (Timko, 2002). Fish ladders allow salmon to move up past dams that would otherwise completely sever their upstream progression. Adult salmon migrate past the Ballard Locks by using the fish ladder or the locks (Seattle Division, 2008). Once salmon have moved into the LWSC they either migrate quickly through the canal or hold in a cool-salty area near the SWD for up to several weeks (Timko, 2002). High canal water temperatures possibly contribute to the decision to move through quickly or hold near the Ballard Locks (Seattle Division, 2008).

Timko et al. (Timko, 2002) used an acoustic transmitter system (ATS) to monitor the migration of adult Chinook salmon through the LWSC. Based on Timko's results, the adult salmon held primary behind the SWD and the small lock, the average hold time was 19 days. One key result from this study was that "there were no observed trends with respect to area of residence and lock operations" (Timko, 2002). This project will hopefully be able to make observed trends as typical locking operations (scenario 1) are compared to when the number of lockings are doubled (scenario 2).

2.1.3 How water quality affects salmon migration

Just as temperature, air pollution, and safety can affect where humans prefer to live. The water temperature, pollution, and safety of river highways can often affect where fish prefer to swim. As temperatures rise, fish swim lower and lower in the water column, preferring to stay in cooler waters (Seattle Division, 2008). Dissolved oxygen (DO) concentrations, salinity, and other water quality parameters can also affect the places salmon are found to swim. In an attempt to quantify the affects water quality (temperature, DO, and salinity) had on salmon migration Timko et al. measured these various water quality parameters throughout the duration of their field study but could not demonstrate any significant trends relating salmon location to water quality (Timko, 2002). Significant water quality changes were observed based on locking operations,

such as salinity increasing after a locking; however, these changes didn't seem to affect the fish (Timko, 2002).

Work done by Hodgson and Quinn (Hodgson, 2002) showed how increased water temperatures affected salmon migration timing. Salmon either migrated to natal spawning grounds and held in the area for several months before peak river temperatures, or they migrated after peak temperatures and spawned shortly thereafter (Hodgson, 2002). When the peak river temperature changed, the salmon migration changed to account for the different temperature. According to (Hodgson, 2002) "high temperatures can increase susceptibility to disease and increase prespawning mortality."

Donald L. Kramer studied the effect dissolved oxygen (DO) has on determining fish behavioral responses (Kramer, 1987). Kramer's approach to fish behavior was based on optimization theory, quantifying oxygen as a limited resource and assuming fish will optimize their environment to meet all basic needs. As the concentration of oxygen decreases, the physical effort required to "breathe" goes up. Therefore, Kramer's theory was that fish will have a certain threshold under which if there is less oxygen, they will move to a new location that is more optimal for survival (Kramer, 1987).

DO concentrations are directly impacted by water temperature and salinity (Spotte, 1970). However, this impact is very small, thus not greatly impacting fish movement unless DO is extremely limited (Kramer, 1987). Hypoxic zones cause fish to move higher in the water column to obtain oxygen more easily. Based on the theory of optimization, if feeding conditions, protective cover, water temperature, etc. are more favorable in a hypoxic zone, fish will choose to stay in the area, despite the greater effort required to breathe (Kramer, 1987).

Modeling DO is very complex and has been removed from the parameters that our FLUENT model will track. Instead we have included DO in the code that converts the FLUENT output files into a format that can be used in the ELAM models. Using the salinity, temperature, and DO, relationship that was developed by Spotte (Spotte, 1970)

we calculated DO values. However, it was determined that this method would be too simplistic to capture the realistic DO changes during a locking operation. Understanding the simplistic approach to resolving DO, the results from Spotte's relationship were still included in the data delivered for the ELAM models to see if the simplistic DO values could help in predicting salmon migration patterns.

The DO levels in Puget Sound are typically higher than in the LWSC. Occasionally, extra "night lockings" are performed to increase the DO levels in the canal. This approach increases the DO level in the canal while at the same time increasing the salt concentration and decreasing the temperature. The immediate effects seem to produce more favorable conditions for fish. However, the overall effect of these extra lockings is unknown (Personal Communication with Frederick Goetz, 2010).

2.2 Numerical simulation of fish migration

Modeling fish migration accurately is extremely difficult. The most common approach is to use optimization theory to determine where a fish will move next. Based on current understanding of how a fish will react to water quality parameters (such as temperature, DO, salinity, or hydrodynamic properties such as turbulence or velocity) helps ultimately determine the direction a fish will swim. The various cues that trigger a fish to move are quantified and written into the algorithms that model fish migration (Goodwin, 2001). By calibrating a numerical model to known fish responses, one can accurately quantify changes that occur to fish migration patterns when management practices are changed. Several numerical models have been developed to better understand fish migration. The following are summaries of the 2D and 3D models that have been developed.

2.2.1 Two-Dimensional Models

Work done by McKillip and Wells (McKillip, 2007) used a CE-QUAL-W2 model to show the water quality and hydrodynamics of a large watershed (see Figure 2.2). The

model analyzed fish bioenergetics (the fish's ability to grow) to determine the prime habitat for migrating fish. This approach resolved more general assumptions as to where fish will be located in a large river reach; it did not however resolve short term movements of fish based on dynamic water quality changes. McKillip's approach was not sufficient for this project because the results produced by our models are three-dimensional; the CE-QUAL-W2 model would be unable to analyze the three-dimensional solutions. The Seattle District is also interested in tracking short-term fish migration which the CE-QUAL-W2 model would be unable to resolve with sufficient detail.

2.2.2 Three-Dimensional Models

Work done by Goodwin et al. (Goodwin, 2001) developed a three-dimensional coupled Eulerian-Lagrangian model (ELAM) that tracked particles based on stimuli responses. The ELAM model was used in work done by Goodwin et al (Goodwin, 2007) to test the feasibility of modeling salmon migration in a small section of the LWSC (see Figure 2.1 for model area). Based on the 2007 results it was determined that testing salmon migration in the entire LWSC could possibly give more insight into how various lock operations affected salmon migration cues.

The model area for this project is much larger than the previous work done on the LWSC (Goodwin, 2007). Once Goodwin receives the water quality and hydrodynamic data from this project he will be able to determine the feasibility of modeling the NFS in such a large domain. The goal of the Seattle District is to model various management practices at the Ballard Locks, using Goodwin's NFS model, to determine the best management practices that will benefit juvenile and adult salmon migration.

2.3 Numerical simulation of salt water intrusion

Salt water that flows from Puget Sound through the Ballard Locks into the LWSC is denser than the fresh water flowing from Lake Washington. This density difference causes the salt water to form a wedge that slowly flows upstream. Depending on the

discharge from Lake Washington, the varying water temperatures, locking operations, and any other management practices around the Ballard Lock and Dam, the salt wedge will move up or down stream. Numerous 1D, 2D, and 3D models have been developed to study density currents at a lock. Known as a lock-exchange problem, sections 2.3.2 through 2.3.4 describe the type of research that has been done previously. Up until now, the lock-exchange problem has only been studied in close proximity to the lock. This project looks at the salt wedge migration upstream, much further away from the lock and dam system than what has been studied in previous models.

2.3.1 Salt Water Intrusion

When salt water and fresh water collide their density differences cause them to flow past each other rather than fully mix. Much like oil on water, fresh water on top of denser salt water acts much the same way. Where fresh water rivers meet the ocean, fresh water surface plumes and salt water river bed wedges are formed. The discontinuity in currents is known as a gravity current or density current. According to (Simpson, 1982), a density current is “the flow of one fluid within another caused by the density difference between the fluids. The difference in specific weight that provides the driving force may be due to dissolved or suspended material or to temperature differences.”

Numerous density-current models have been made in an attempt to simulate salt water intrusion, turbidity currents, atmospheric-sized flows, deep-ocean currents, and the basic lock-exchange problem. Although many of these models have been created specifically with one type of density-current in mind, often the models can overlap and be used in other situations. The various models also help demonstrate the diverse approaches that have been developed in modeling density-currents.

The next three sections discuss a history of density-current models and their complexities.

2.3.2 One-Dimensional Models

In the past, several 1D density-current models have been created. The work of (Bonnecaze, 1993) modeled two-layers of fluids interacting. The 1D model predicted the approximate movement of the denser layer in a lock-exchange type situation. The work of (Choi, 1995) modeled unsteady turbidity currents (density currents caused by sediment) using a depth-integrated approach. Both Bonnecaze and Choi's models focused on locating the head of the denser current as it moved through time. These 1D models were not able to resolve some of the detailed disturbances that happen along the density-current fronts. These models were also developed using idealized model flumes. In our case, a 1D model would not be sufficient to model the LWSC bathymetry, salt concentrations, and water temperatures needed to analyze fish movements in the three-dimensional system.

2.3.3 Two-Dimensional Models

(Daly, 1968) was one of the first to do a 2D model of the lock-exchange problem. Using the computing power that was available at the time, Daly was able to accurately model the structure of a density current at a lock.

Numerous people have used 2D models to study atmospheric density-currents. (Mitchell, 1977) pioneered looking at 2D structures of thunder clouds where the density differences are much more acutely recognized by the buoyancy of air pockets. (Crook, 1985) looked at 2D atmospheric density currents, particularly at the waves that are created in the less dense clouds in front of a dense cloud front. (Haase, 1989) also modeled 2D atmospheric currents. During a National Center for Supercomputing Applications (NCSA) conference held in September 1990, (Straka et al., 1993) analyzed various 2D models in the diffusive-only situation of a denser air mass moving along a surface. The Kelvin-Helmholtz instabilities were resolved accurately in the finer meshed

models. It was noted that the results were noticeably inaccurate when the mesh size became too coarse.

Modeling turbidity currents helps analyze river bed movement and how the river sediment settles in large reservoirs or lakes. The work done by (Bradford, 1999) looked at “unsteady, two-dimensional, single-layer, depth-averaged turbid underflows driven by nonuniform, noncohesive sediment.” The model was able to determine the changes in an erodible bed by including a sediment-bed conservation equation. (Khan, 2008) modeled 2D density-currents when encountering a bump in the bed. The model accurately showed that the dense liquid was forced to backup until it could go through a critical depth where it spilled over the bump. In our case, a 2D model would not be sufficient to model the depth-varying salt concentrations and water temperatures needed to analyze fish movements in the three-dimensional system.

2.3.4 Three-Dimensional Models

Three-dimensional models are much more difficult to create and run than 1D or 2D models. The time required to develop the model, the base data required for inputs, and the computational time required to solve 3D problems are all reasons three-dimensional models are not used unless completely necessary. In recent years, computing power has reached a level where many 3D computational fluid dynamic models can be resolved in a reasonable amount of time. Numerous complex 3D problems are still limited by the computing power required. Assuming computers continue to get faster and faster, more and more models with more and more detail will be developed studying all three dimensions.

Imran et al. (Imran, 2004) studied 3D density-currents in long straight channels. Imran looked at channels with high side walls and channels with low sidewalls leading into open floodplains and then compared them. The model focused mostly on the densities in various areas and not so much on the 3D structures created by the density

flow. (Kassem, 2004) was the follow up study to Imran et al. (Imran, 2004) in which density-currents in sinuous channels were modeled. Again the study focused on the densities of the liquid as flow moved through a curved channel instead of the 3D structures created by the density flows.

Various models have been developed to look at turbidity currents flowing into reservoirs (Bournet, 1999), (De Cesare, 2001), (Huang, 2005), (Huang, 2007), and (Dallimore, 2004). Dallimore (Dallimore, 2004) used a 3D hydrodynamics model, coupled with a 2D turbidity current model. Modeling aeration bubble plumes as a density current have also been studied in the past by (Cantero, 2002), and (Bombardelli, 2004a). (Imran, 2004) and (Kassem, 2004) used the commercial software code FLUENT for their models. Species mass conservation was used to track the density-current.

The lock-exchange problem was studied in detail by (Ooi, 2006). Using an LES model Ooi was able to resolve very detailed Kelvin-Helmholtz instabilities within the lock. In a related project, Ooi developed the $k-\epsilon$ models used by Goodwin et al. (Goodwin, 2007) to study adult Chinook salmon movement directly upstream of the Ballard Locks. The project was done as a feasibility study and was thus limited to a very small area, as shown in Figure 2.1.

The Reynolds Averaged Navier-Stokes (RANS) equations were used almost exclusively in the 3D model approaches. They were used by (Bournet, 1999), (De Cesare, 2001), (Cantero, 2002), (Bombardelli, 2004a), (Imran, 2004) (Kassem, 2004), (Huang, 2005), (Huang, 2007), and (Dallimore, 2004). The RANS equations have been seen as the standard approach for reasonable results. Modeling turbulence with the two equation $k-\epsilon$ model has also become standard. More advanced options such as LES and DNS are available; however, the computational expense is often the limiting factor.

The model for this project was created using the same basic approach as Imran and Kassem, by using the commercial code Ansys FLUENT which incorporates species mass conservation to track the density-current, as explained in detail in chapter four.

This project model encompasses the area shown in Figure 4.16 which expands upon the small area used in Goodwin et al. (Figure 2.1) (Goodwin, 2007). In addition, our model is an unsteady boundary condition model, meaning, the physical properties along some of the boundaries change dynamically. This allows the model to simulate the opening and closing of lock gates based on modeled management practice. The results from our model were used to provide the Seattle District with the hydrodynamics and water quality data needed to run their ELAM model, which was used to predict salmon migration. Given the large scale of the project, modeling dynamic gravity currents, hydrodynamics, and water quality parameters, and using the results to analyze salmon migration, all make this project very unique to any other work that has been done in the past.

2.3.5 Summary

Due to the way water quality, fish migration, salt water intrusion, and locking operations were all strongly inter-related; this chapter was dedicated to reviewing the literature of these various topics, and showing how they were all connected. Fish migration will be modeled using the 3D ELAM model developed by ERDC. The ELAM model uses water quality and hydrodynamic parameters to determine where fish will swim. The commercial software Ansys FLUENT will be used to model the 3D hydrodynamic and water quality changes of the project scenarios. Similar to other studies, species conservation will be used to track the salt water intrusion. The various equations used in FLUENT to model the hydrodynamics and water quality will be presented in Chapter 3.

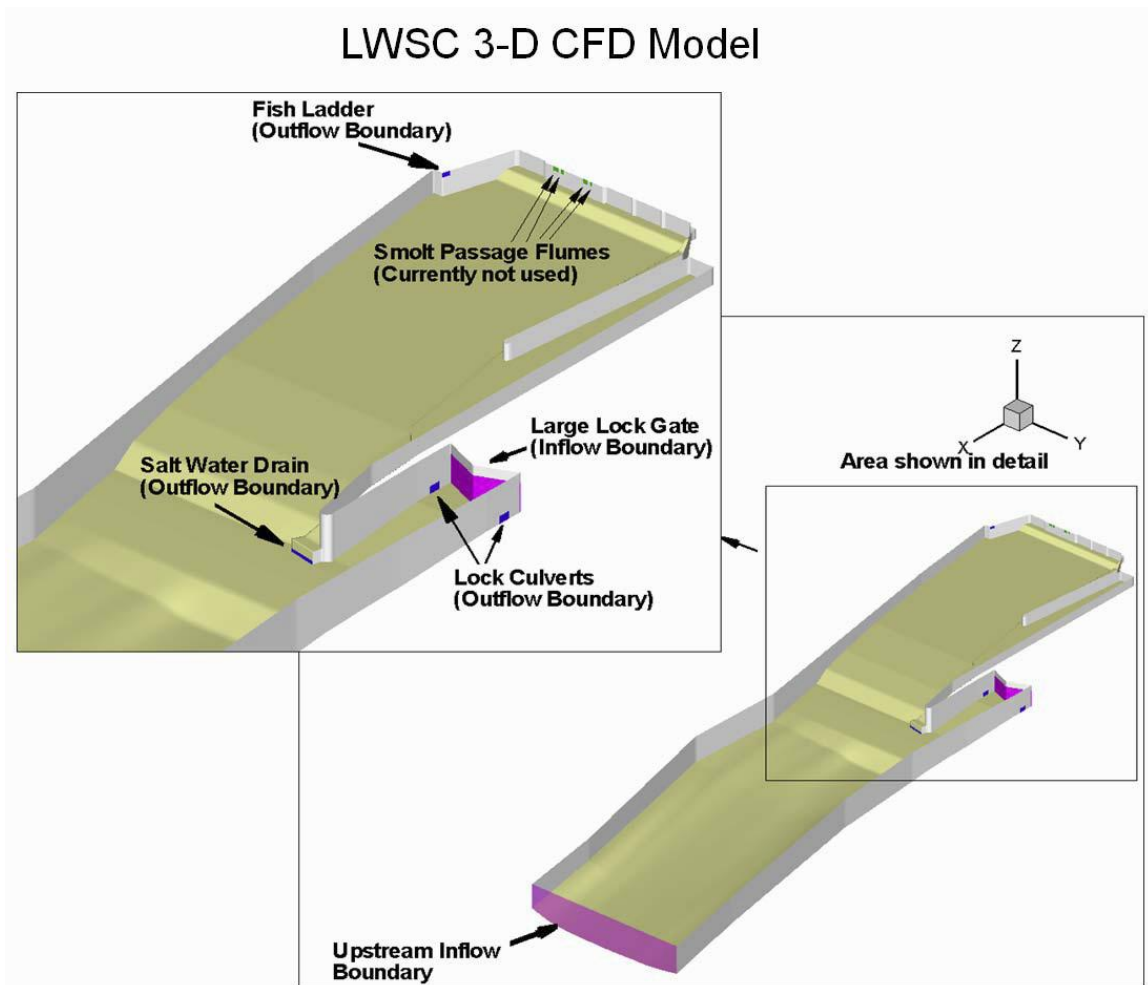


Figure 2.1 Illustration of the volume modeled by Ooi's computational fluid dynamics (CFD) model and Goodwin's ELAM NFS model. (Goodwin, 2007)

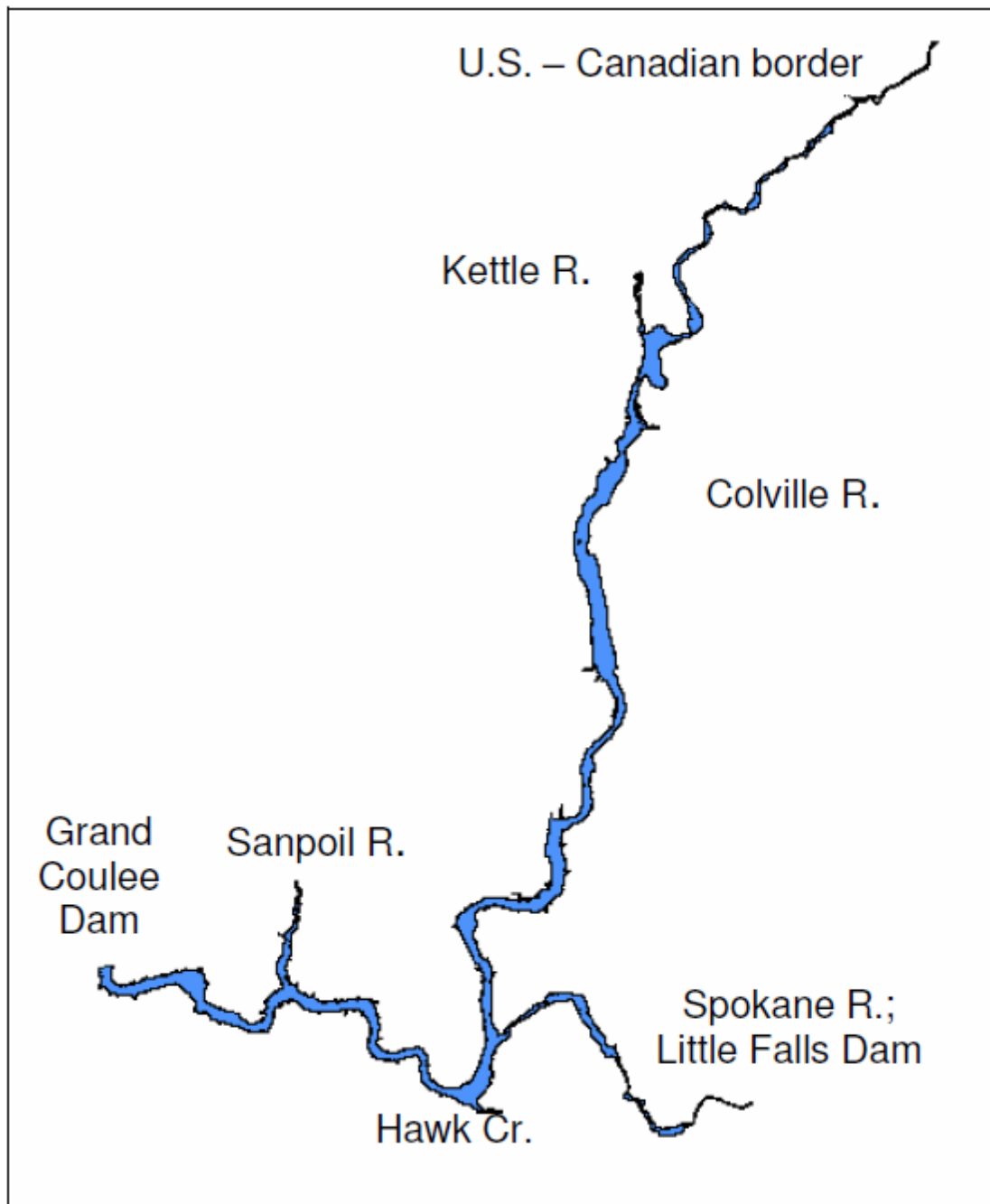


Figure 2.2 Lake Roosevelt model area (McKillip, 2007)

CHAPTER 3: NUMERICAL METHODS

Computers continue to get faster and faster. In recent years, the computational power needed to solve advanced computational fluid dynamics (CFD) has reached a level where many complex models can be resolved in a relatively short amount of time. ANSYS FLUENT 12.0 Commercial CFD Software (FLUENT) was used to run the models that were developed for this project. FLUENT uses discretized forms of the Navier-Stokes equations to accurately solve the hydrodynamics of the model.

FLUENT is capable of doing one, two, and three-dimensional modeling. The three-dimensional code used for this project was a finite volume scheme, which is a very common way to model fluid flow for numerous applications. Mechanical, bio-medical, aerospace, water resources, and environmental applications have all used FLUENT to solve complex three-dimensional problems (ANSYS Inc., 2009). FLUENT's ability to model the hydrodynamics of the system (x, y, z velocities and pressure), the energy equation (change in temperature), and the species transport (salt water intrusion) makes it a great tool for this research.

The general Navier-Stokes equations solve for seven unknowns: density (ρ), x-velocity (u), y-velocity (v), z-velocity (w), pressure (p), total energy (e) and temperature (T). Assuming that the flow is incompressible simplifies the equations by removing pressure. The six remaining variables are solved with six equations: the continuity equation, the three, three-dimensional momentum equations, the energy equation, and the species equation.

The general form of the continuity equation can be written as follows:

$$\frac{\partial \rho}{\partial t} + \frac{\partial (\rho u)}{\partial x} + \frac{\partial (\rho v)}{\partial y} + \frac{\partial (\rho w)}{\partial z} = 0 \quad (3.1)$$

Making the assumption that the fluid is incompressible results in the following form:

$$\frac{\partial \rho}{\partial t} + \frac{\partial \rho u}{\partial x} + \frac{\partial \rho v}{\partial y} + \frac{\partial \rho w}{\partial z} = 0 \quad (3.2)$$

The general form of the three-dimensional momentum equations are:

$$\tau_{xy} = \mu \left(\frac{\partial u}{\partial y} + \frac{\partial v}{\partial x} \right) \quad (3.3)$$

$$\tau_{yz} = \mu \left(\frac{\partial v}{\partial z} + \frac{\partial w}{\partial y} \right) \quad (3.4)$$

$$\tau_{zx} = \mu \left(\frac{\partial w}{\partial x} + \frac{\partial u}{\partial z} \right) \quad (3.5)$$

In our case we are modeling Newtonian fluids, therefore the viscous stresses ($\tau_{(x,y,z)(x,y,z)}$) can be expressed in terms of velocity and viscosity as:

$$\tau_{xx} = 2\mu \frac{\partial u}{\partial x} - \frac{2}{3}\mu \nabla \cdot \mathbf{u} \quad (3.6)$$

$$\tau_{yy} = 2\mu \frac{\partial v}{\partial y} - \frac{2}{3}\mu \nabla \cdot \mathbf{u}$$

$$\tau_{zz} = 2\mu \frac{\partial w}{\partial z} - \frac{2}{3}\mu \nabla \cdot \mathbf{u} \quad (3.7)$$

Applying these expressions for viscous shear the equations simplify to:

$$\rho \frac{D u}{D t} = \rho g_x - \frac{\partial p}{\partial x} + \mu \nabla^2 u \quad (3.8)$$

$$\rho \frac{D v}{D t} = \rho g_y - \frac{\partial p}{\partial y} + \mu \nabla^2 v \quad (3.9)$$

$$\rho \frac{D w}{D t} = \rho g_z - \frac{\partial p}{\partial z} + \mu \nabla^2 w \quad (3.10)$$

3.1 Reynolds-Averaged Navier-Stokes (RANS) Model

The hydrodynamics of the model were solved by implementing the Reynolds Averaged Navier Stokes (RANS) equations. The closure of the turbulence variables were solved by using a turbulence k-ε model. Reynolds-averaging is used to average the turbulent effects and calculate a mean flow condition. This method separates the mean flow from the turbulent velocity fluctuations. Instantaneous velocities are defined as:

$$\mathbf{u} = \bar{\mathbf{u}} + \mathbf{u}' \quad (3.11)$$

Where the instantaneous velocity equals the mean velocity ($\bar{\mathbf{u}}$) plus the deviation from that average (\mathbf{u}'). Applying Reynolds-averaging to equations 3.8 through 3.10, the RANS equations can be expressed as:

$$\rho \frac{D \bar{u}}{D t} = \rho \bar{g}_x - \frac{\partial \bar{p}}{\partial x} + \mu \nabla^2 \bar{u} - \frac{\partial \overline{u'u'}}{\partial x} \quad (3.12)$$

$$\rho \frac{D \bar{v}}{D t} = \rho \bar{g}_y - \frac{\partial \bar{p}}{\partial y} + \mu \nabla^2 \bar{v} - \frac{\partial \overline{v'v'}}{\partial y} \quad (3.13)$$

$$\rho \frac{D \bar{w}}{D t} = \rho \bar{g}_z - \frac{\partial \bar{p}}{\partial z} + \mu \nabla^2 \bar{w} - \frac{\partial \overline{w'w'}}{\partial z} \quad (3.14)$$

Three terms are derived from the fluctuation terms and are known as turbulent stresses or Reynolds stresses. A turbulence model is required to solve for the Reynolds stresses thus closing the system of equations. The k- ϵ turbulence model was used in this project.

3.2 k- ϵ turbulence model

As stated in the FLUENT theory manual (section 4.4.1 Standard k- ϵ model), the Reynolds stresses can be represented in terms of an eddy viscosity, μ_T , as:

$$\tau_{ij} = -\mu_T \left(\frac{\partial u_i}{\partial x_j} + \frac{\partial u_j}{\partial x_i} \right) \quad (3.15)$$

where k is the turbulent kinetic energy (TKE), δ_{ij} is the Kronecker delta matrix, and eddy viscosity is expressed as:

$$\mu_T = C_\mu \rho k^2 / \epsilon \quad (3.16)$$

where ϵ is the turbulent dissipation rate (TDR) and C_μ is a constant. The standard k- ϵ turbulence model solves for k and ϵ using the following equations:

$$\frac{dk}{dt} = G_k - \epsilon \quad (3.17)$$

$$\frac{d\epsilon}{dt} = G_\epsilon - \epsilon^{3/2} / L \quad (3.18)$$

where G_k represents the production of TKE due to the mean velocity gradients as:

$$G_k = \rho \overline{u_i' \frac{\partial u_i}{\partial x_j} \frac{\partial u_j}{\partial x_i}} \quad (3.19)$$

and G_b represents the generation of TKE due to buoyancy as:

$$G_b = \beta g \overline{u_i' \theta'} \quad (3.20)$$

where Pr_t is the Prandtl number for energy, g_i is the component of the gravitational vector in the i th direction, and β is the coefficient of thermal expansion, defined as:

$$\beta = -\frac{1}{\rho} \left(\frac{\partial \rho}{\partial T} \right)_p \quad (3.21)$$

The standard k- ϵ coefficients recommended by FLUENT were used in this study:

3.3 The Energy Equation

FLUENT is able to couple the energy equation with the hydrodynamics and species transport models, thus being able to take into account the changing temperatures throughout the model. FLUENT solves the energy equation in the following form:

$$\rho \frac{dE}{dt} + \nabla \cdot (\rho \mathbf{u} E) = \nabla \cdot (\mathbf{k} \nabla T) - \nabla \cdot (\sum_j \rho_j \mathbf{u}_j h_j) + \rho \epsilon \quad (3.22)$$

where \mathbf{k} is the effective conductivity, $\rho_j \mathbf{u}_j h_j$ is the diffusion flux of the species, caused by a gradient in the species concentration and temperature, expressed as:

$$-\rho_j \mathbf{u}_j h_j = -D_m \nabla c_j - D_t \nabla c_j \quad (3.23)$$

where D_m is the molecular diffusivity and D_t is the turbulent diffusivity. Sc_t is the turbulent Schmidt number. The default value of Sc_t in FLUENT is 0.7. In turbulent flows, D_t is generally much larger than D_m and accounts for the vast majority of the diffusion.

ϵ is the effective viscous dissipation, defined as:

$$\epsilon = \mu \nabla^2 \mathbf{u} \cdot \nabla \mathbf{u} \quad (3.24)$$

where μ is the effective viscosity.

E is the total energy, and defined as:

$$E = \frac{1}{2} \mathbf{u} \cdot \mathbf{u} + \sum_j c_j h_j \quad (3.25)$$

where sensible enthalpy h_j , is defined as:

$$h_j = \int_{T_{ref}}^T c_p^j dT \quad (3.26)$$

where c_j is the mass fraction of the species j and c_p^j is defined as:

$$c_p^j = \sum_k c_k^j c_p^k \quad (3.27)$$

where T_{ref} is 298.15 K.

3.4 Species Fate and Transport

FLUENT models mixing and transport of a species by solving for species conservation based on diffusion and convection of the species mass fraction. This capability can be used in conjunction with the hydrodynamic solver to calculate a species

concentration at any given time, thus allowing one to simulate the concentration over time.

The governing equation for species conservation is:

$$\frac{dY}{dt} + \nabla \cdot (\rho Y \mathbf{u}) - \nabla \cdot (\rho D \nabla Y) = S_Y \quad (3.28)$$

where Y is the species mass fraction, and \mathbf{u} is the turbulent diffusion flux.

3.5 Volume-weighted-mixing-law

The standard density function, when dealing with multiple elements, is the ideal gas law. When dealing with a non-ideal gas mixture, density is defined by the following function:

$$\rho = \sum_i Y_i \rho_i \quad (3.29)$$

where Y_i is the mass fraction and ρ_i is the density of species i .

3.6 Solution Methods

FLUENT has various standard discretization options when solving the complex computational model. The pressure-velocity coupling discretization method used in this model was SIMPLE. The spatial discretization methods were as follows: gradient – Green-Gauss cell based; pressure – STANDARD; momentum, TKE, TDR, energy, and species transport were solved using a 1st order upwind stepping method. The model was set to solve for the 1st order implicit solution. The frozen flux formulation was used in this study.

3.6.1 Summary

This chapter presented the governing equations that were used to model the hydrodynamics, turbulence, energy, and species transport of each project scenario. Chapter 4 will present the physical model area and the numerical boundary conditions that were resolved by the numerical equations.

CHAPTER 4: CFD MODEL SIMULATION SETUP

The LWSC is a complex water system. Detailed descriptions of the various key features affecting the LWSC are discussed. The numerical boundary conditions and parameters that went into the 3D CFD model are presented.

4.1 Physical Description

4.1.1 General Layout

Figure 4.1 shows a general map of Seattle (courtesy of Google Earth). Water flowing through Lake Washington serves as the main inflow into the LWSC at Montlake Cut. Water flows through the canal, through Lake Union, and finally flows out into Puget Sound through the Ballard Locks. Lake Washington and its tributaries are all fresh water habitats. Puget Sound is a large estuarine sound branching off the Pacific Ocean. The water exchange that takes place at the Ballard Locks allows salty water to diffuse into the LWSC. The Seattle District closely monitors the salt water wedge that forms and migrates upstream through the canal because of state legislation standards set in the “Water Quality Standards For Surface Waters Of The State Of Washington” chapter 173-201A (WAC 173-201A). WAC 173-201A states that the state of Washington “imposes a special condition on the Ship Canal from the Ballard Locks to Lake Washington such that salinity shall not exceed one part per thousand (1.0 ppt) at any point or depth along a line that transects the Ship Canal at the University Bridge.” (Department of Ecology, State of Washington, 2006).

4.1.2 Lake Washington Ship Canal (LWSC)

The LWSC is the stretch of water that connects Puget Sound to Lake Washington (see Figure 4.1). The USACE is responsible for maintaining lake water levels as well as controlling the water quality for fish passage. The LWSC begins at the Ballard Locks and ends where the Montlake Cut opens up into Lake Washington. The LWSC is

approximately 13.8 km (8.6 miles) long (Celedonia, 2009). The canal contains several bodies of water, including: Salmon Bay, Lake Union, and Portage Bay (see Figure 4.2). Historically Salmon Bay and Lake Union branched off of the Puget Sound estuary. When the Ballard Locks blocked Salmon Bay from Puget Sound the water rose and the area became mostly a fresh water habitat. The canal does serve as an acclimation zone for fish traveling between the fresh and salty waters.

4.1.3 Lock and Dam

The Ballard Locks and Dam have several main features: the large and small locks, the smolt flumes and spillways, the salt water drain, and the fish ladder.

4.1.3.1 Large Lock

The large lock is 80 feet wide, 825 feet long, and about 50 feet deep (Seattle Public Utilities, 2008). The large lock has two sections; an upper and a lower chamber (see Figure 4.3 through Figure 4.5). The two chambers allow for quicker locking when only half of the entire lock area needs to be filled. The large lock is filled/drained through the filling culverts that run along either side of the lock chamber. The large lock is mainly used for commercial boats.

The Large Lock is the dominate source of salt water entering the LWSC, it also serves as a passage way for migrating fish to travel past the lock and dam complex. The two filling culverts are 14 feet high by 9 or 14 feet wide (Seattle Public Utilities, 2008). The filling culverts are cleaned seasonally to remove the barnacles that are known to grate off the scales of fish traveling through these highly turbulent chambers (Seattle Public Utilities, 2008).

The large lock has a floating wall that comes up from the bed, which is typically used unless there is an extremely deep-drafting boat or if the floating wall is under repair. The wall helps hold back denser salt water from flowing into the LWSC unnecessarily.

4.1.3.2 Small Lock

The small lock is 30 feet wide, 150 feet long, and over 16 feet deep (Seattle Public Utilities, 2008). The small lock has one section, unlike the large lock (see Figure 4.3 through Figure 4.5). The small lock is used mainly to accommodate non-commercial or small boats. The small lock also serves as a passage way for migrating fish, but at a much smaller level.

4.1.3.3 Smolt Flumes and Spillways

There are six spillways that span the 235 feet between the small lock and the southern canal edge. Four smolt flumes are located in 2 spillway sections. The smolt flumes are paired such that each spillway section has two smolt flumes. In the center of each spillway is a 12 foot section that passes water into the smolt flumes (see lock design drawings in Figure 4.6 and Figure 4.7). The majority of the water is filtered off to the sides of the flumes, allowing fish and water to travel through the flumes at a safe speed (Seattle Public Utilities, 2008). The smolt flumes were designed to improve fish passage for juvenile salmon moving downstream, past the locks. Depending on spring runoff and lake levels, the smolt flumes are only in operation in the early spring through mid-summer. For this project, various scenarios include smolt flume flow, where other scenarios do not. The hypothetical June scenario puts a floating wall in the forebay of the dam. The hope is that water will be forced to flow under the wall, pulling up cooler water up in front of the smolt flumes. As the surface warms up through the summer smolts begin to find exits that are cooler than the smolt flumes. If the floating wall can extend the time period when cooler water flows through the smolt flumes, it is possible that smolts will use this migration route later into the summer.

4.1.3.4 Salt Water Drain

The salt water drain (SWD) is located between the large and small locks, directly south of the eastern-most edge of the pier that separates the two locks (see Figure 4.5 and

Figure 4.8). The SWD has a box entrance that is 48 feet wide by 4 feet high (Seattle Public Utilities, 2008). The drain was created to help control salt water intrusion in the canal. After water flows into the SWD it is split and sent in two directions. A large portion is sent to a diffuser well that services the fish ladder. The rest of the flow spills directly into the tailrace of the dam.

4.1.3.5 Fish Ladder

The fish ladder was designed to help adult salmon move upstream past the dam. There are 23 sections to the fish ladder, 5 sections have adjustable weirs that help with the fish passage during varying tide heights. The fish ladder receives a constant discharge of 23 cfs. On average 160 cfs flows from the SWD to a diffuser well next to the fish ladder where the water is pumped into the ladder to help attract migrating salmon, as well as help the salmon acclimate to the fresh water conditions in the forebay of the dam.

4.1.4 Water quality collection stations

Various water quality collection stations have been installed throughout Puget Sound, the LWSC, and Lake Washington and have collected water quality data in some cases for several decades. The Army Corp of Engineers (ACOE), King County, and other agencies have vested interests in the water quality of the area. The management practices at the lock and dam are directly affected by the water quality data that is collected in the canal. Salt concentration, dissolved oxygen (DO) levels, and water temperatures are of specific concern. Salt concentrations flowing upstream past University Bridge are under state law (WAC 173-201A) that they cannot exceed one part per thousand (1.0 ppt) (Department of Ecology, State of Washington, 2006). As mentioned in chapter 2, dissolved oxygen and temperature levels can greatly affect the movement patterns of the migrating salmon. When water temperatures or DO levels get below accepted levels for fish, an influx of water from Puget Sound can increase DO

levels and drop water temperatures back to safer levels. Figure 4.9 shows the locations of water quality collection stations that are located inside the LWSC. Data collected from these stations was used to help validate the water quality in the CFD models that were created.

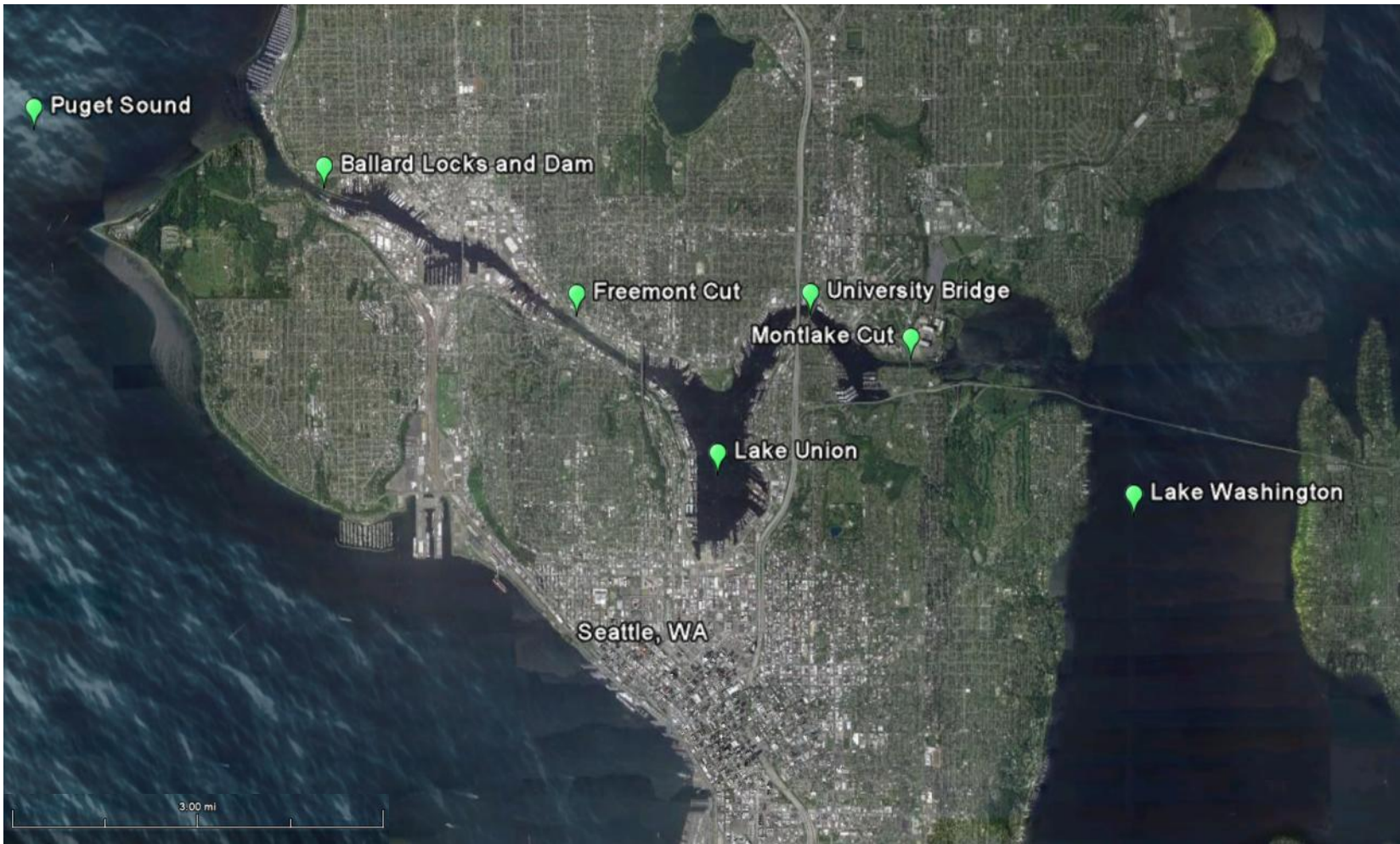


Figure 4.1 General Map of Seattle (Google Earth)



Figure 4.2 Features of the LWSC (Seattle Public Utilities, 2008)

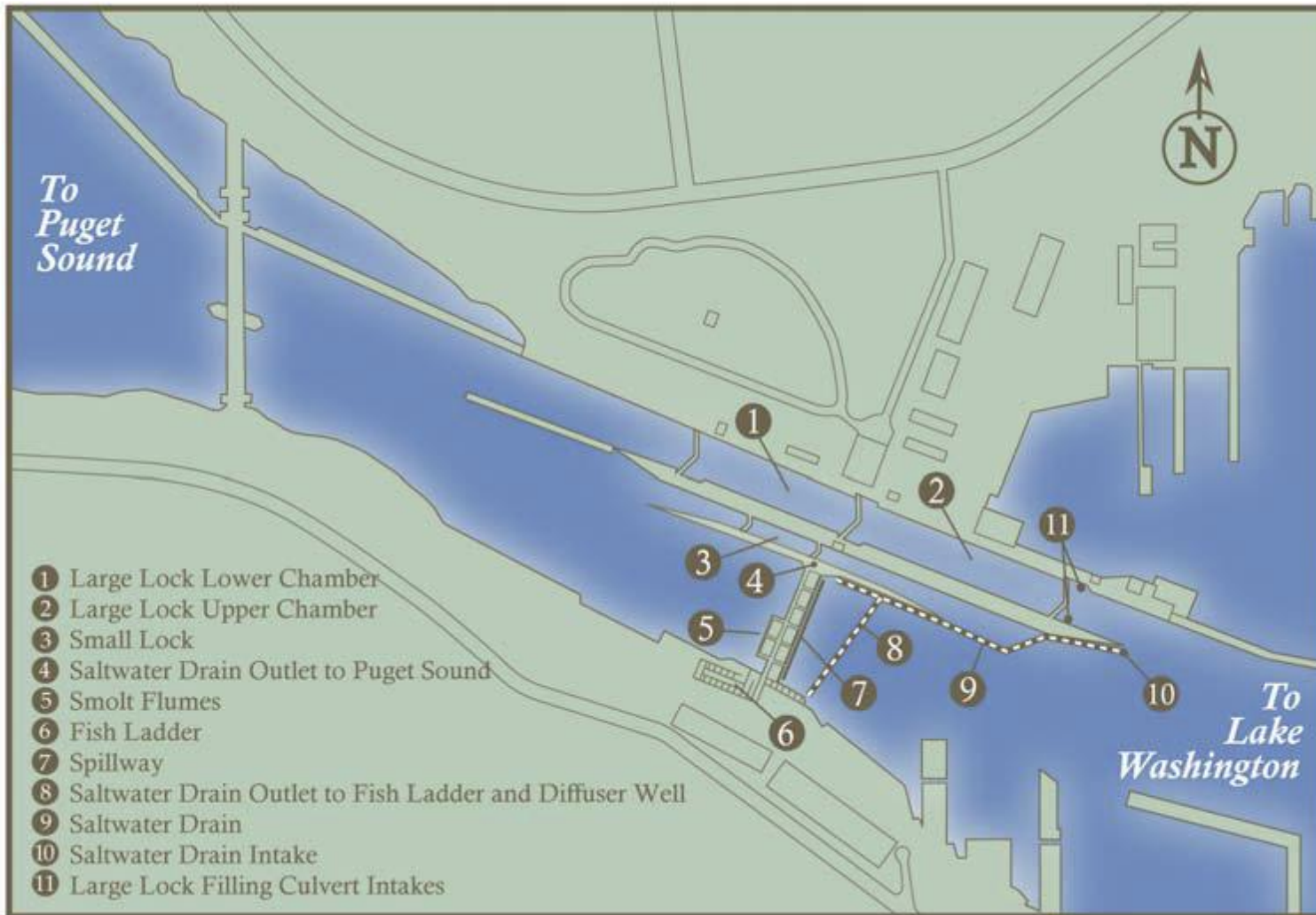


Figure 4.3 Major Physical Features of the Locks (Seattle Public Utilities, 2008)

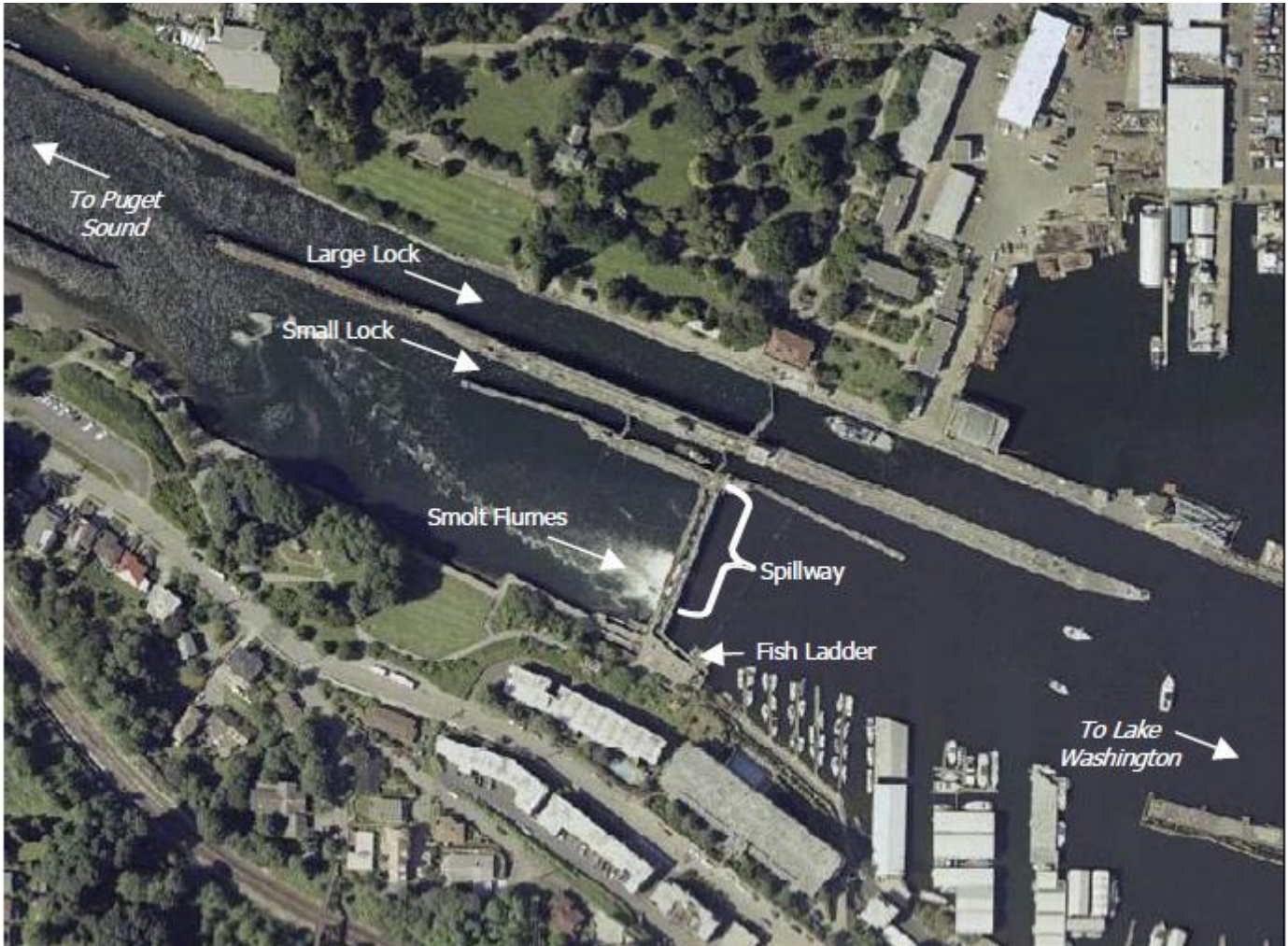


Figure 4.4 Major physical features of the Locks. Large lock chamber upper and lower gates are open and middle gate is closed. Small lock chamber is closed. Smolt flumes are operating (Seattle Public Utilities, 2008)

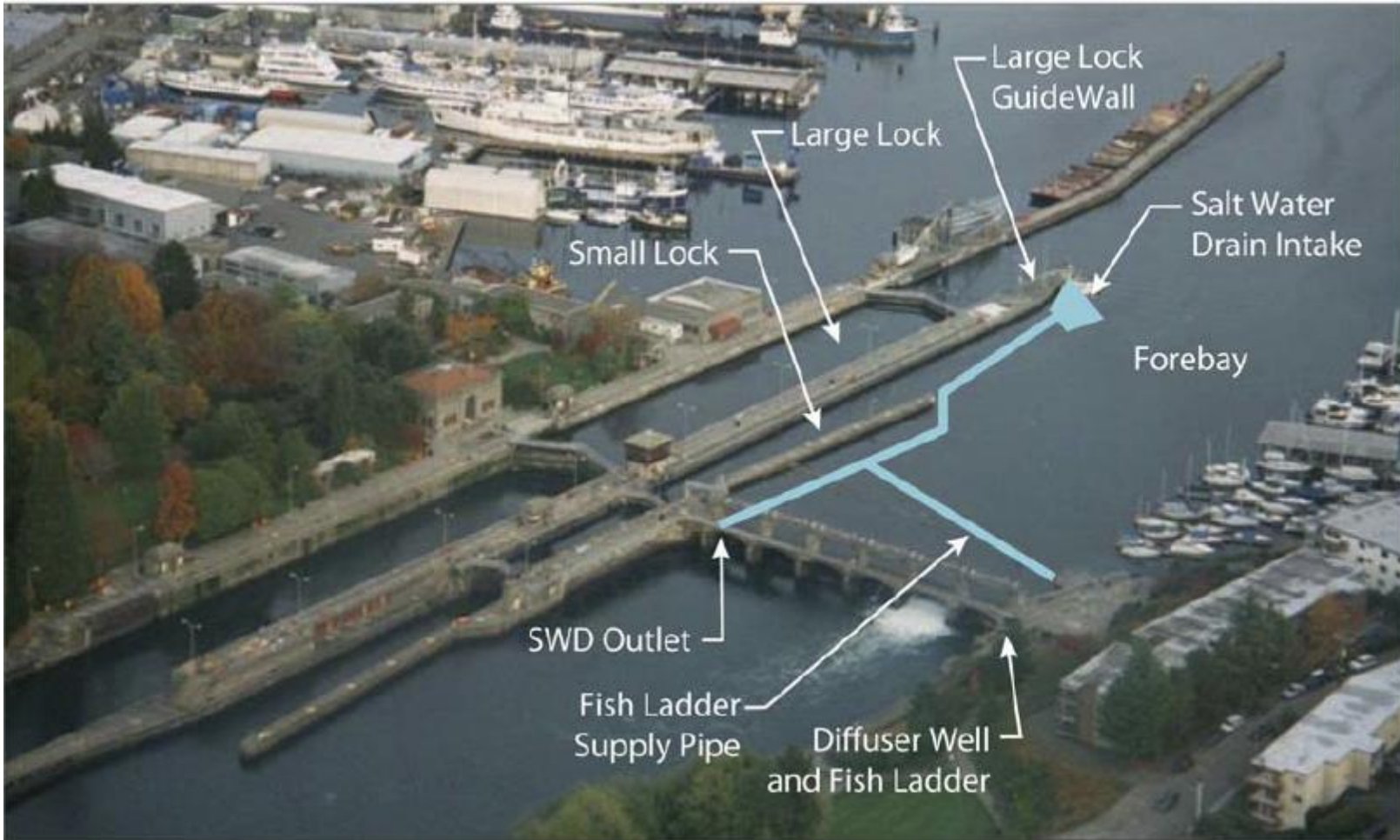


Figure 4.5 Saltwater drain, showing outlet to Puget Sound and pipe to fish ladder (Seattle Public Utilities, 2008)

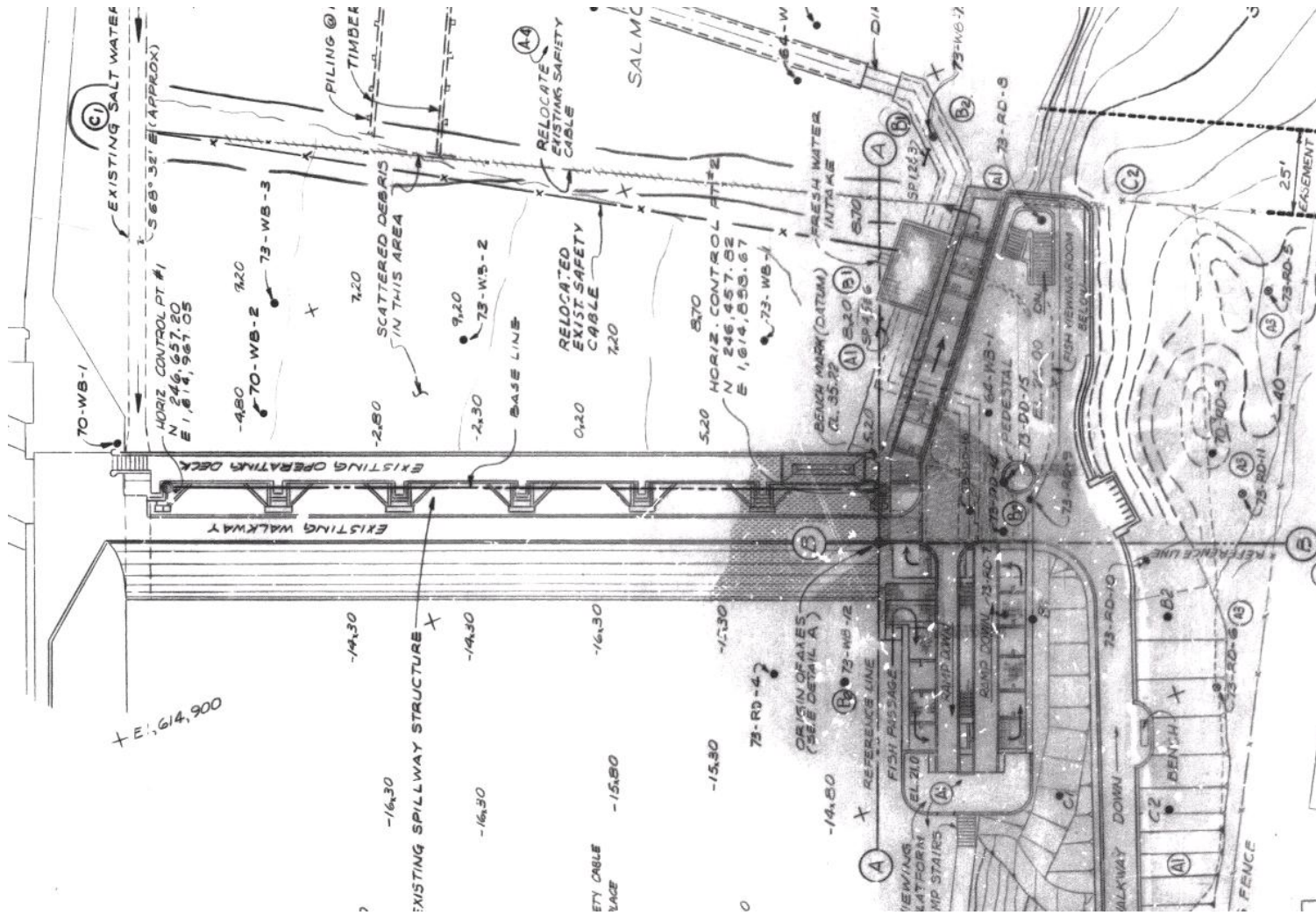


Figure 4.6 Plan view of Ballard Locks spillway and fishladder , courtesy of Lynne Melder, Seattle District

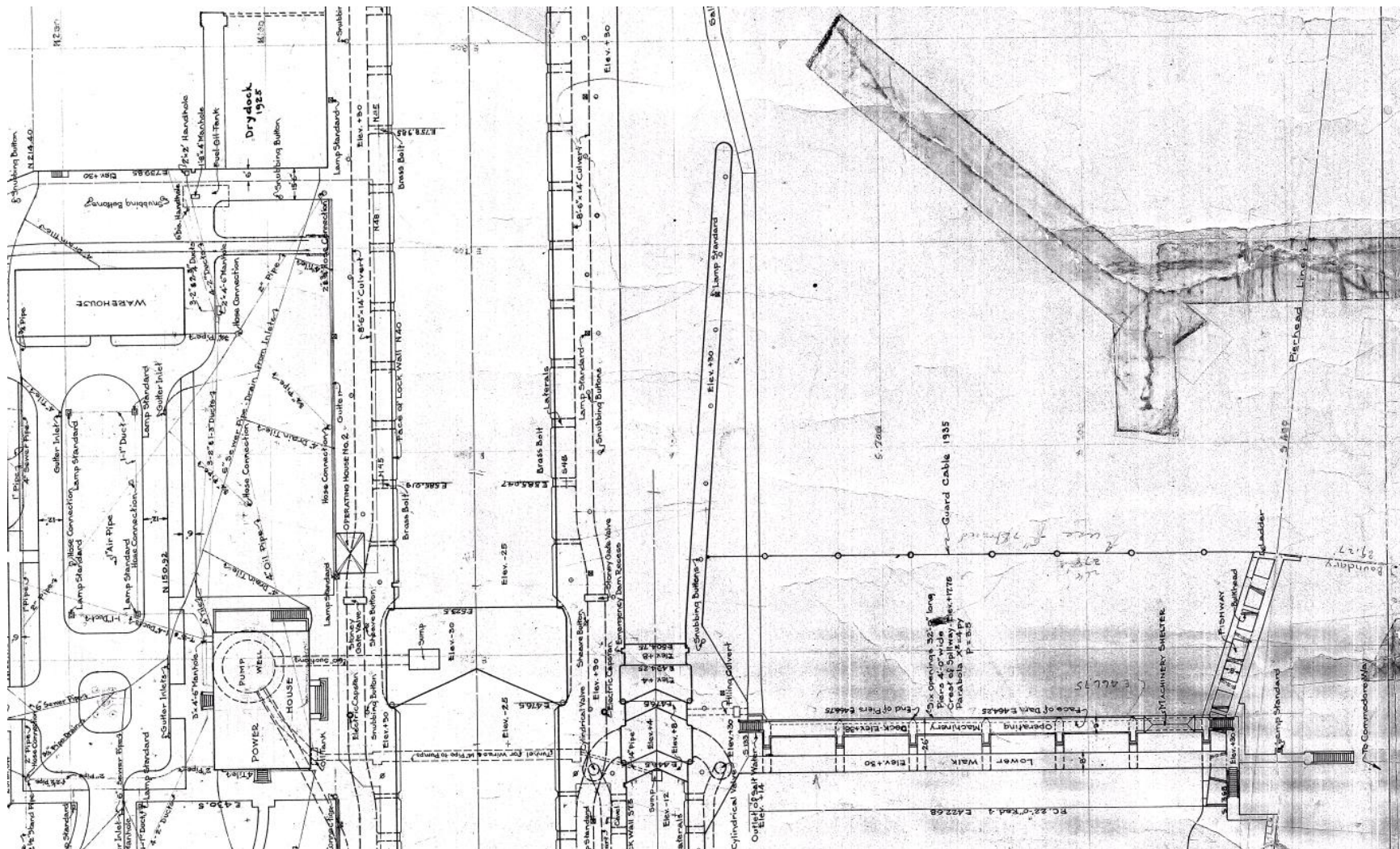


Figure 4.7 Plan view of Ballard Locks, courtesy of Lynne Melder, Seattle District

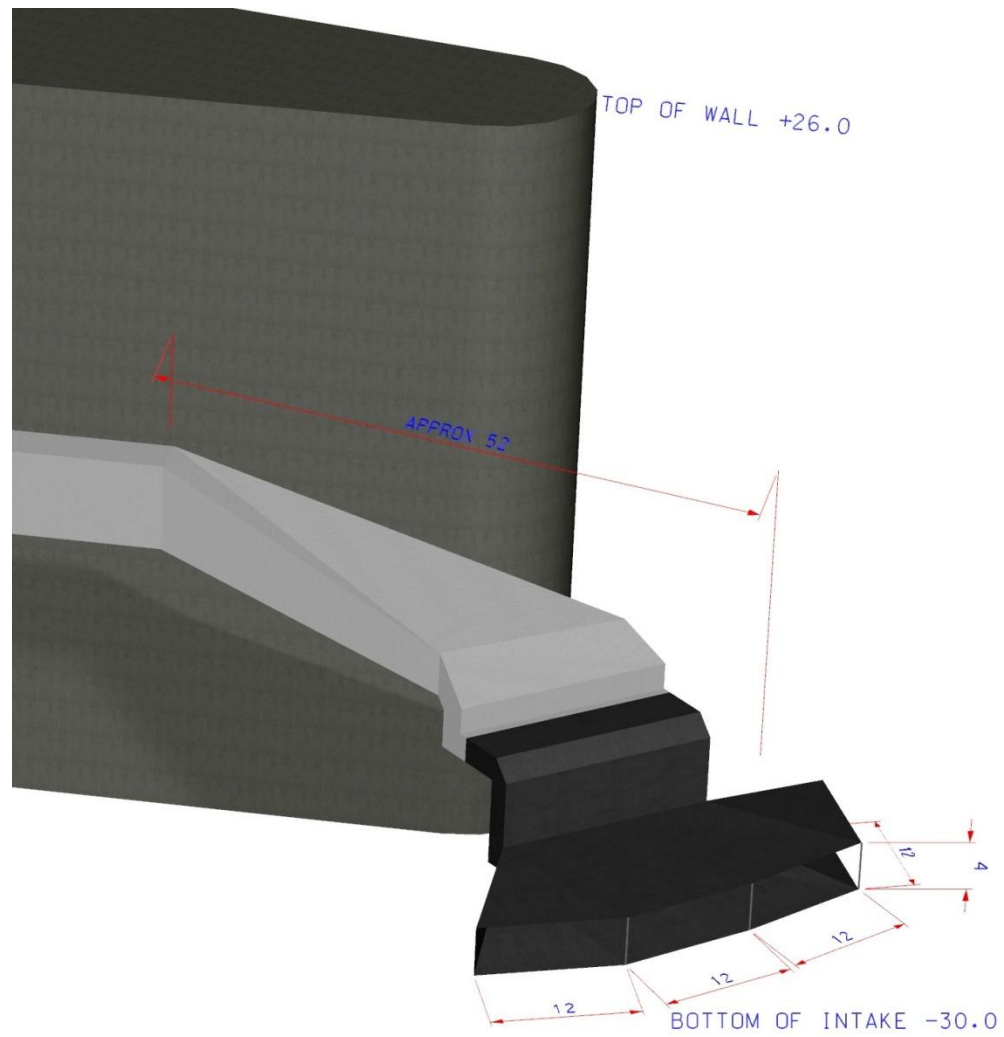


Figure 4.8 Isometric view of SWD, courtesy of Lynne Melder, Seattle District

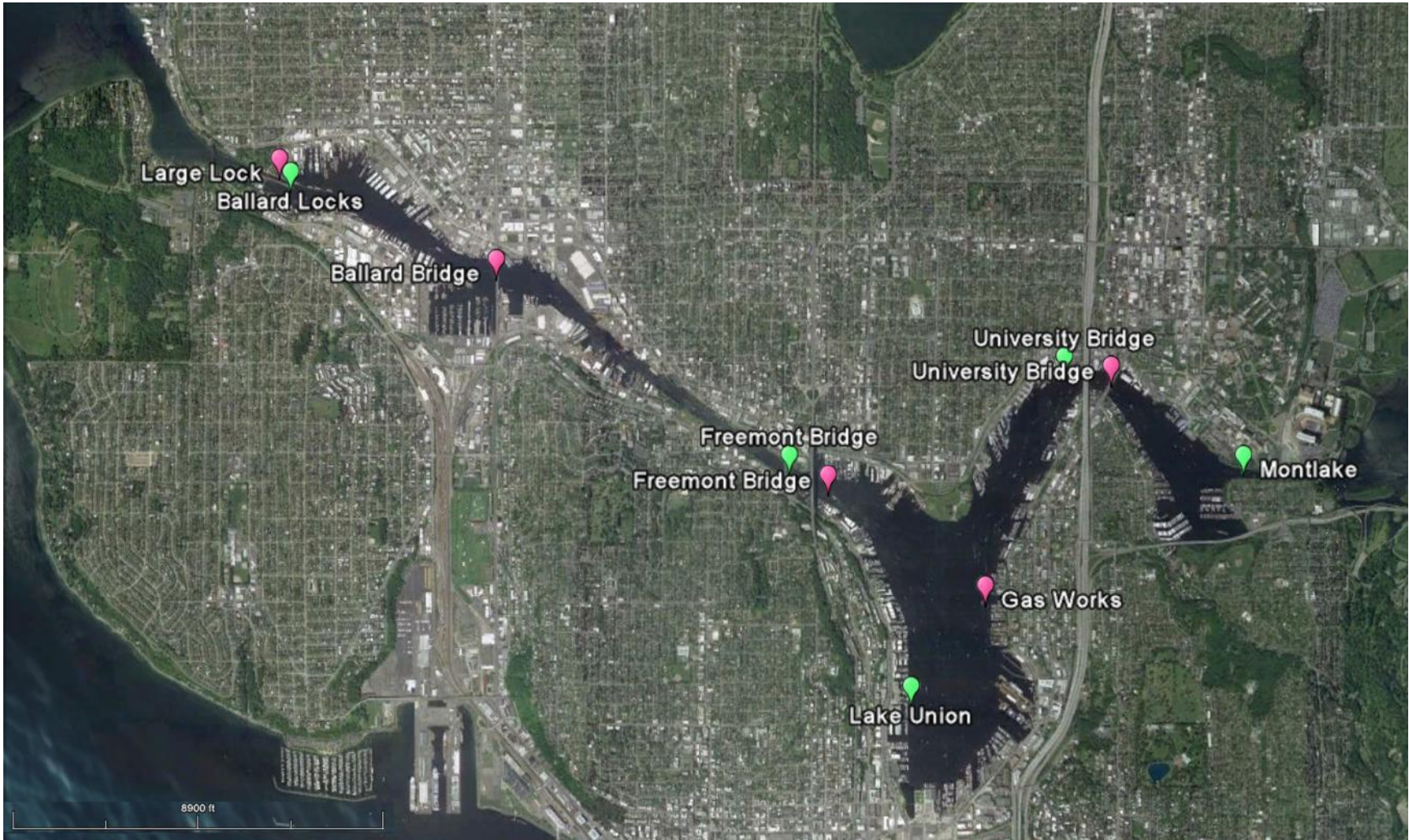


Figure 4.9 Water quality data collection stations. ACOE (Pink), King County (Green)

4.2 Numerical Description

FLUENT applies the numerical methods described in chapter three to a finite volume mesh that is imported into FLUENT. This section presents the construction of the mesh and the boundary conditions that were applied in FLUENT.

4.2.1 Mesh Generation

GRIDGEN version 15.0 computational mesh generation software was used to develop the mesh that was used by FLUENT to analyze the LWSC system. The entire model contains a structured mesh. This was much more labor intensive than creating an unstructured mesh, however the model was much more stable and able to converge quicker with the structured mesh. Creating structured blocks also allows for better control in mesh density. The blocks near the dam have a much higher mesh density than the blocks further out in the canal or in Lake Union. The total mesh consisted of approximately 1.81 million nodes and 1.66 million block elements. The mesh density in the majority of the canal was kept fairly coarse to help speed up the simulation time required. Future work could include creating a denser mesh.

The June mesh and August mesh are slightly different. Based on Figure 4.15 the June water surface was set to 21.8 feet and the August water surface was set to 20.8 feet. The first two scenarios therefore have the same number of nodes and block elements as mentioned above. The surface of the third and fourth scenarios was one foot higher than the August mesh. The fourth scenario also included an impermeable wall near the spillways. These minor changes slightly increased the overall number of nodes and block elements in their respective model scenarios.

The mesh size is a very difficult parameter to correctly scale. As the mesh becomes finer the solution will become more accurate; however, the computational time needed to resolve the model can increase exponentially. Due to the large scale of our model, we were limited on how dense the mesh could be to resolve the model in a

practical time frame. Figure 4.16 shows the final mesh overlaid on GoogleEarth. As shown in the figure, the mesh covered the key elements of the actual LWSC.

4.2.1.1 Constructing the mesh in steps

The mesh that was used in this project was created in steps. First, the lock and dam was reconstructed by examining an older model that was used by SK Ooi (see Figure 2.1). The main LWSC bathymetry was constructed from University of Washington bathymetric data collected in 2000 (see Figure 4.10). Using ArcGIS, the data was converted to the Seattle District lock datum and imported into Tecplot (see Figure 4.11). The lock datum is exactly the same as NAD 27 state plane zone 4601 with a slight vertical adjustment. This vertical adjustment was based off Figure A.1 in the appendix. Various bathymetric surveys of the LWSC have been done over the years, their datums and vertical reference frames were all adjusted to help determine that the University of Washington 2000 survey was the most accurate and useful map to construct the project mesh (based on emails sent on August 19, 2010).

4.2.2 Boundary Conditions

FLUENT requires boundary conditions to accurately solve for a solution. The boundary conditions are the physical characteristics of the system in question. The following sections explain the boundary conditions that were used at the various zones of the various model scenarios that were generated in FLUENT.

4.2.2.1 Mass Flow Inlet

The average flow coming into the LWSC varies over the year and is completely determined by snow melt throughout Lake Washington's contributing watershed. The two periods of the year that were modeled ran flows of 390 cfs (11,048 kg/s) for June 2007 and 313 cfs (8,863 kg/s) for August 2000. To maintain the mass balance, when high outlet velocities were imposed to simulate the filling of a lock, the inlet mass flow

rate was adjusted to account for the change. These changes are included in Tables A.3 to A.8 in the appendix.

4.2.2.2 Walls

The channel bed, dam face, small pier, medium pier, large pier, and river walls, were all treated as fixed no-slip walls.

4.2.2.3 Diffusive Walls

The large and small lock gates were treated as no-slip walls in the model. This means that no hydrodynamic fluxes were modeled moving in or out of the locks. The walls were given a salt concentration of 19 ppt and a wall temperature of 53.6°F (285.15°K) for a typical June 2007 day and 57.2°F (287.15°K) for a typical August 2000 day. Modeling diffusion, a salt wedge was formed and flowed up the LWSC. It is important to note that the locks were not constantly diffusing salt. To simulate the opening of the locks a FLUENT user defined function (UDF) was written to change the wall salt concentration from 0 ppt to 19 ppt each time the lock was considered open. Summary Tables A.3 through A.8 in the appendix shows the 15 minute intervals when the locks were open or closed.

4.2.2.4 Free Surface

The free surface was treated as a zero shear wall. This allows the air/water heat transfer relationship to be established while maintaining a zero flux wall for all other parameters. The coefficient of heat transfer between air and water can be between 10 and 100 W/m², our model assumed 50 W/m² (Rohsenow, 1998). The air temperature was held constant at 60°F (288.71°K) for a typical June 2007 day and 63.7°F (290.76°K) for a typical August 2000 day.

4.2.2.5 Outlets

To simplify the model, zero losses were assumed between the mass flow inlet and the various outlets. The smolt flumes, spillways, large and small lock filling culverts, salt water drain, and fish ladder cumulatively equaled 100% of the outflow of the system. Due to the UDFs that adjusted the flow percentages each time the filling culverts were opened, the actual outflow percentages of each outlet during the different model scenarios are shown in 15 minute increments in Tables A.3 through A.8 in the appendix.

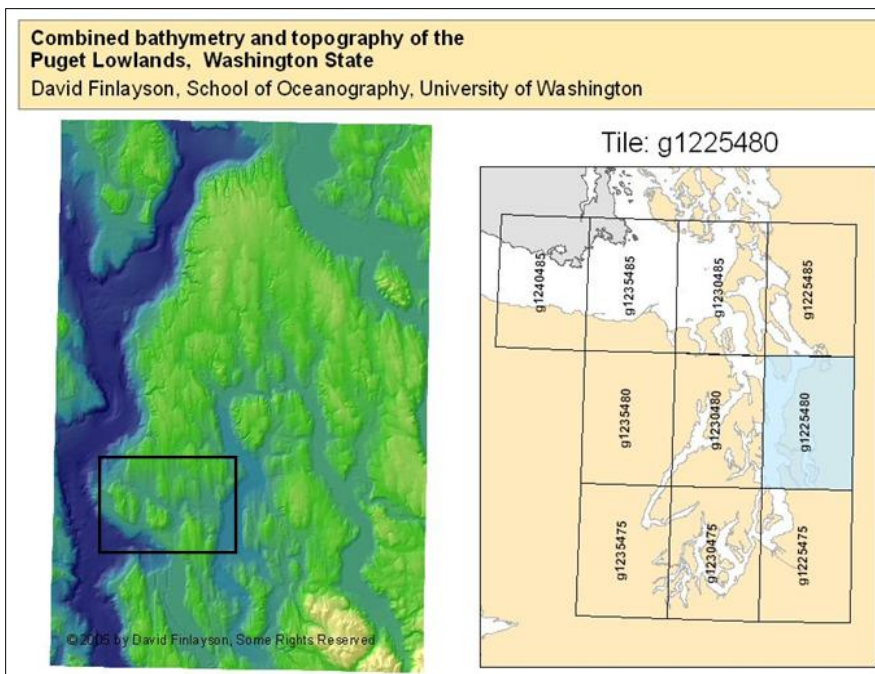


Figure 4.10 Combined bathymetry and topography of Seattle Washington area, University of Washington

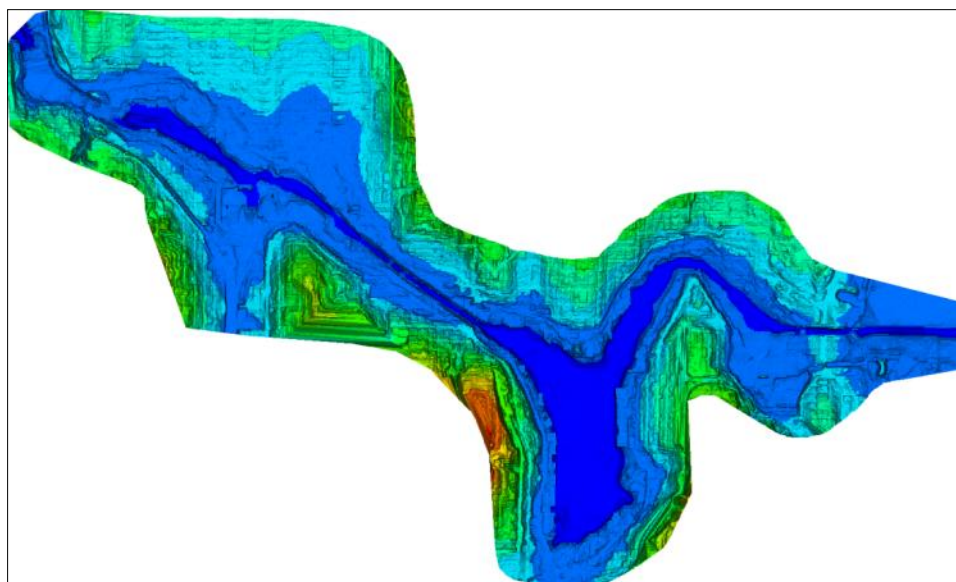


Figure 4.11 ArcGIS cut bathymetry

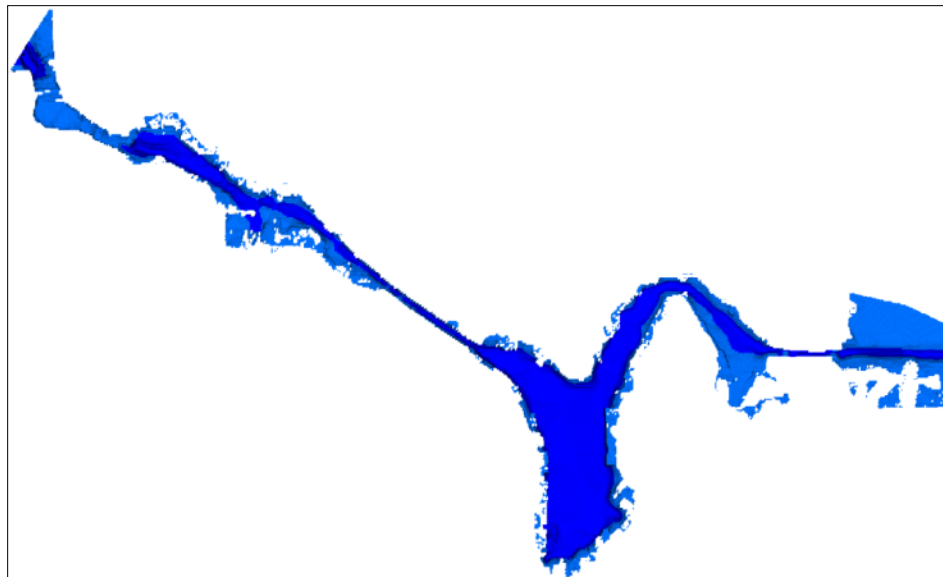


Figure 4.12 Bathymetry used to create mesh river bed



Figure 4.13 Mesh of LWSC Model

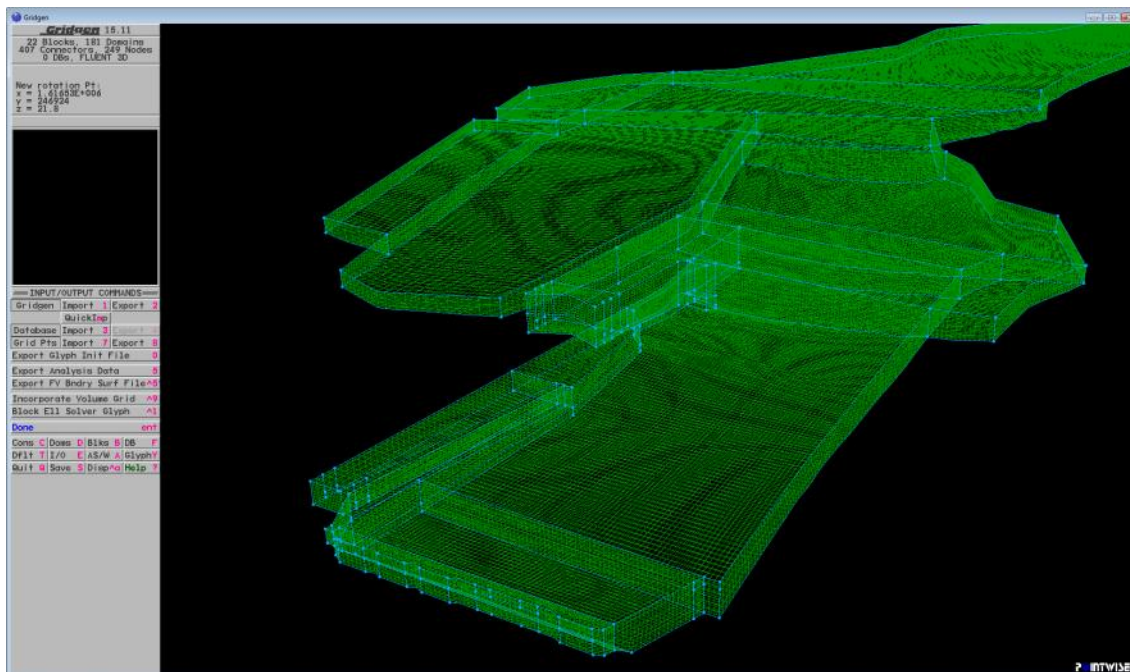


Figure 4.14 Mesh of LWSC Model – Close up of Ballard Locks

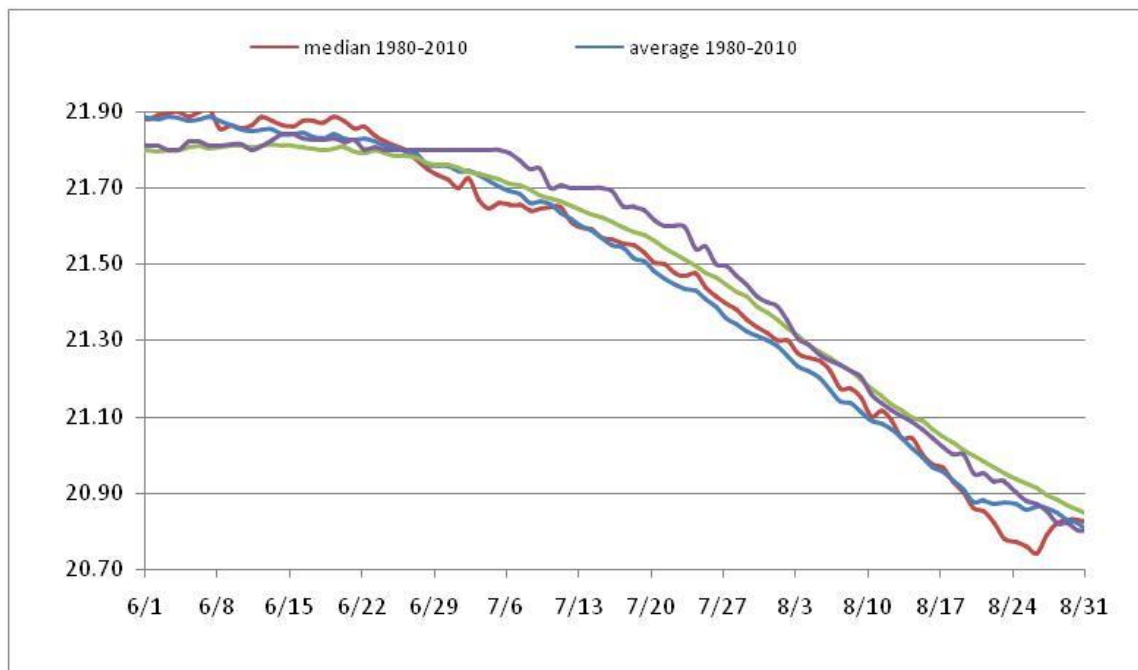


Figure 4.15 Water surface elevation in the LWSC



Figure 4.16 Model overlaid on GoogleEarth

4.3 Methods, and Controls

4.3.1 Mesh dependency test

Early on in the project various mesh densities were compared to make sure that the final mesh density would produce an accurate result, independent of the mesh size. The mesh around the lock and dam was kept dense throughout the tests; while the rest of the canal was adjusted several times to capture the best mesh density to use. To keep the entire mesh structured, the number of nodes on the base and the height of the canal were kept the same as those in the dense lock and dam area. The number of nodes along the length of the canal were changed four times and the structure of the salt plume was compared in each case.

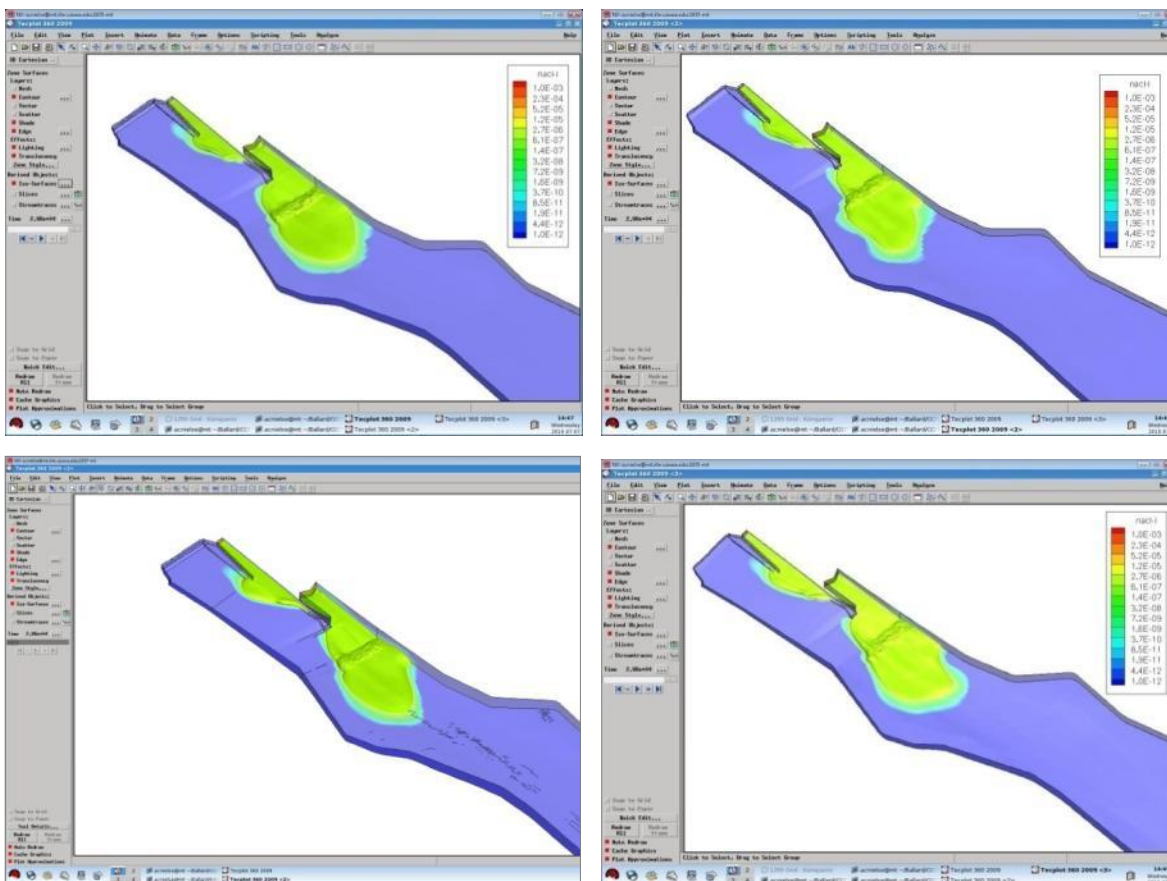


Figure 4.17 Top Left: 1000, Top Right: 1250, Bottom Left: 1500, Bottom Right: 2000

Each scenario was numbered based on the total number of nodes along the length of the canal. After eight hours of iterations Figure 4.17 showed that, for the work being done, any of these meshes would be sufficiently dense to address the questions being asked. When looking at the time it took to iterate each of the different mesh sizes it became clear that using the 1500 mesh would be the most advantageous. As shown in Table 4.1, this mesh was selected because it was the highest density mesh that was able to still iterate quickly. Figure 4.18 is a visual of this table and reiterates why the 1,500 mesh density for the length of the canal was used.

Table 4.1 Mesh density vs. iteration time

Mesh Density	Time between 15 minute save intervals
1000	11 minutes
1250	12 minutes
1500	15 minutes
2000	30 minutes

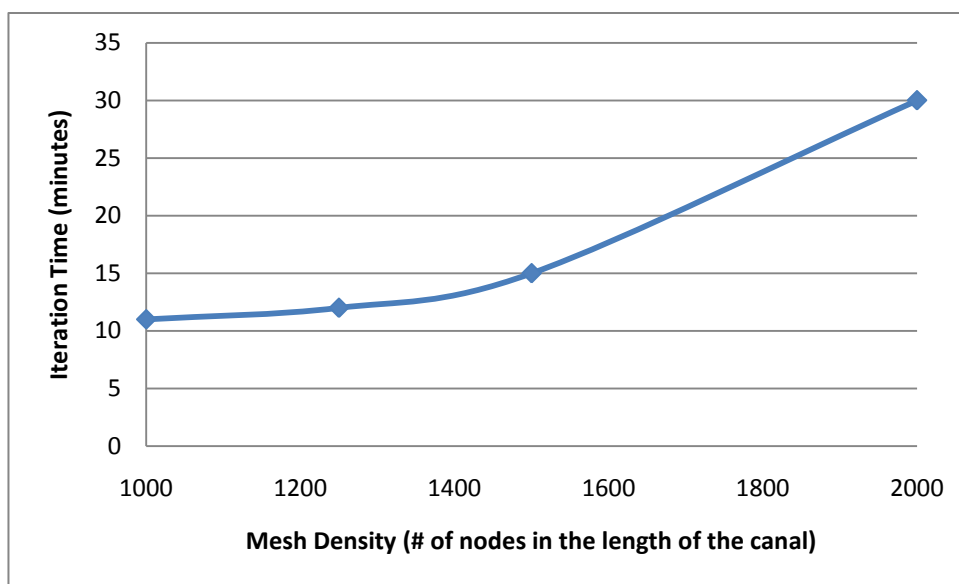


Figure 4.18 Mesh density vs. iteration time

The final mesh used for the project was much more detailed than the preliminary mesh that was used for the GDT. However, the density of the mesh along the main canal was kept at 1,500 nodes. When details such as Salmon Bay and Lake Union were added, the mesh density was kept consistent with past models to ensure that the GDT still held.

4.3.2 Time-step dependency test

The time-step dependency test was also done on the preliminary model. Time-step sizes of 1, 5, 10, and 20 seconds were selected for this test. Both the 10 and 20 second models crashed before being able to converge. In hindsight, these time-step sizes were too large to start with, but it might have been possible to ramp up to these step sizes once the model had begun to converge. The 1 and 5 second models both ran smoothly, the 1 second model converged the fastest.

A secondary time-step dependency test was done as the final model was being prepared. In this case the time-step size was ramped up from 1 second to 10 seconds in steps (see Table 4.2). After the model converged using 1 second time-steps, the time-step was bumped up to 2, then 4, 5, 6, 8, and finally 10 seconds. Observing the convergence of the model, up to the 5 second time-step, the model converged quickly and used only 2 internal iterations to solve each time-step. Above the 5 second time-step size, the model required much more internal iterations to converge inside each time-step. Comparing the time-step size to the number of internal iterations required to solve each time-step gave a ratio, that can essentially be thought of as the speed of the model (seconds per iteration). Figure 4.19 shows that using a 5 second time-step gave the fastest running model.

The final model ran 5 second time-steps on a mesh that maintained a mesh density very similar to the 1500 mesh used in the GDT. These parameters were used assuming that they would create the optimum mesh for the project.

Table 4.2 Computational speed

Time-step (sec)	# of Internal Iterations per time-step	Time per iteration
1	2	0.5
2	2	1
4	2	2
5	2	2.5
6	3	2
8	5	1.6
10	7	1.4

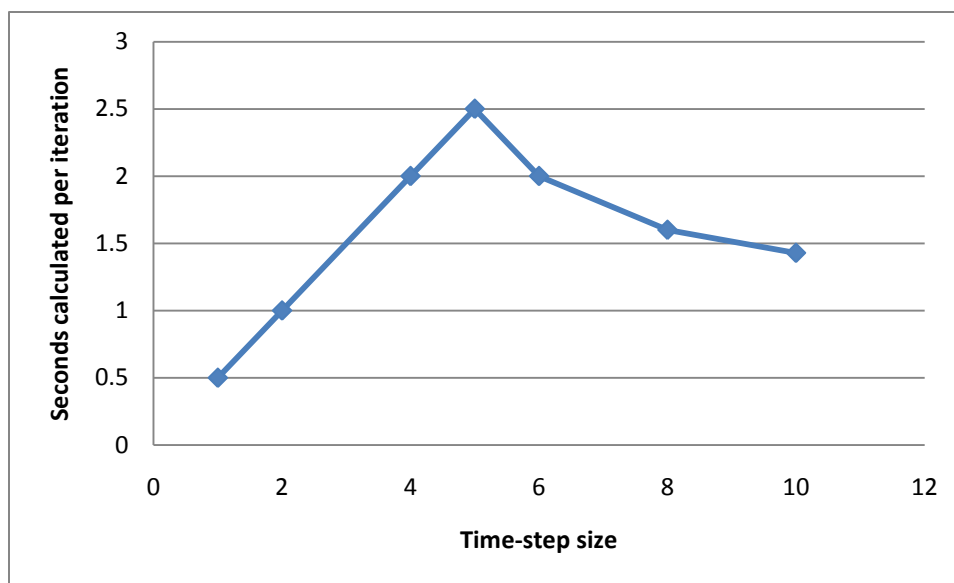


Figure 4.19 Computational speed

4.3.3 Summary

This chapter presented the development of the physical model area. The process used to develop and determine the best numerical boundary conditions was also discussed. Time and grid dependency studies were done to determine the best conditions

to use in the setup of each project scenario. The results from the four project scenarios are presented in Chapter 5.

CHAPTER 5: RESULTS AND DISCUSSION

5.1 Project Development and Evolution

The four model scenarios that were ran for this project were relatively small in magnitude compared to the effort of the various approaches that were taken in trying to solve for the most accurate solution. With that in mind, this section shows the project development and evolution. As various scenarios were simulated, new ideas and approaches were developed, leading to new model runs. The final four model scenarios that were outlined in chapter 2 were developed after incorporating the results and understanding that went into the previous model results.

5.1.1 Preliminary Model Geometry Development

The preliminary model was limited to only the main LWSC channel. Salmon Bay, Lake Union, and Portage Bay were not included because they were not present in the bathymetric data that was provided at the time (see Figure 5.1). A large portion of model development, grid dependency and time dependency tests were all studied using this preliminary structure (as mentioned in Chapter 4).

Using this model, preliminary results were presented to the client and it was determined that inclusion of Lake Union and the other LWSC water bodies would be crucial in developing an accurate model for the final model scenarios. The fore bay of the Ballard Locks was appended to a new canal model geometry that included the various large bodies of water in the canal. These changes required detailed construction of the mesh to allow the model to continue to converge quickly. The mesh size was kept as close to the preliminary design mesh size as possible. This was done assuming that the grid dependency and time dependency tests that were done on the preliminary model would still hold in the expanded model. The final model geometry is shown in Figure 4.13 and Figure 4.14.

5.1.2 Development of the Initial Condition

One of the key parts to setting up a CFD model is to select appropriate boundary conditions and to then apply them to an appropriate initial condition. When the model geometry was first brought into FLUENT, the fluid domain hydrodynamics and water quality were undefined. The first approach to developing an initial condition model was to run the model for an extended period, allowing salt entering from the locks to form a plume that migrated upstream. The idea was that when the plume matched closely to the field data that the initialization model could be stopped and final model scenarios would be ran on the calibrated model.

The time period needed to initialize the model was grossly underestimated. After the June 2007 had been running for 10 weeks and had still not reached a satisfactory condition the model was stopped and other options were investigated. The June 2007 model was able to resolve 40 days worth of “real-time solutions” over the 10 week run period. Using TecPlot 2009, the salt mass balance over the 40 days was calculated. Based on the average accumulation of salt per day that had built up in the June 2007 initialization model, 252 m³/day (see section 5.2.5 on salt mass balance) the model would have taken approximately 100 days worth of simulation to fill the canal with salt concentrations of 1 ppt. This would have taken at least 10 more weeks of simulation time. Similar results were obtained from the August 2000 model.

Because the model was not operating as initially anticipated, several tests were developed to better understand the hydrodynamics of the salt plume. Based on a study done by Rattray et al. in the early 1950’s (Rattray 1954) that focused on salt concentrations in Lake Union over the course of 2 years, it was determined that understanding Lake Union’s hydrodynamics would be critical in understanding the system as a whole. A patch was inserted into the FLUENT model, giving a salt concentration equal to August 2000 data throughout the Lake Union portion of the LWSC (see Figure 5.3). This was done to see how the hydrodynamics of the model

would affect the salt plume once a larger concentration base was developed in the lake. After a relatively short simulation of 2 weeks, 8 days worth of “real time” results were simulated (see Figure 5.4). These results showed that the hydrodynamics in the LWSC was such that a significant amount of salt was able to be suspended in solution and deposited further upstream. When salt diffusing from the lock faces took several months to propagate upstream to University Bridge, compared to salt that diffused from within Lake Union up to the same point within a matter of a few days, it was deemed as a very significant player in how salt concentrations would propagate upstream to University Bridge.

After discussing the results of the “Lake Union only patch” with the client, it was concluded that salt diffusing from the Ballard Locks was not immediately affecting salt concentrations at the University Bridge. However, as salt migrated upstream and filled up Lake Union, salt that was sitting in Lake Union could migrate up to the University Bridge in a relatively short amount of time. Further understanding of how the hydrodynamics in the LWSC near Lake Union affect salt migration would greatly benefit future model development and project research.

After presenting our findings to Seattle from the initialization models and the Lake Union patched model, new LWSC water quality data was presented to help understand how the system worked. Based on the data presented by Seattle, salt changes near the Ballard Locks had noticeable effects on salt concentrations further upstream over a short period of time. Figure 5.5 (conversation with Lynne Melder 01/07/2011) shows salt concentration recordings at four different water quality monitoring stations in the LWSC during the 2010 season. As concentrations near the Ballard Locks increased, the effects were felt further upstream as shown by the increase in salt concentration at the various monitors upstream.

Even though high salt concentrations near the Ballard Locks caused increases in concentrations upstream, the effects were not felt within the 24 hour window that the four

project scenarios were developed under. Even though the 24 hour simulations would possibly only show significant results near the Ballard Locks, the 4 project simulations were still completed so that they could be used in the ELAM model to see if any conclusive results could be obtained from the short term approach. Thus, the results from the various monitors throughout the canal, further upstream than Salmon Bay, would not be strongly influenced by lock operations within the first 24 hours of simulation.

The four final model scenarios were initialized by patching known August 2000 and June 2007 water quality data over the model domain. The salt concentrations and water temperatures recorded at various depths in the respective scenarios were used to create the initial conditions used in the models. Section 5.2 describes in further detail the final scenarios and their results.

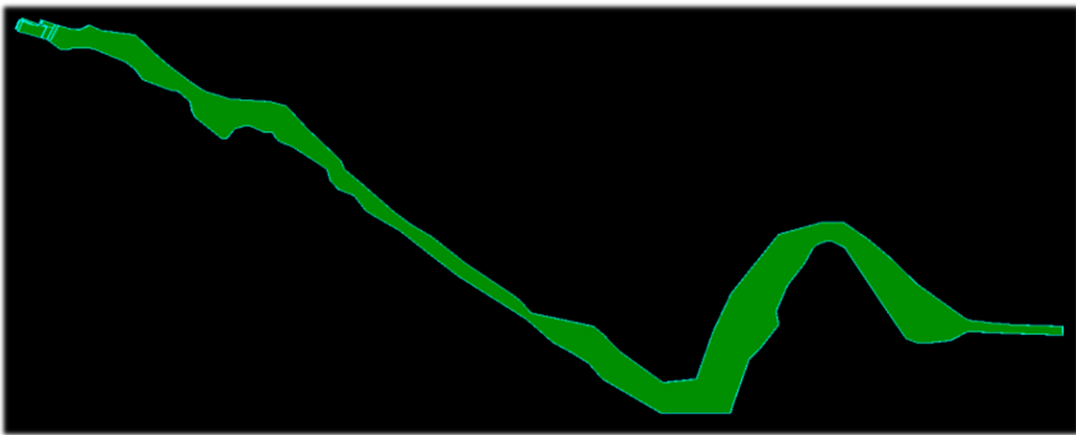


Figure 5.1 Preliminary Model Mesh

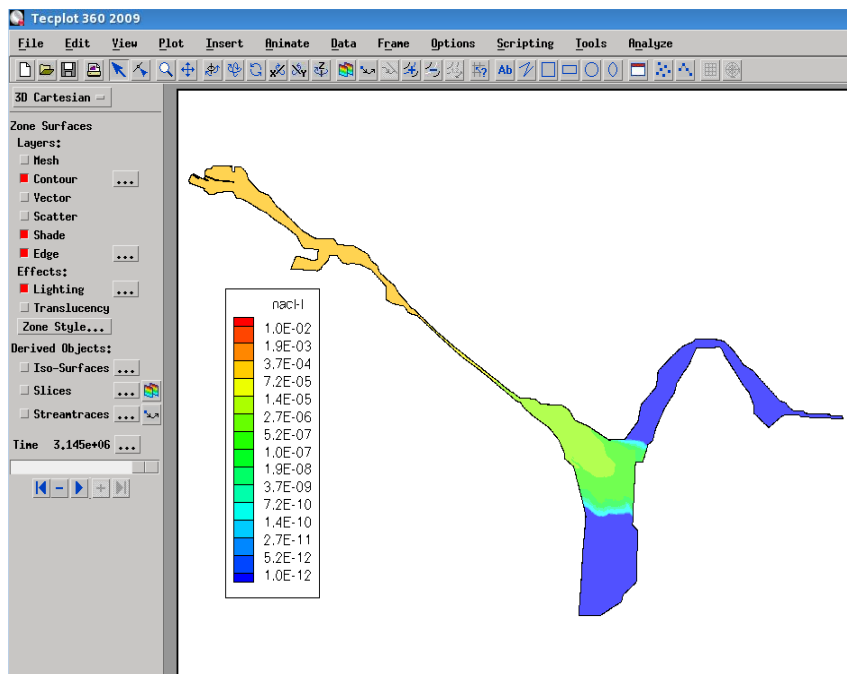


Figure 5.2 June 2007 salt plume after 10 weeks of simulation

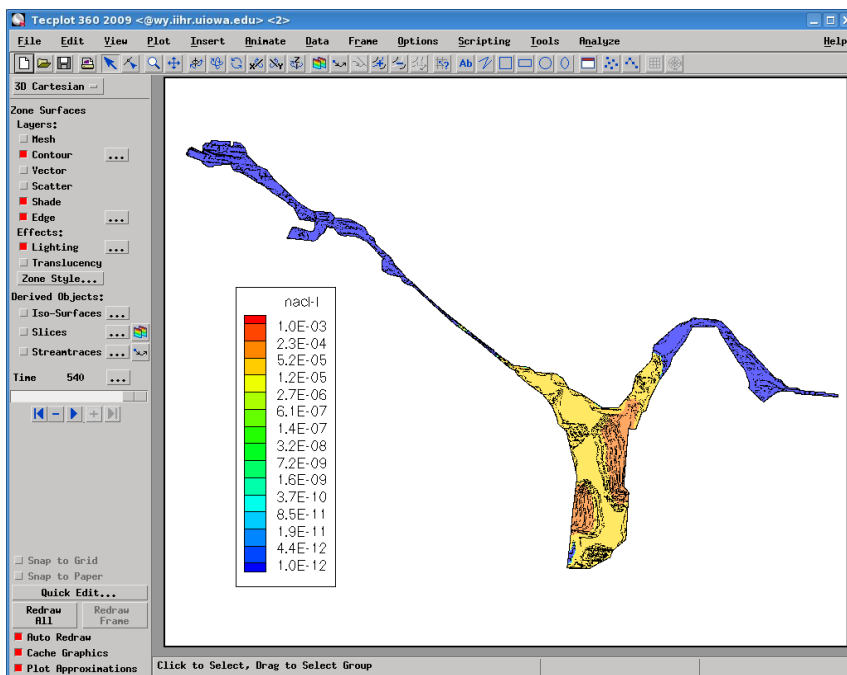


Figure 5.3 Lake Union patch, using August 2000 data

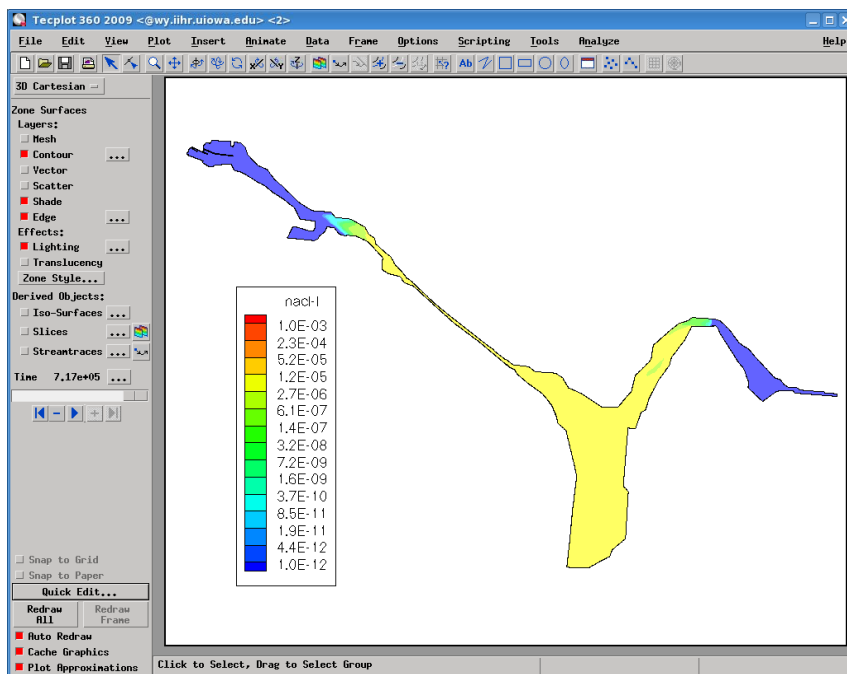


Figure 5.4 Lake Union patch, Solution after 6 days of simulation

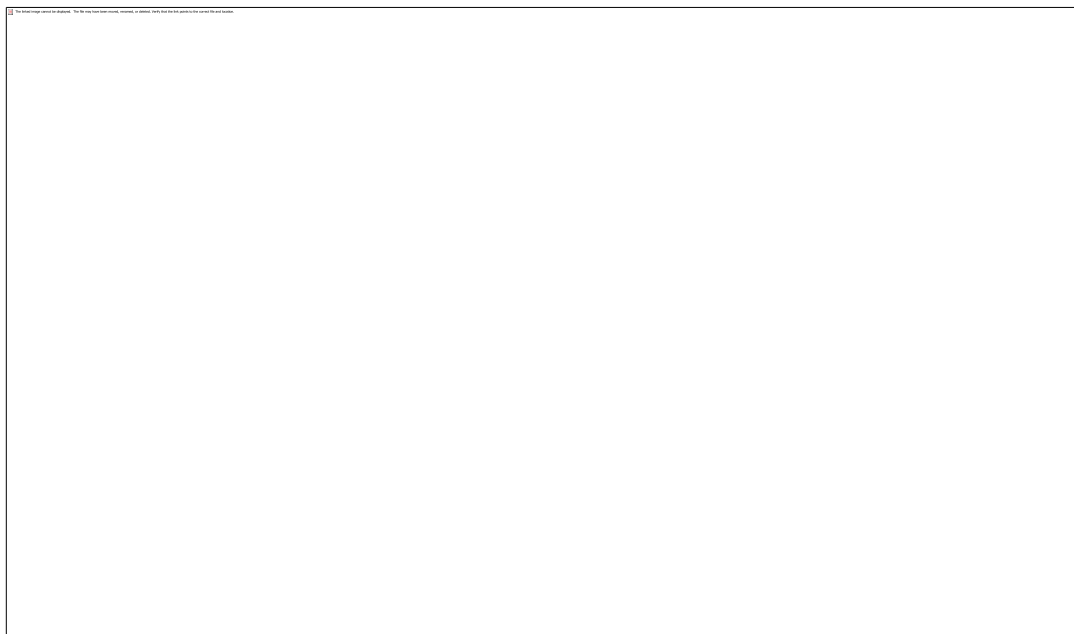


Figure 5.5 Salt Concentrations in the LWSC for 2010

5.2 Salt Water Intrusion and Temperature Analysis

For Final Four Scenarios

While the four scenarios were being run, salinity and temperature monitors were placed in the same locations and depths as the ACOE water quality monitors in the LWSC. Four monitors were also placed at the same location and depth as the King County water monitor in the southern end of Lake Union. The August models had 42 monitors and the June models had 40 monitors (the deepest monitor level was not available in June at the Gas Works station for both June scenarios). Of the 40 or 42 monitors, 5 representative salinity and temperature monitors were selected from each scenario to plot and analyze. This was done to avoid plotting all 162 monitor graphs.

The results are broken into 4 sections for the 4 different scenarios. At the beginning of each section comments and analysis are provided before moving on to the next scenario. At the end of the fourth section a general assessment is made comparing all 4 scenarios. In general, only the monitors near the Ballard Locks show any significant results that can be analyzed. Due to simulating only 24 hours, the other monitors are simply tracking the mixing and settling of the initial conditions.

5.2.1 Scenario 1 – August 2000

Using the boundary conditions that were outlined in chapter 4, scenario 1 simulated 24 hours worth of data. Figure 5.6 shows lock and dam monitor 3 which was the deepest monitor near the Ballard Locks. As the day developed and locking operations were simulated, the salinity concentration near the locks spiked in unison with the locking operations. Overall the number of lockings was not high enough to increase the salt concentrations in the fore bay of the dam. This shows that the SWD and fish ladder removed more salt than the locking operations brought in. The overall change in salt concentration over the 24 hour period was small. After the system stabilized around a concentration of 1.3 ppt, the model only decreased to approximately 1.1 ppt. Allowing

the model to simulate more time would help show the long term trend of the locking operations set up in scenario 1.

The Fremont Bridge, Gas Works, and Lake Union salt monitors (Figure 5.7 through Figure 5.9) all show a mild downward trend. This means the system as a whole was losing salt. In other words, the initial conditions that were set up were higher than the stable solution, therefore during the 24 hours that were simulated the model was moving towards a steady state that had less salt in the system. The University Bridge salt monitor (Figure 5.10) increased half way through the simulation, however the concentrations at this point were so small that this small change was insignificant.

The lock and dam temperature monitor (Figure 5.11) shows the dips each time the lock opened and brought in colder Puget Sound water. The overall trend downward also incorporates the cooler surface air that was simulated. The other 4 monitors (Figure 5.12 through Figure 5.15) all show fluctuations that can be attributed to the model stabilizing after having initial conditions imposed on the system.

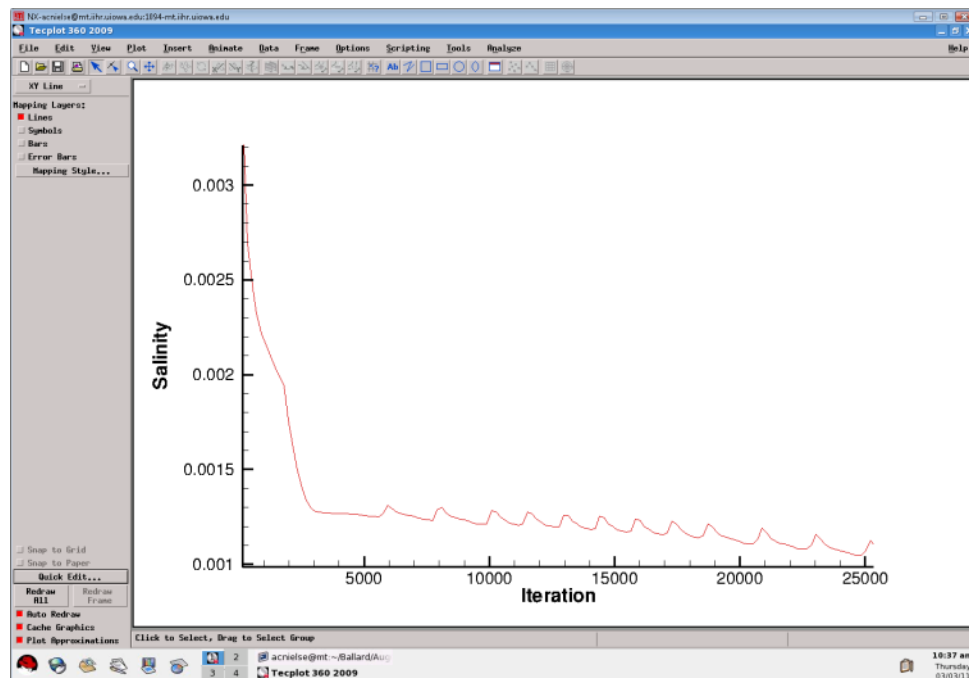


Figure 5.6 Scenario 1 - Lock and Dam salt monitor 3

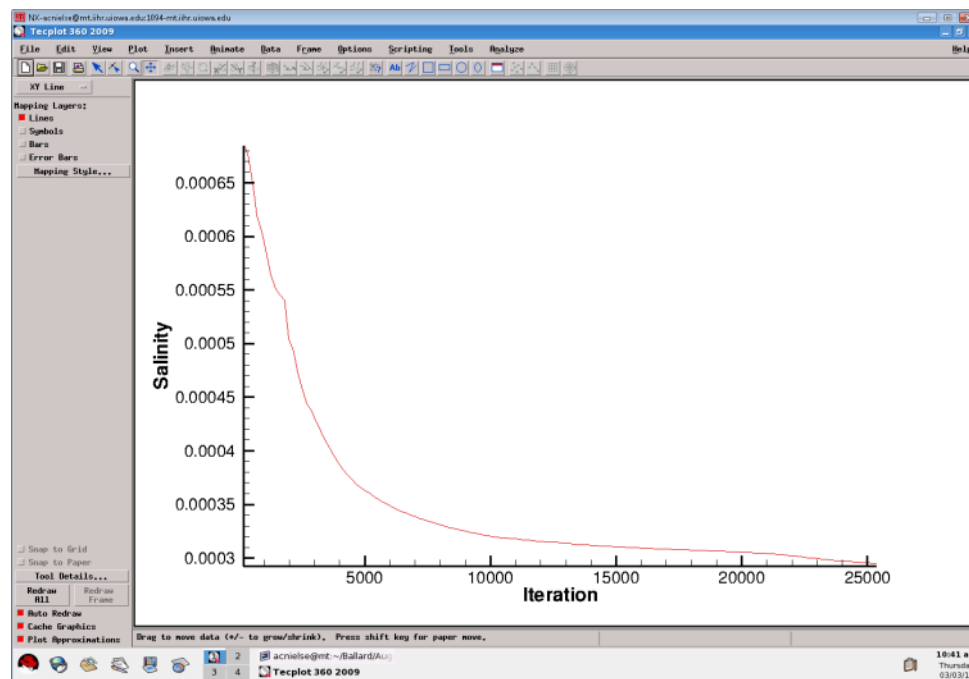


Figure 5.7 Scenario 1 - Fremont Bridge salt monitor 3

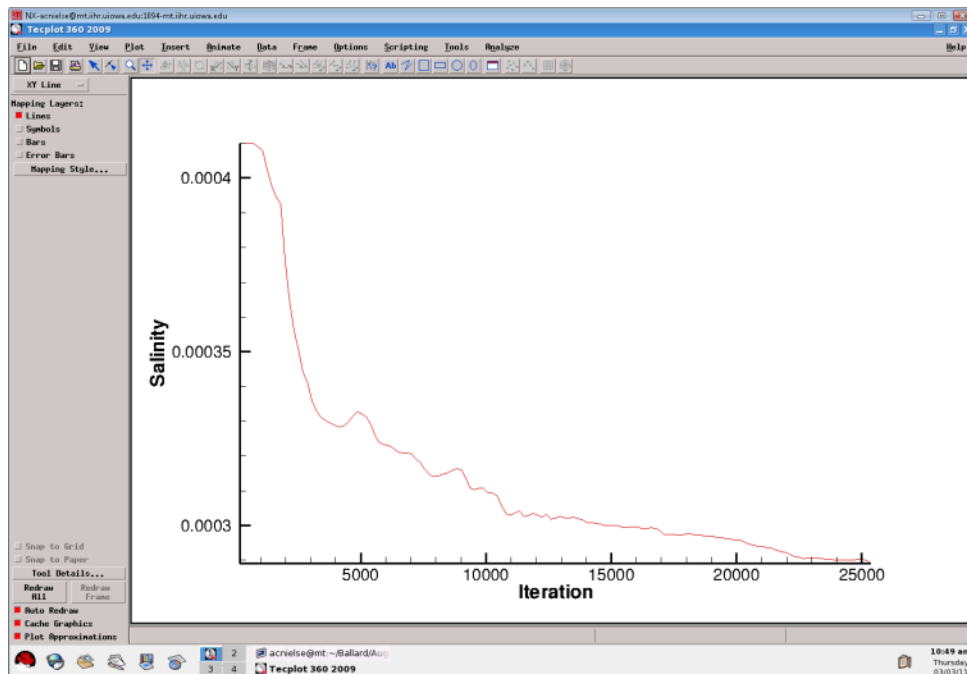


Figure 5.8 Scenario 1 - Gas Works salt monitor 4

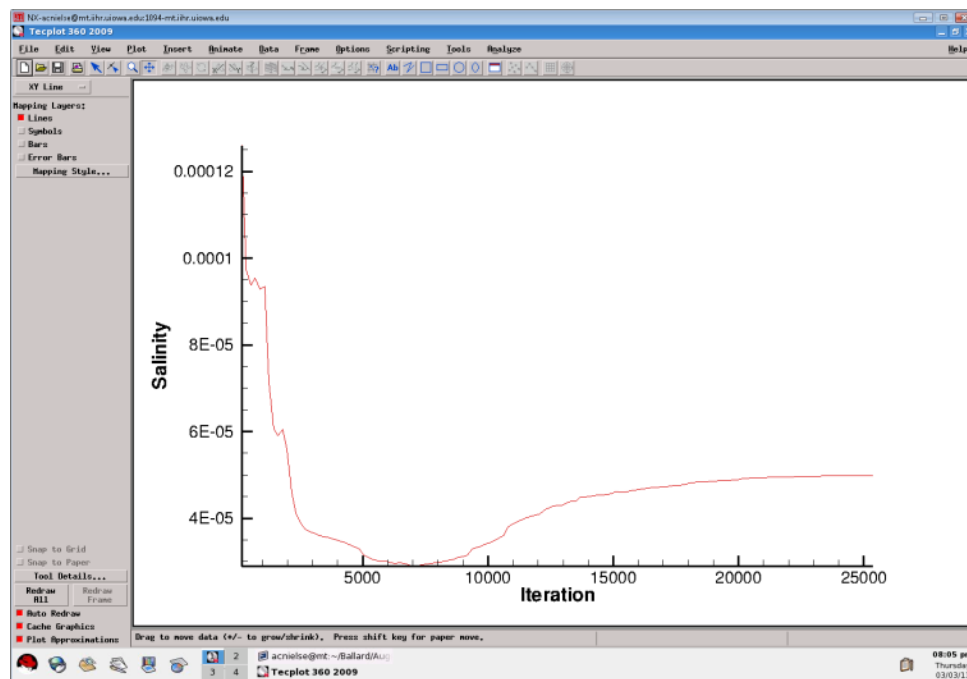


Figure 5.9 Scenario 1 - Lake Union salt monitor 4

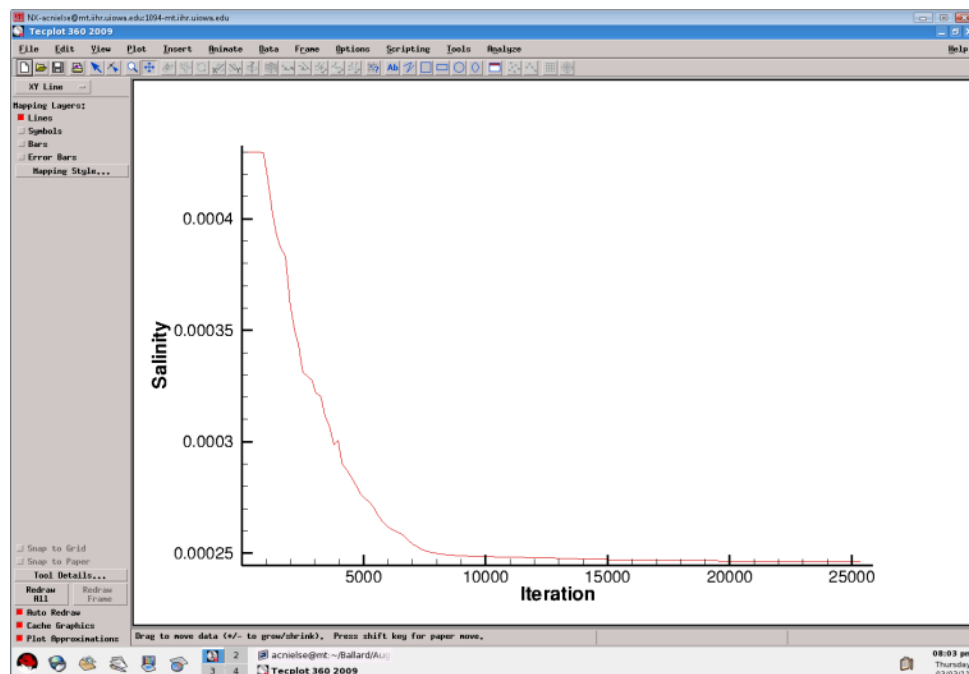


Figure 5.10 Scenario 1 - University Bridge salt monitor 2

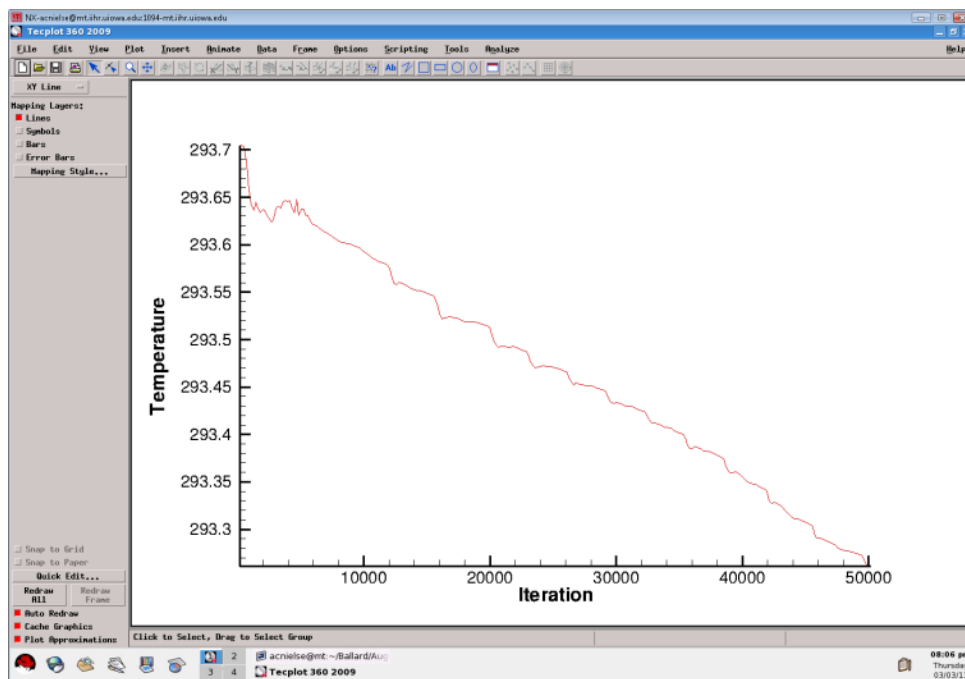


Figure 5.11 Scenario 1 - Lock and Dam temperature monitor 1

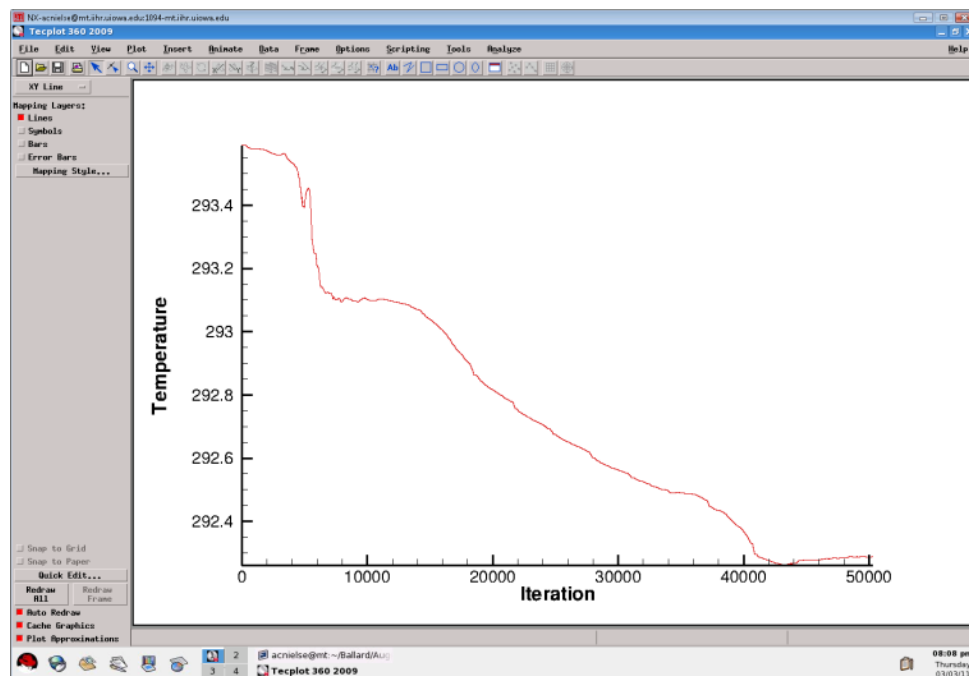


Figure 5.12 Scenario 1 - Fremont Bridge temperature monitor 1

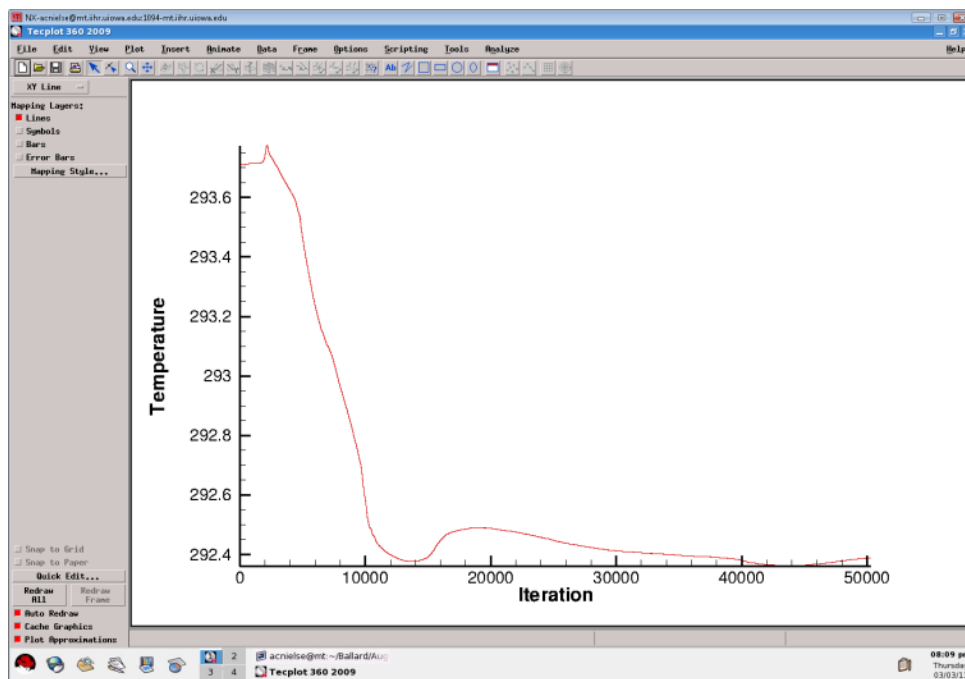


Figure 5.13 Scenario 1 - Gas Works temperature monitor 1

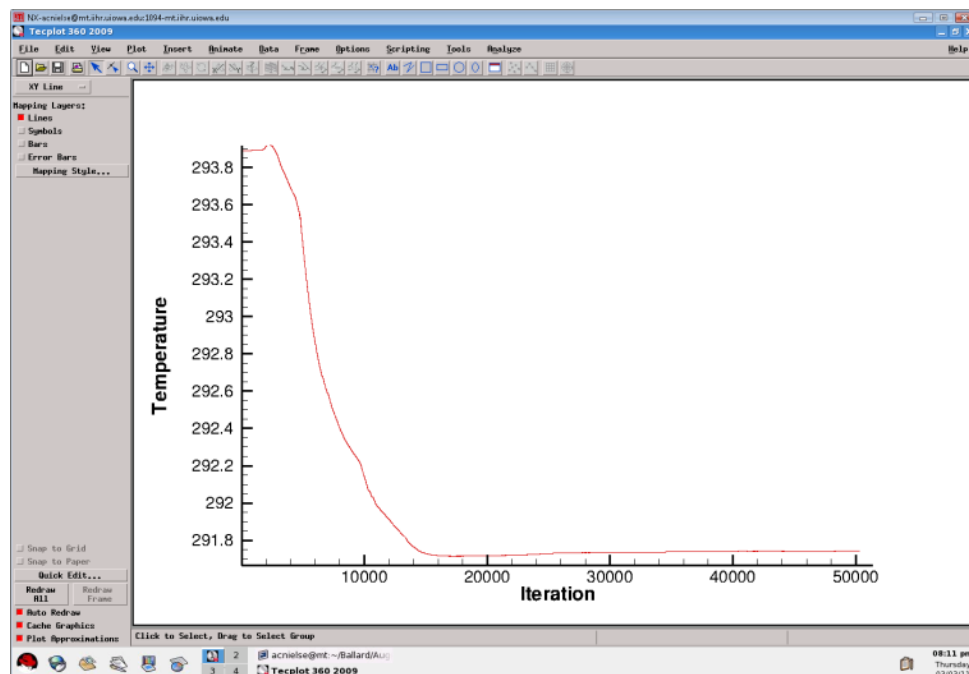


Figure 5.14 Scenario 1 - Lake Union temperature monitor 1

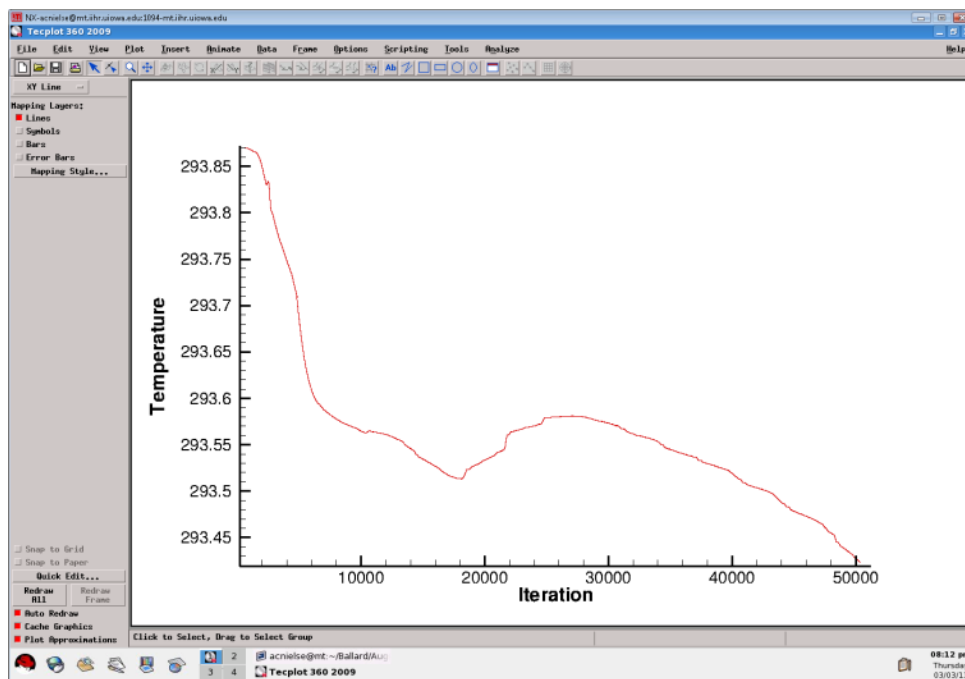


Figure 5.15 Scenario 1 - University Bridge temperature monitor 1

5.2.2 Scenario 2 – August 2000 (x2)

Using the boundary conditions that were outlined in chapter 4, scenario 2 simulated 24 hours worth of data. Scenario 2 was developed to have exactly twice as many lockings during a typical August 2000 day to see how this would affect water quality, hydrodynamics, and the changes that would be produced in the ELAM fish model. Figure 5.16 shows the increased spikes in salt concentration by the dam in agreement with the simulated increased lock operation. The overall salt concentration change between scenario 1 and 2 was almost the same. Both models started around 1.3 ppt and ended around 1.1 ppt. This means that the increased number of lockings had limited effect on the overall salt concentration in the system. The salinity at the other monitors didn't show much change when compared to scenario 1. This is because the model has only had 24 hours to simulate. Longer simulations could show more of the long term effects of these selected locking operations.

The temperature monitors in scenario 2 were very similar to those of scenario 1. As described above, the temperature drop near the lock and dam and the gradual decline over the whole system can all be attributed to the same reasons as in scenario 1.

Where scenario 1 and scenario 2 had the exact same setups, other than changing the number of lockings, the results from the first 24 hours of simulation are very similar.

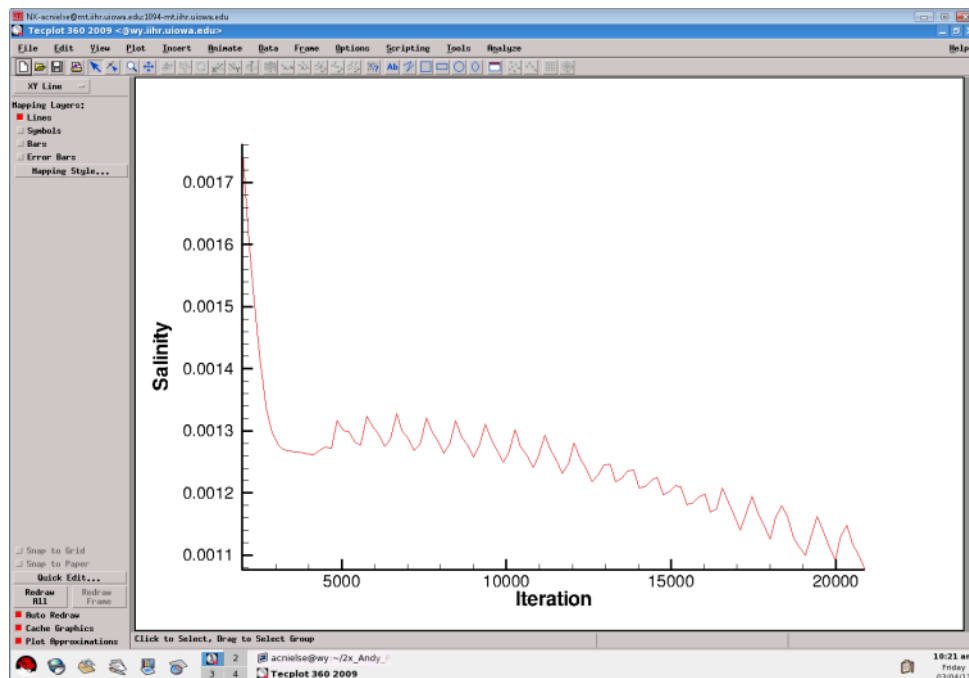


Figure 5.16 Scenario 2 - Lock and Dam salt monitor 3

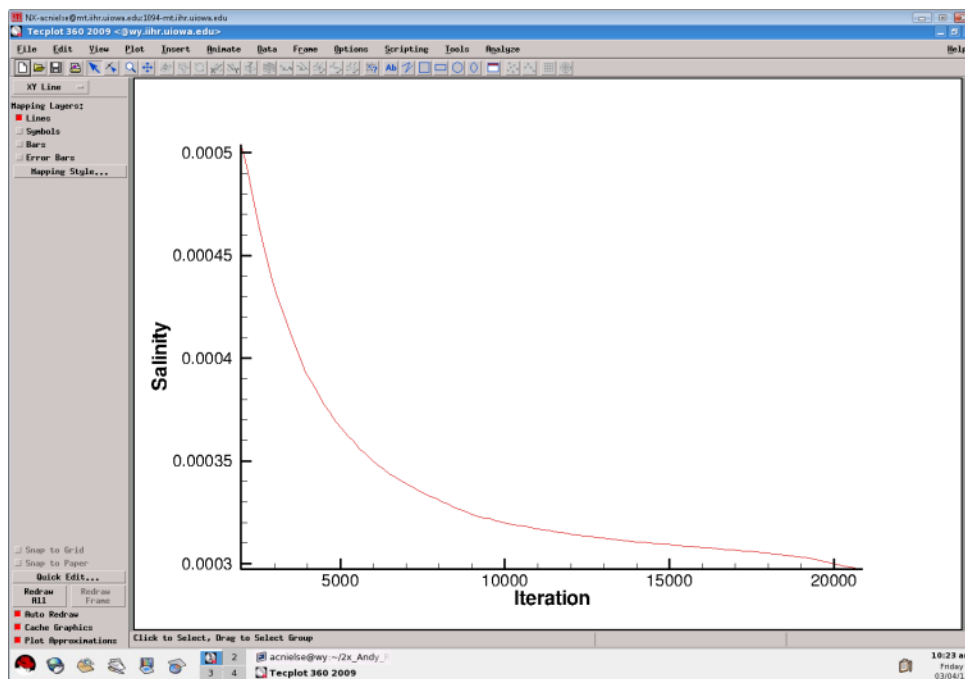


Figure 5.17 Scenario 2 - Fremont Bridge salt monitor 3

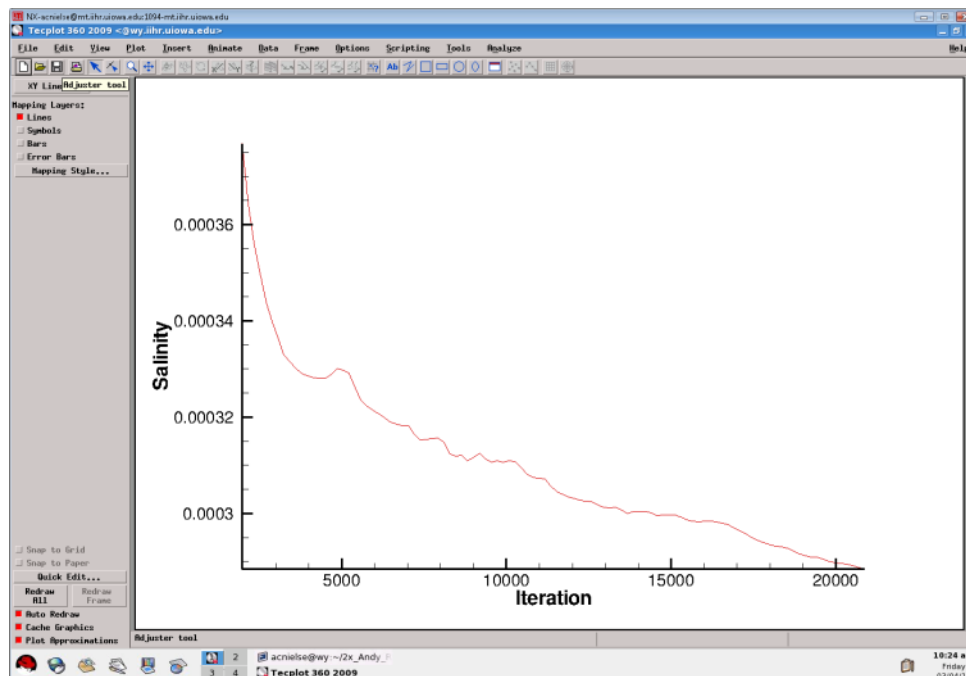


Figure 5.18 Scenario 2 - Gas Works salt monitor 4

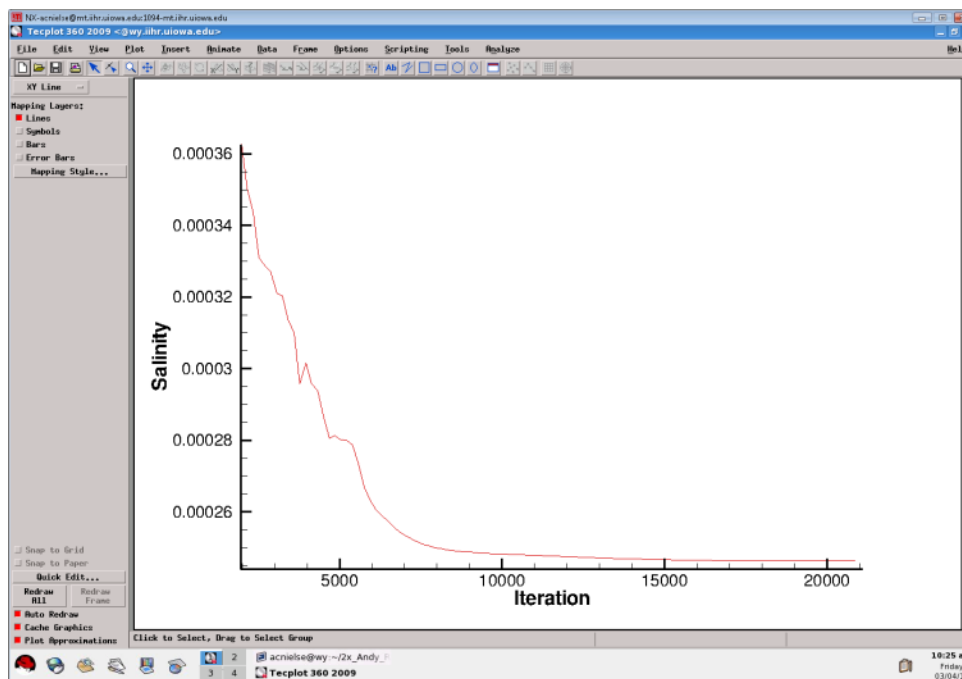


Figure 5.19 Scenario 2 - Lake Union salt monitor 4

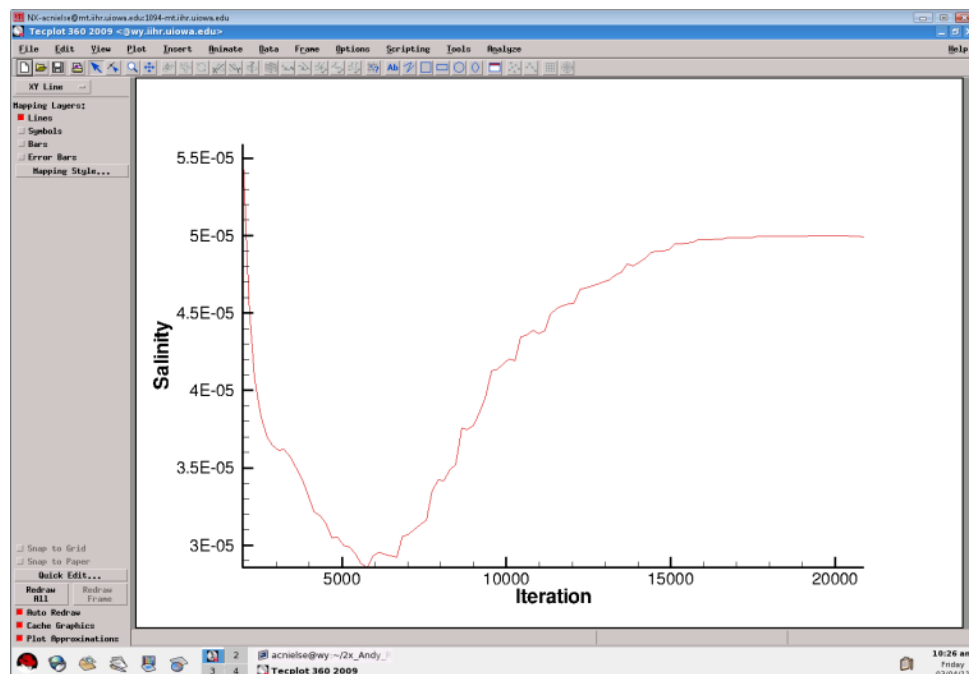


Figure 5.20 Scenario 2 - University Bridge salt monitor 2

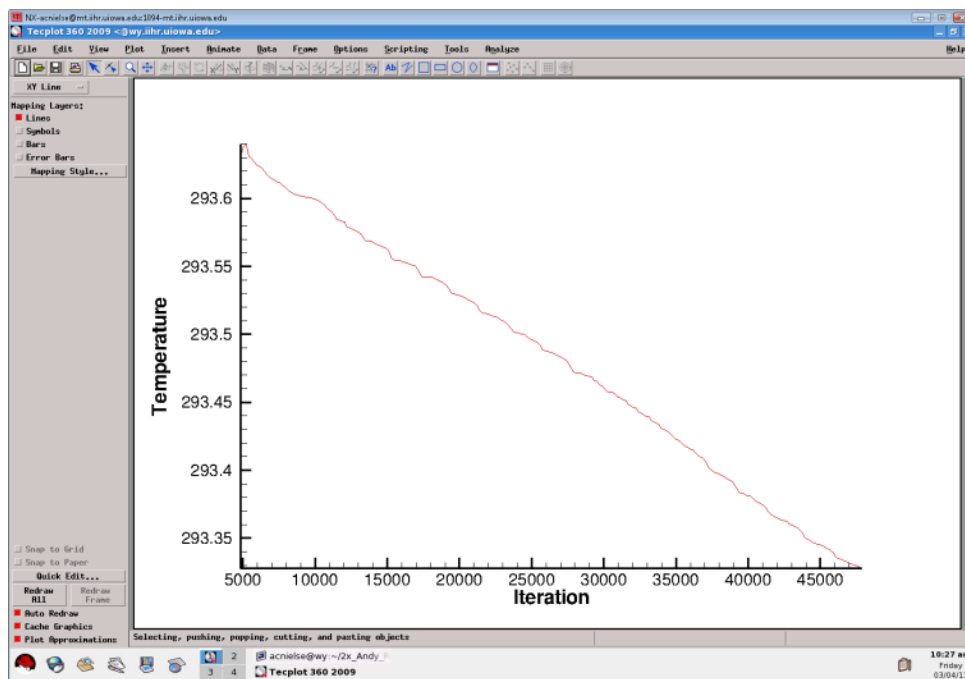


Figure 5.21 Scenario 2 - Lock and Dam temperature monitor 1

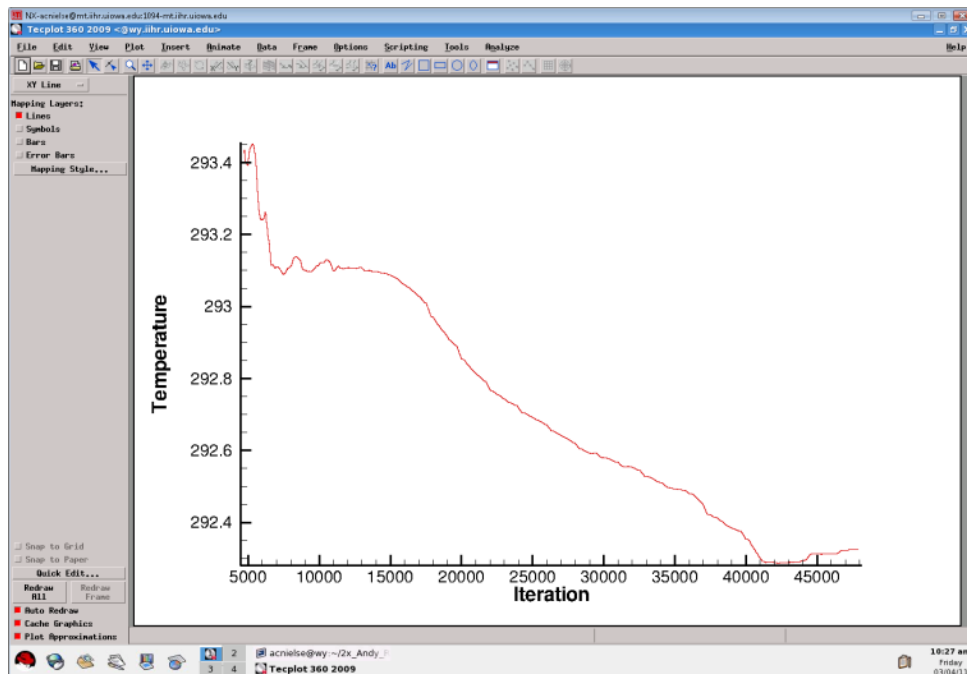


Figure 5.22 Scenario 2 - Fremont Bridge temperature monitor 1

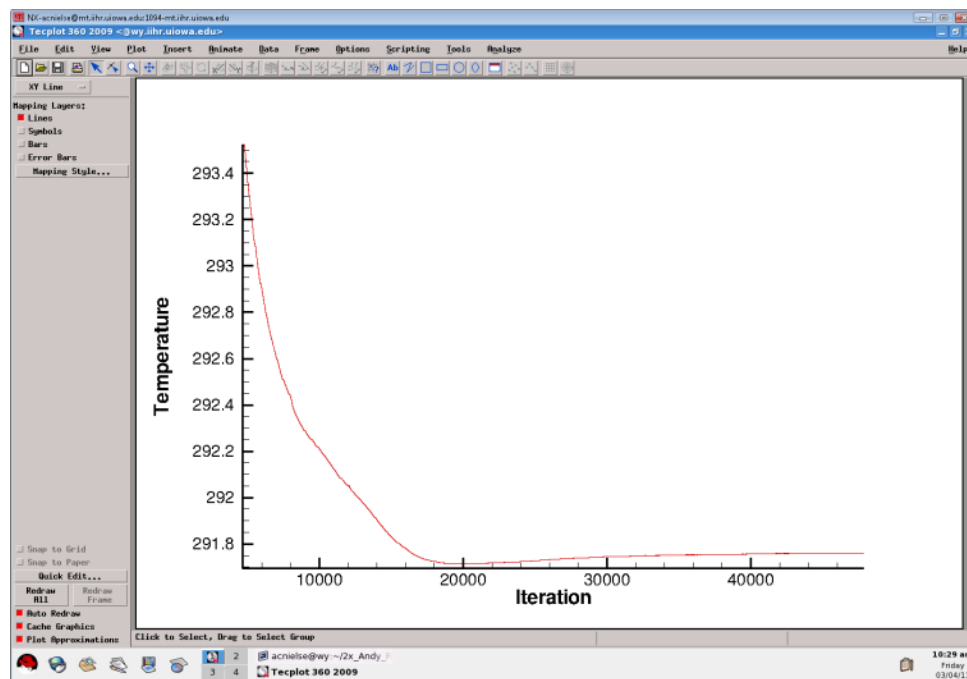


Figure 5.23 Scenario 2 - Gas Works temperature monitor 1

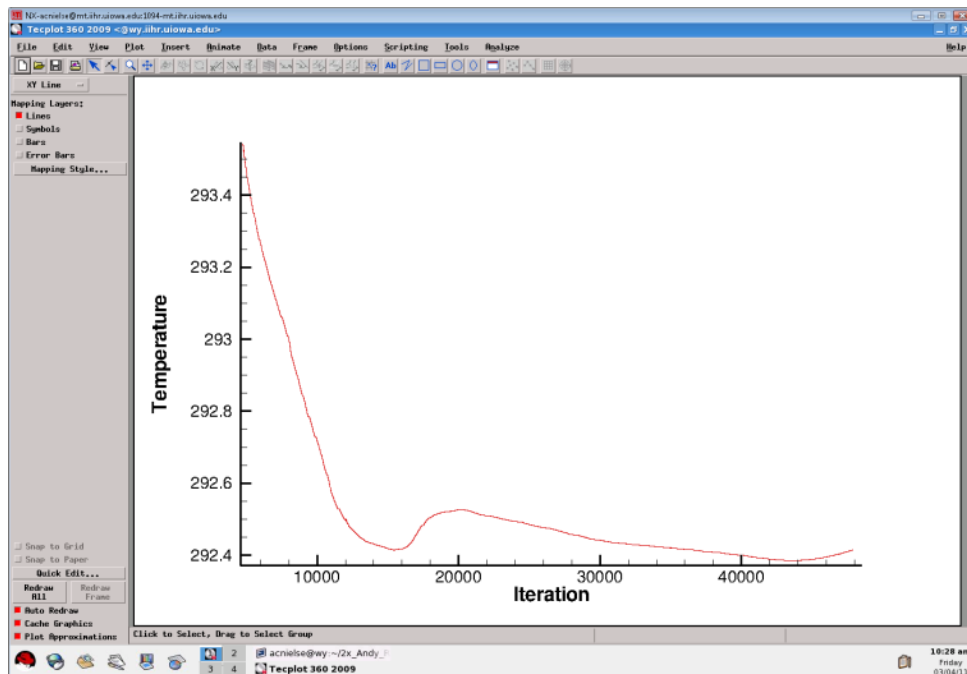


Figure 5.24 Scenario 2 - Lake Union temperature monitor 1

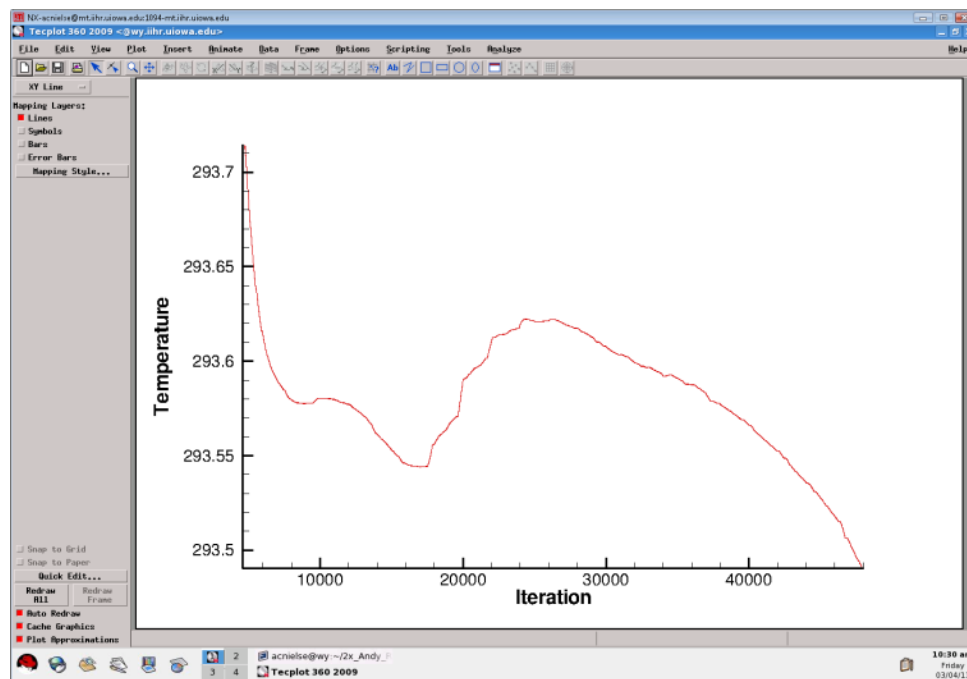


Figure 5.25 Scenario 2 - University Bridge temperature monitor 1

5.2.3 Scenario 3 – June 2007

The monitor plots from scenario 3 are very similar to those in the previous scenarios in that the small peaks in salt and drops in temperature during each locking is very noticeable in the lock and dam monitors. The rest of the monitors show the general trend of decreasing salt concentrations. Allowing the simulation to run for more than 24 hours would allow for lock operation effects to be seen further upstream.

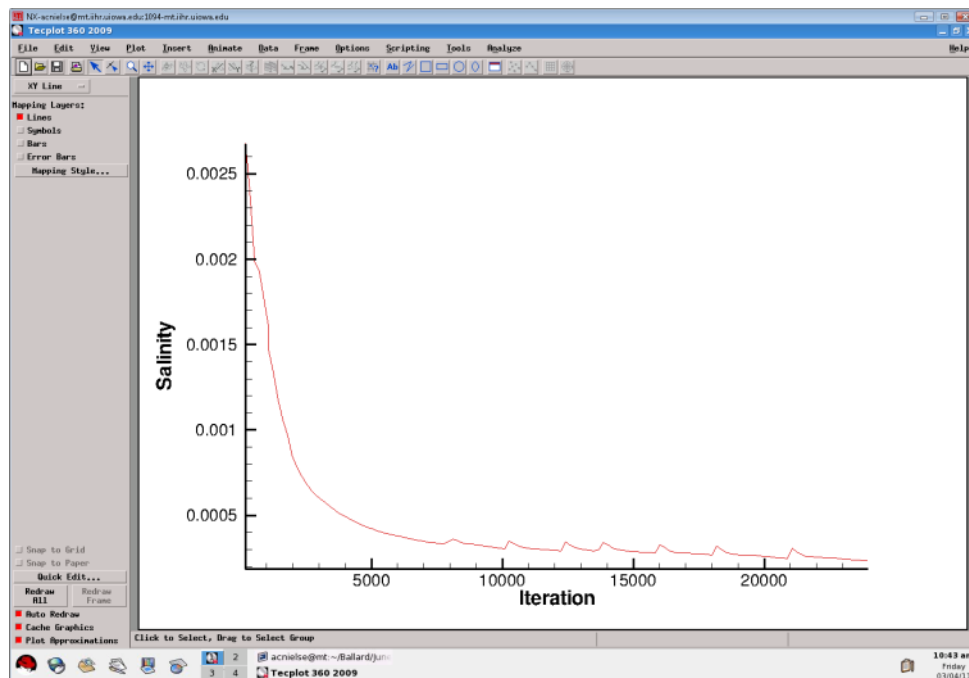


Figure 5.26 Scenario 3 - Lock and Dam salt monitor 3

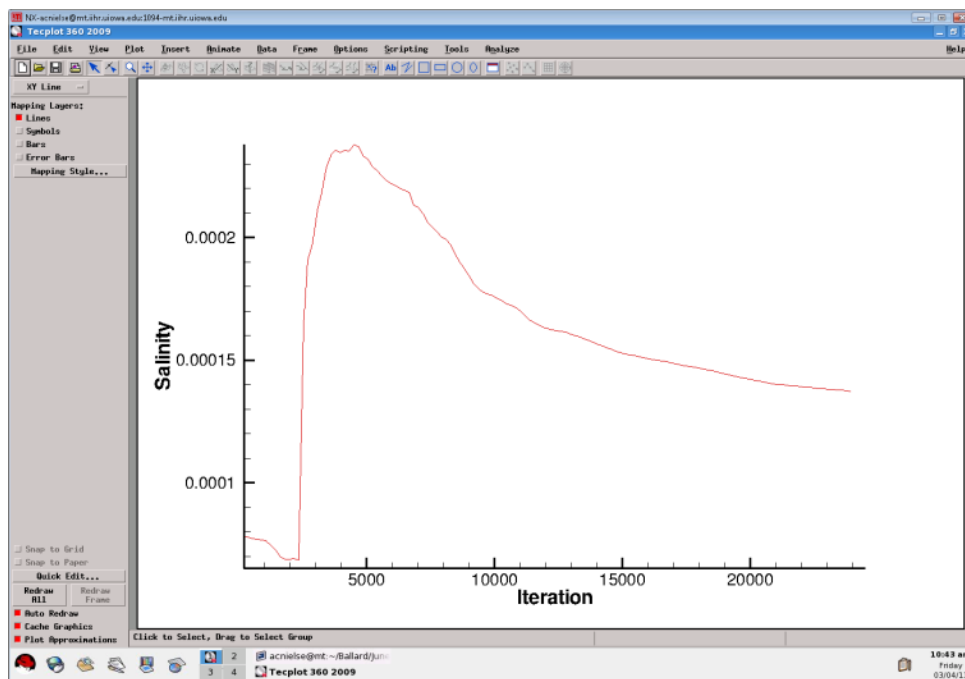


Figure 5.27 Scenario 3 - Fremont Bridge salt monitor 3

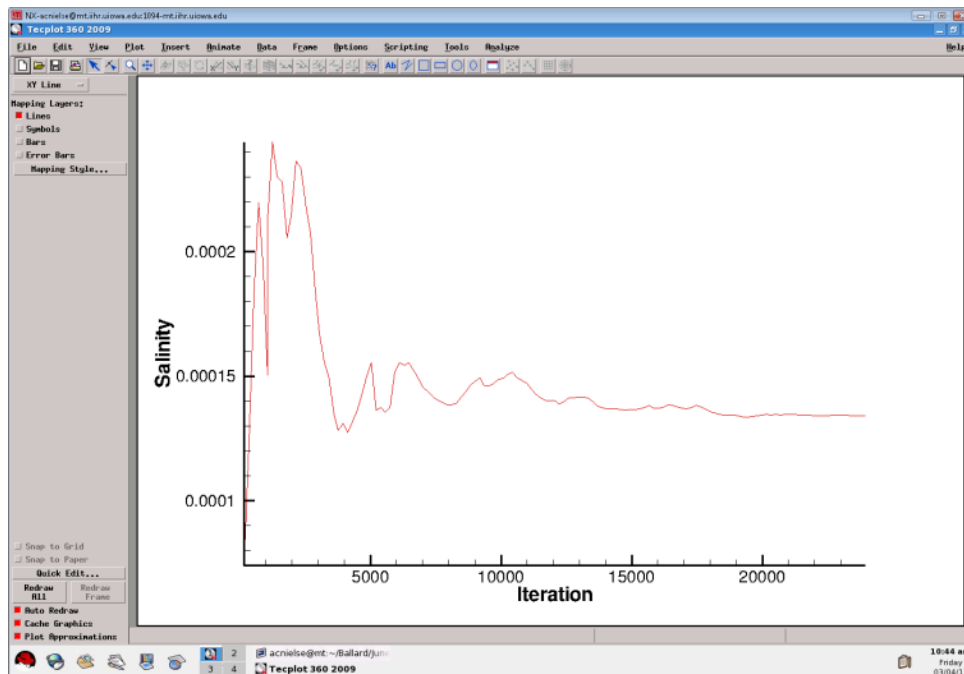


Figure 5.28 Scenario 3 - Gas Works salt monitor 3

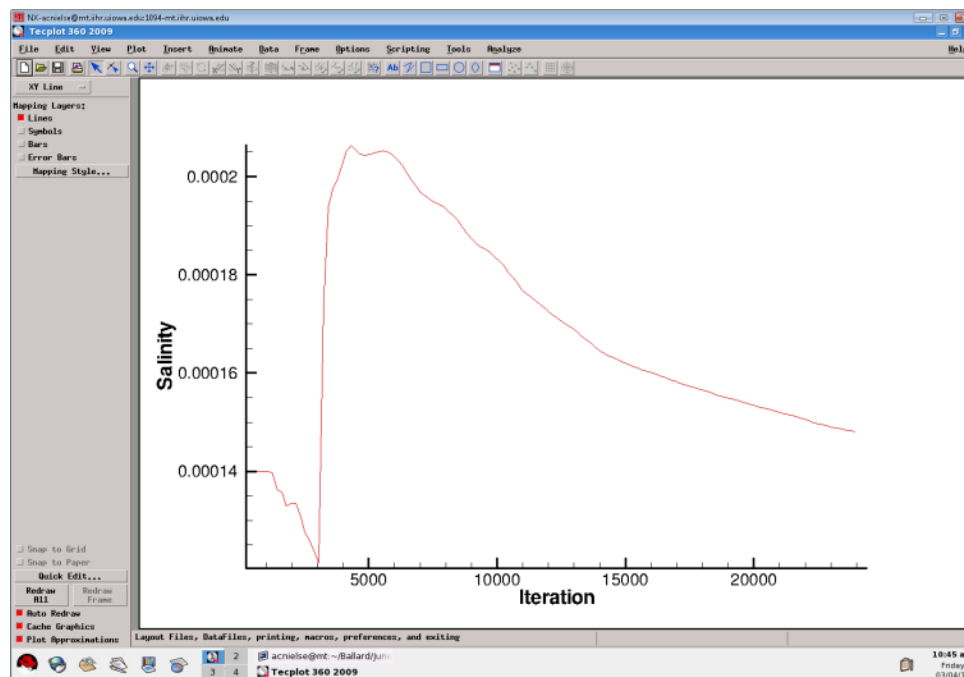


Figure 5.29 Scenario 3 - Lake Union salt monitor 4

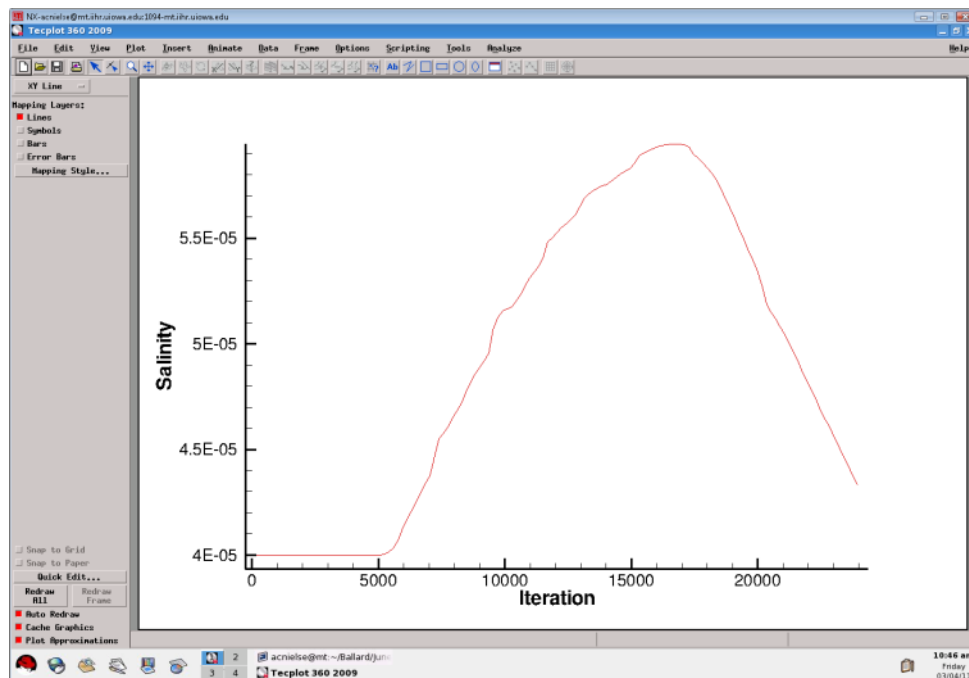


Figure 5.30 Scenario 3 - University Bridge salt monitor 2

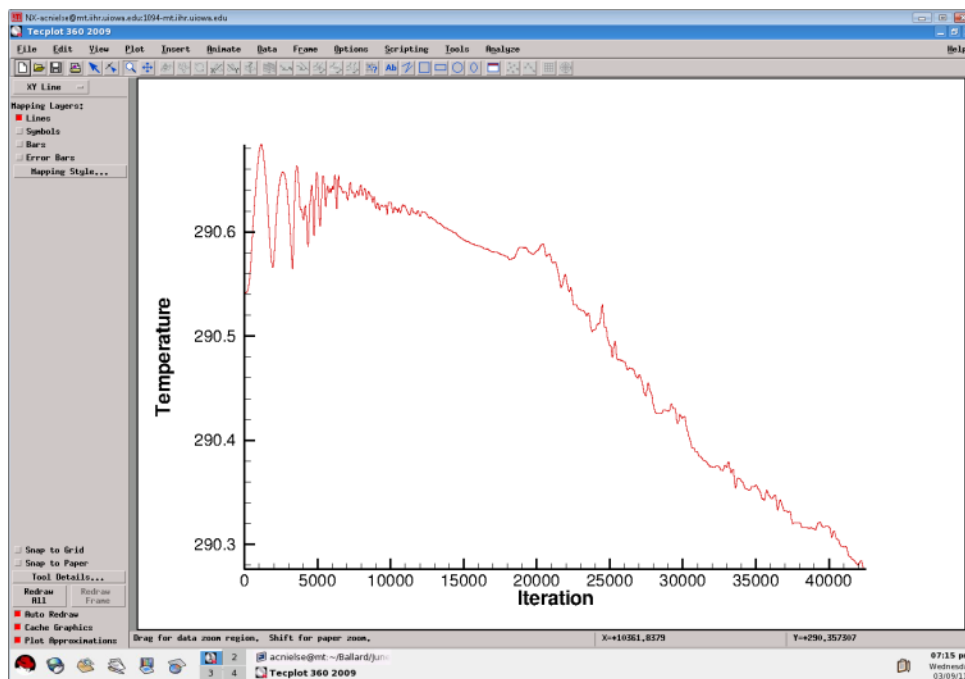


Figure 5.31 Scenario 3 - Lock and Dam temperature monitor 1

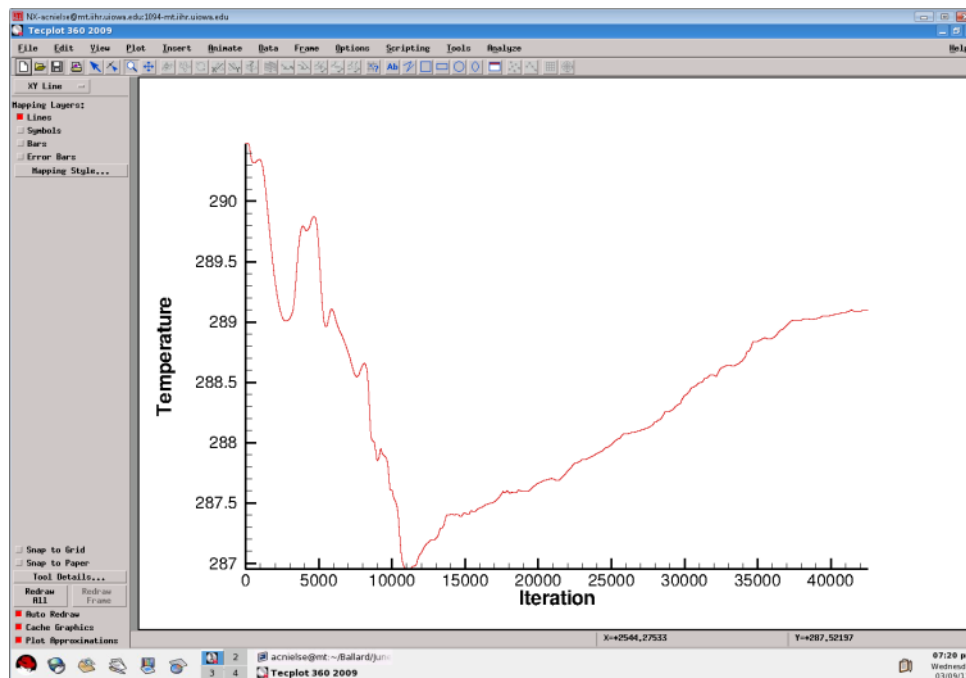


Figure 5.32 Scenario 3 - Fremont Bridge temperature monitor 1

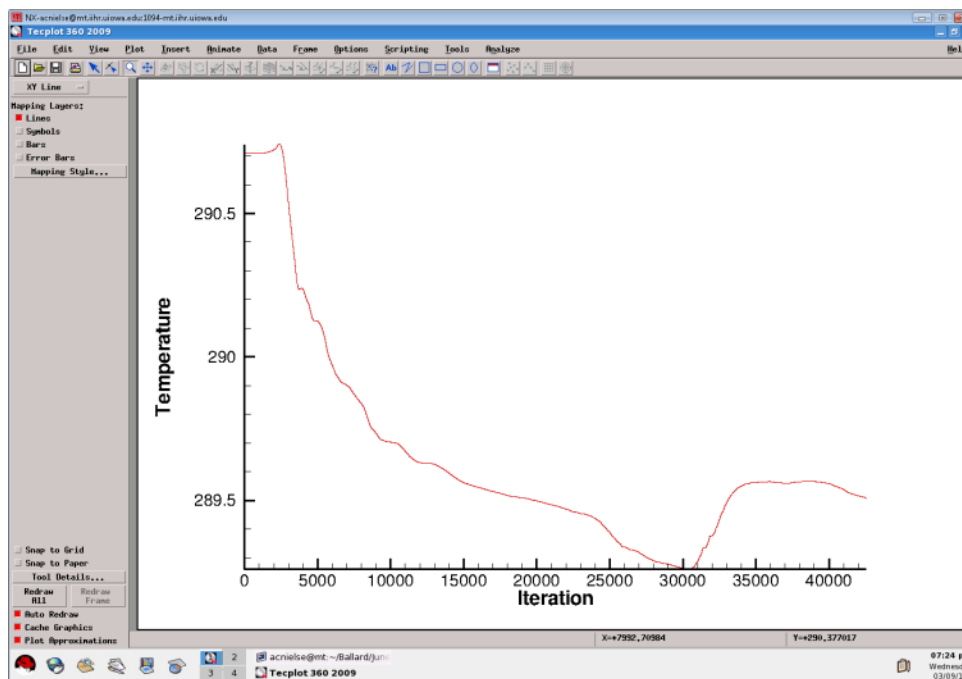


Figure 5.33 Scenario 3 - Gas Works temperature monitor 1

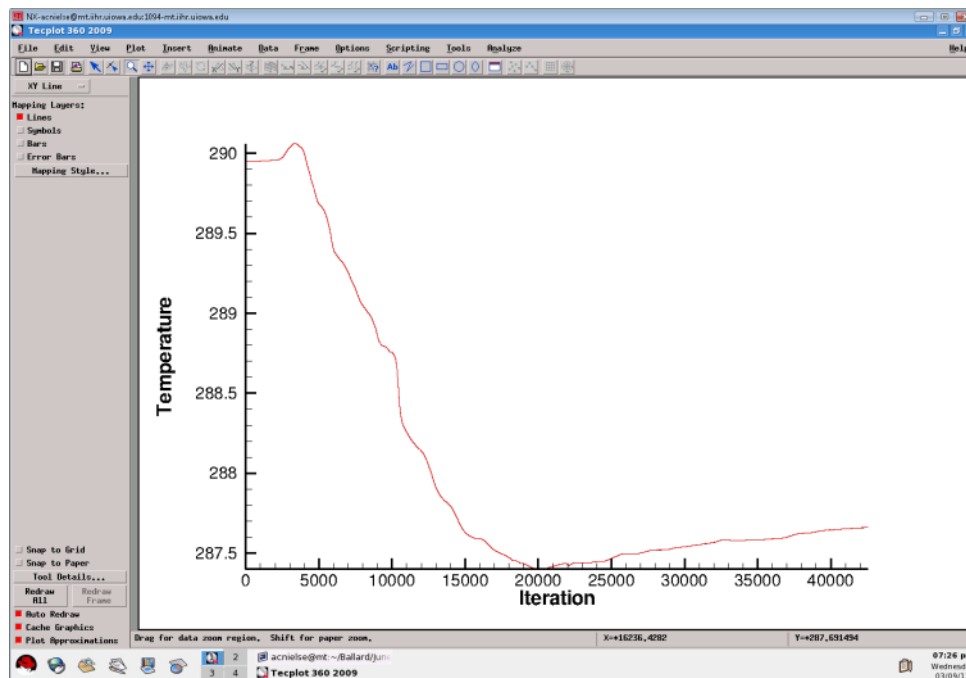


Figure 5.34 Scenario 3 - Lake Union temperature monitor 1

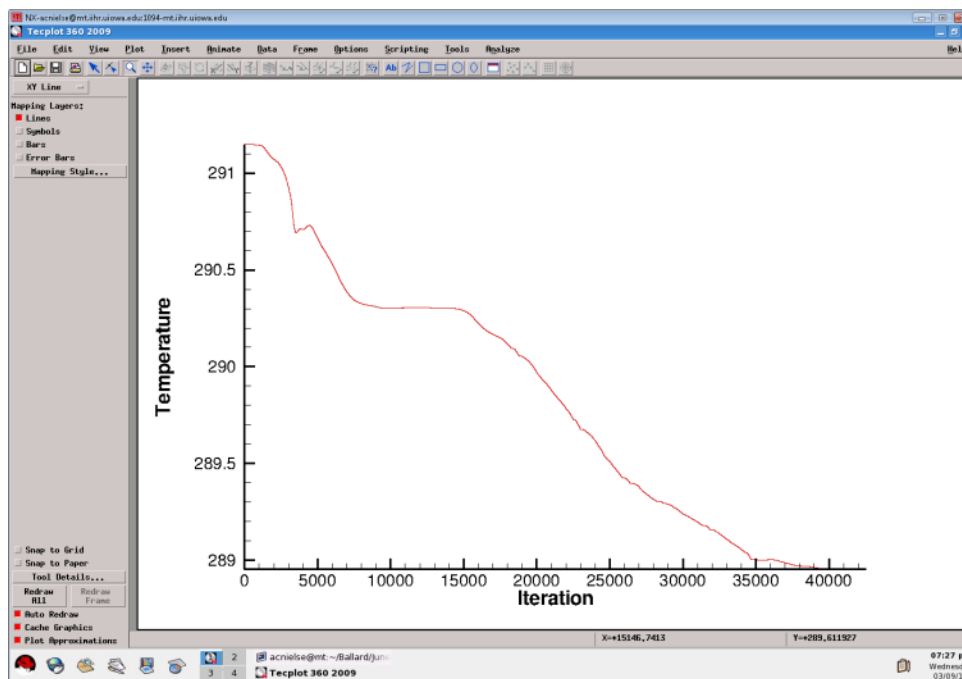


Figure 5.35 Scenario 3 - University Bridge temperature monitor 1

5.2.4 Scenario 4 – June 2007 (Fish wall)

The monitor plots from scenario4 are almost identical to those in scenario 3. This shows that including the floating wall in the fore bay did not affect the overall water quality of the system. The changes in the flow field near the spillways will be modeled in the ELAM fish model to determine if the wall helps more smolts use the smolt flumes. For all of the scenario 4 graphs, the same analysis that was done on scenario 3 can be applied to the results from scenario 4.

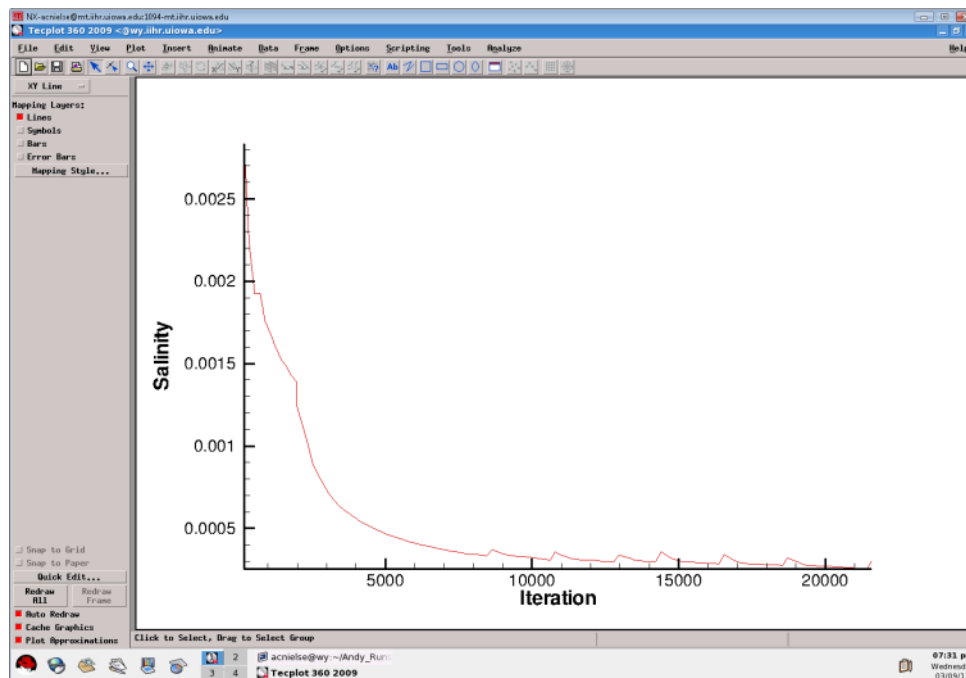


Figure 5.36 Scenario 4 - Lock and Dam salt monitor 3

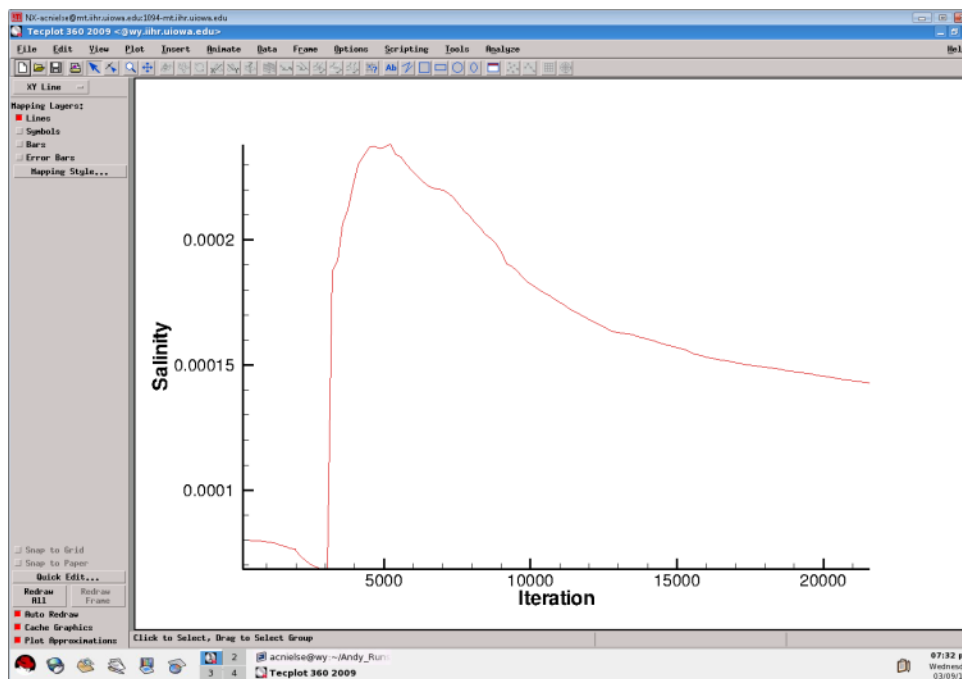


Figure 5.37 Scenario 4 - Fremont Bridge salt monitor 3

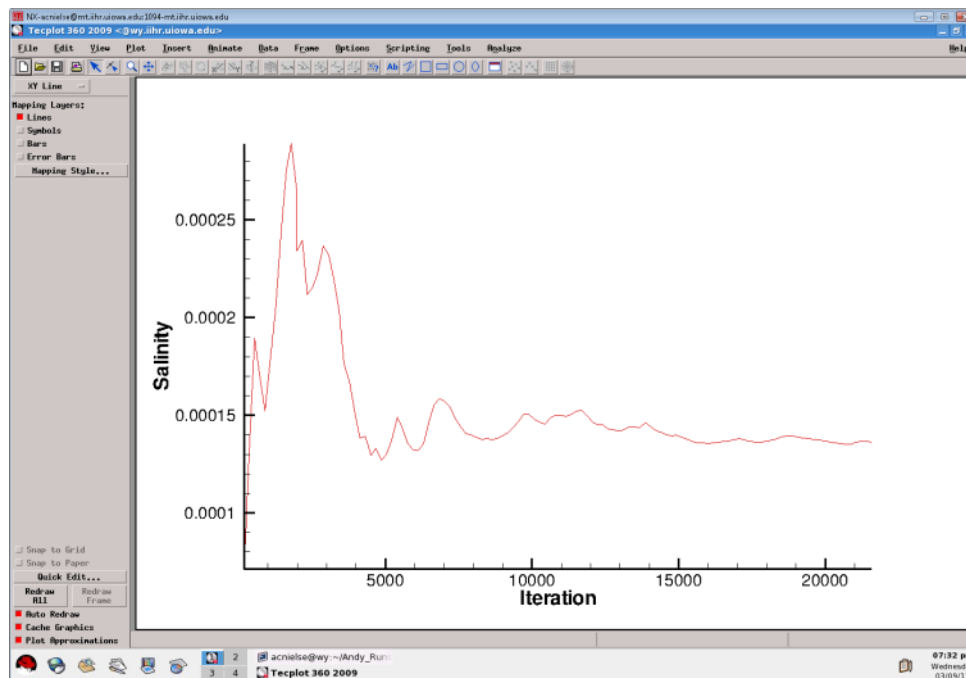


Figure 5.38 Scenario 4 - Gas Works salt monitor 3

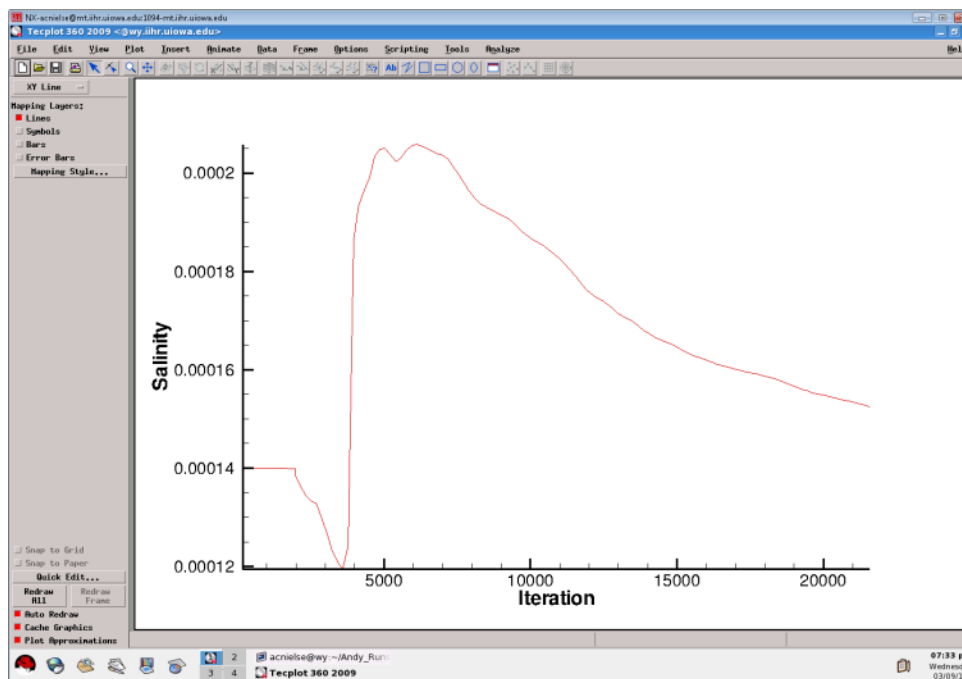


Figure 5.39 Scenario 4 - Lake Union salt monitor 4

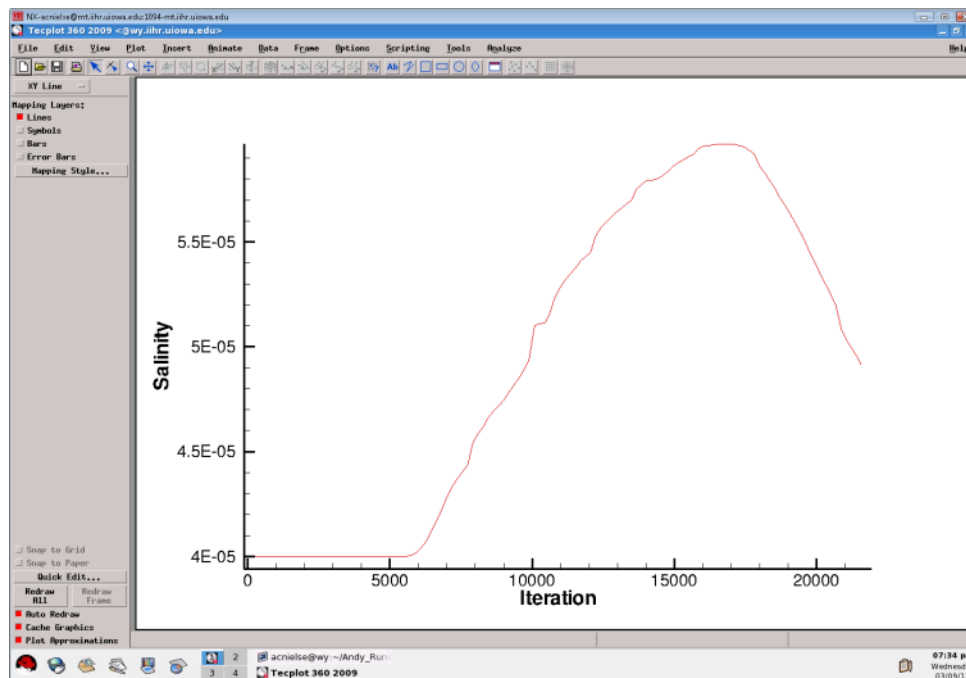


Figure 5.40 Scenario 4 - University Bridge salt monitor 2

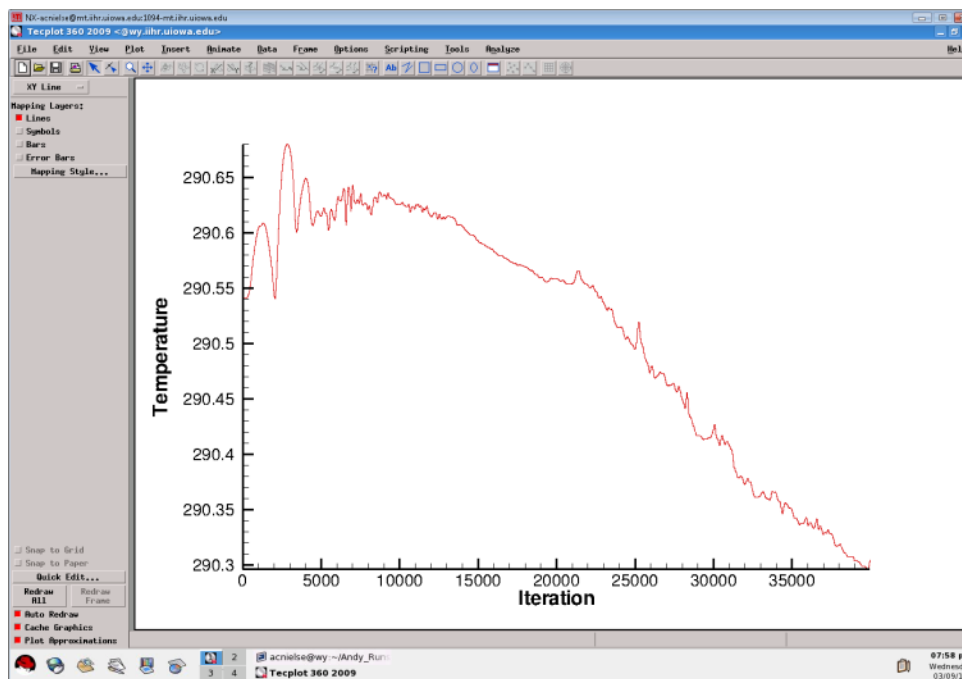


Figure 5.41 Scenario 4 - Lock and Dam temperature monitor 1

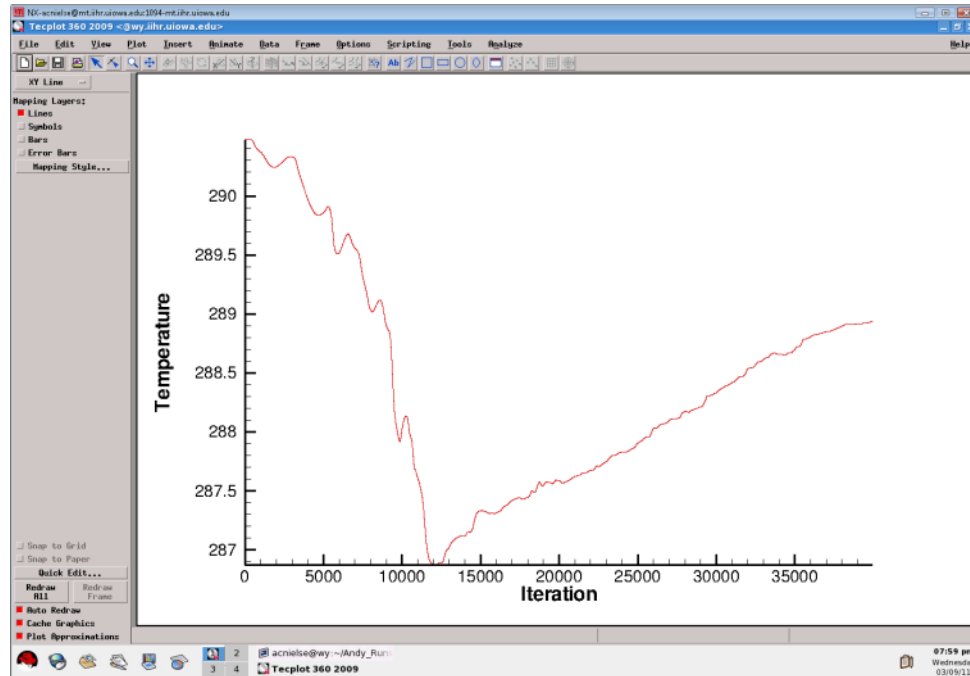


Figure 5.42 Scenario 4 - Fremont Bridge temperature monitor 1

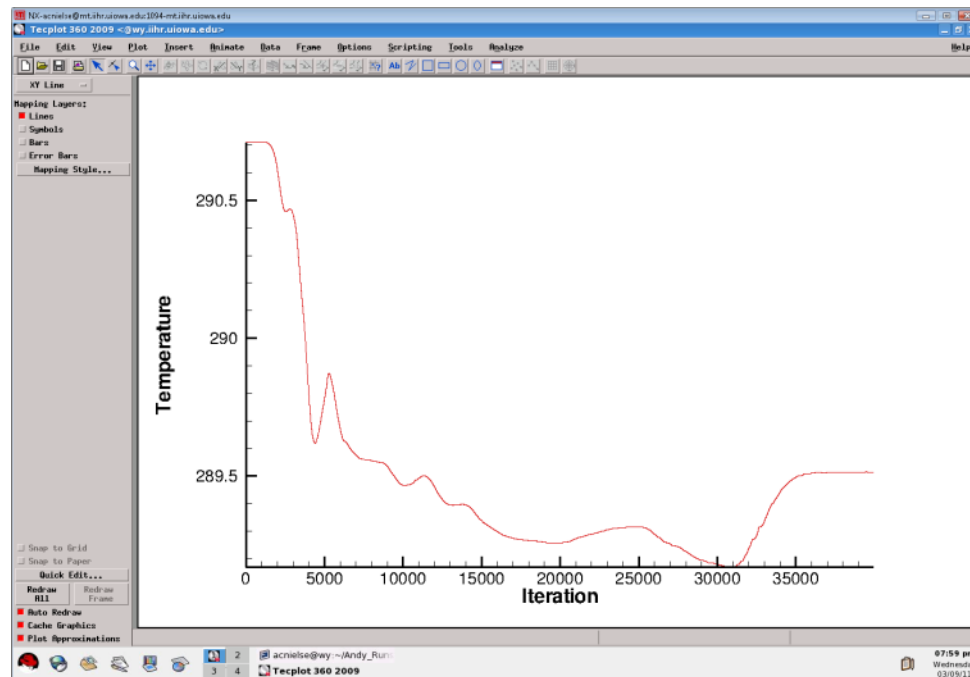


Figure 5.43 Scenario 4 - Gas Works temperature monitor 1

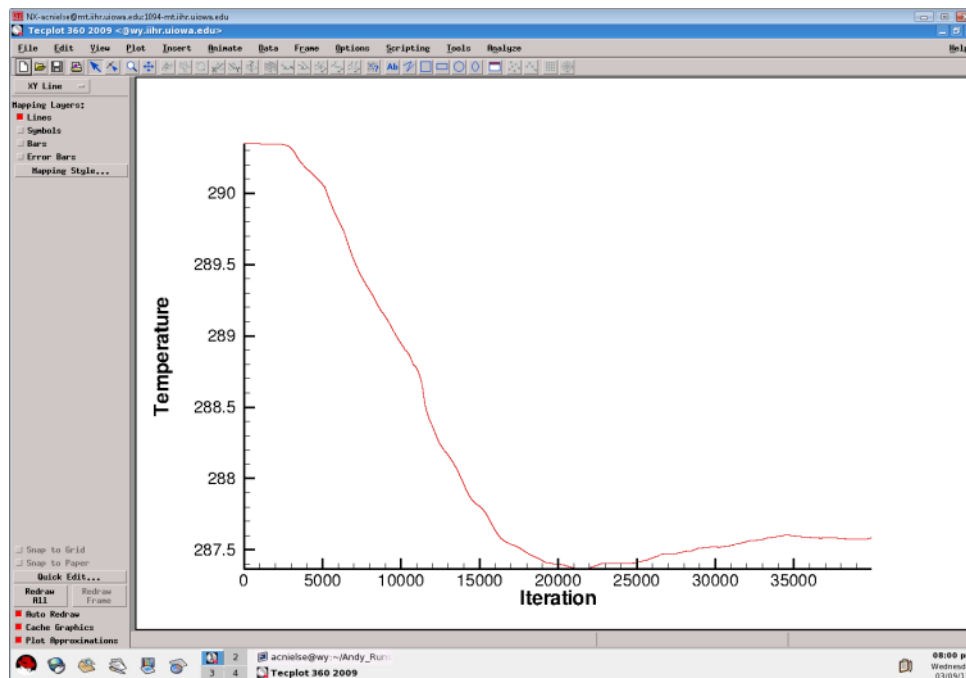


Figure 5.44 Scenario 4 - Lake Union temperature monitor 1

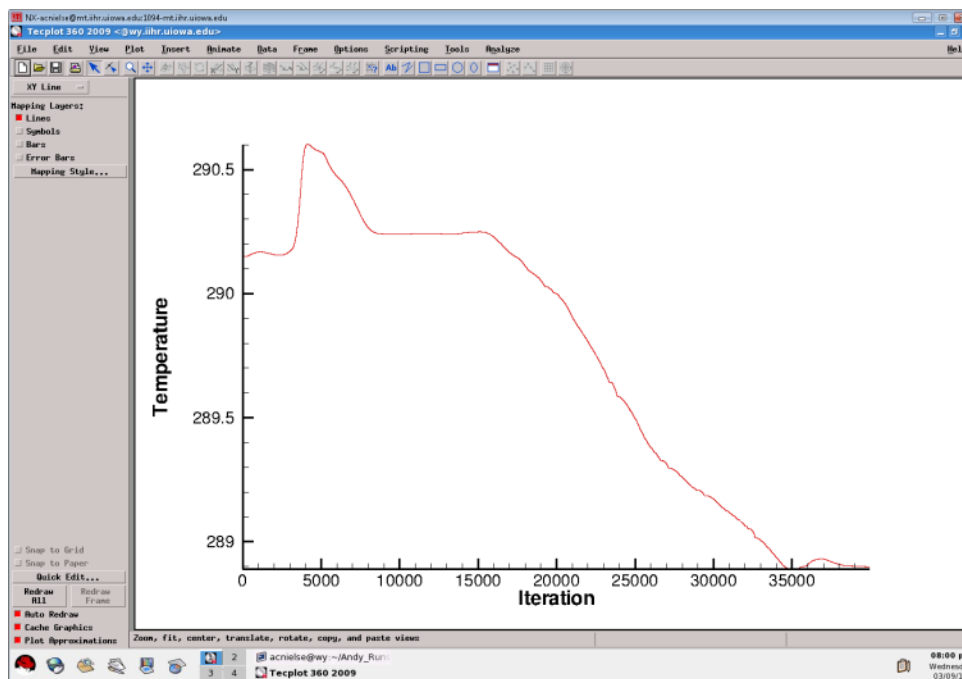


Figure 5.45 Scenario 4 - University Bridge temperature monitor 1

5.2.5 Comparison and Summary of Scenarios 1 through 4

The majority of the monitors did not see changes due to the lock and dam operations over the first 24 hour period. All of the monitors show some of the “noise” going on as the initial conditions that were superimposed on the system began to settle or move due to the hydrodynamics of the model. The salt and temperature monitors that were located directly upstream of the large lock do show concentration and temperature changes that occur with every locking that was modeled.

The general trend in all four models shows that the salt concentration was slowly decreasing at all monitoring locations. This means that the amount of fresh water coming in upstream as well as the amount of salty water leaving the system through the salt water drain, spillways, fish ladder, and lock filling culverts, was greater than the amount of salt being infused into the system at the lock walls.

Table 5.1 shows a summary of the total change in salt in the system over the 24 hour period. Figure 5.46 shows graphically the total salt change in each scenario. The fact that scenario 2 salt concentrations decreased more than scenario 1 shows that a salt concentration of 19 ppt at the locks is not large enough to cause salt to build up in the system with the given locking setup. In fact, the higher number of lockings causes more fresh water from upstream to enter to the system, causing a faster decrease in the overall salt volume in the LWSC.

These results show that there is a refinement needed in the boundary conditions to model the physical conditions more accurately. Chapter 6 discusses some of the approaches that could be used to further the work done by this research.

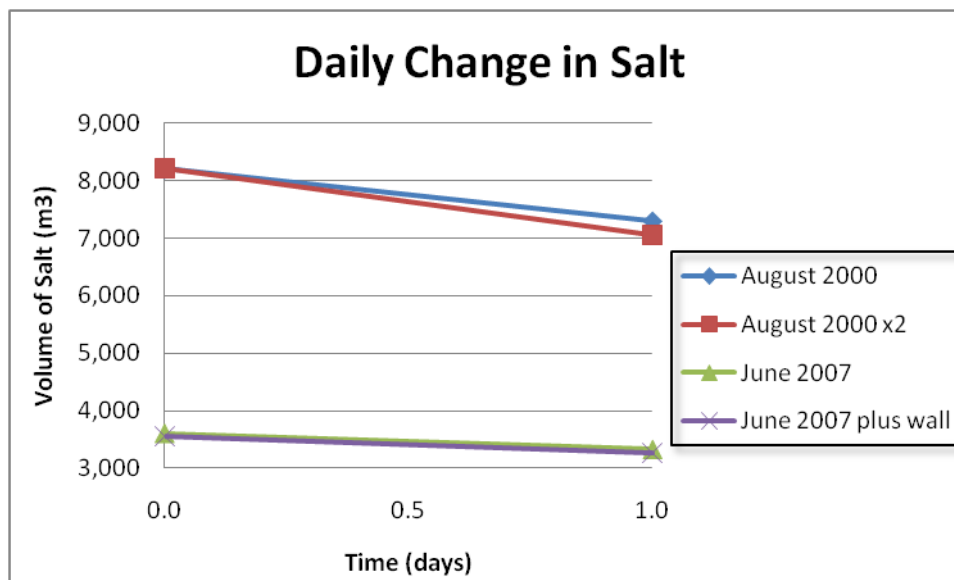


Figure 5.46 Salt Flux over 24 hours

Table 5.1 Salt Flux over 24 hours

#	Scenario	Change in total volume (m ³) of salt in the system		
		t = 0 sec	t = 86,400 sec	Δ salt/day
1	August 2000	8,203	7,298	-905
2	August 2000 x2	8,220	7,052	-1,168
3	June 2007	3,607	3,323	-284
4	June 2007 plus wall	3,551	3,266	-285

CHAPTER 6: SUMMARY AND FUTURE WORK

6.1 Summary

Salmon migration is extremely important in the Pacific Northwest. For many, their way of life depends on the successful migration and spawning of salmon. Improving the water quality and overall habitat for salmon is critical in assuring their future environmental and economic viability.

CFD was used to model the hydrodynamics and species transport of salt in the LWSC. Two historical situations and two hypothetical scenarios were modeled to help better understand the sensitivity of the LWSC system as a whole. These results will be used to simulate the changes in fish migration patterns over a 24 hour period.

6.2 Future Work

Work done in 2004 (Goodwin, 2007) laid the groundwork to show that CFD can accurately model large complex hydrodynamic systems. This work has expanded that model from the area directly around the Ballard Locks, inside the forebay before entering Salmon Bay, to the entire LWSC. This model encompasses the key water bodies and hydraulic structures from the Ballard Locks to the Montlake Cut. Future work that has already been proposed would be to refine the boundary conditions at the lock gates. Instead of modeling the entire LWSC, analyzing a small area directly behind the locks, and looking at trends based on various lock boundary conditions could help determine the most accurate conditions that model the real physical changes. Some of the boundary conditions to analyze would be the salt concentration at the locks, a possible inlet velocity gradient, and comparing fixed lid versus volume of fraction (VOF) models. Using lock operation and large lock monitoring station records one could calibrate the salinity concentrations and velocities that most accurately represent the results that are being seen in the field. The calibration could be done by plotting salt concentration over time and comparing the results to salt concentrations seen at the monitoring station.

Once the lock boundary conditions have been refined, modeling various historical situations in a larger stretch of the LWSC could help validate the accuracy of the model boundary conditions. Once specific guidelines are developed for modeling various locking operations, hypothetical scenarios could be tested to analyze how fish would react to different lock operations.

Two key model parameters that should be carefully studied are giving the salt concentration an initial velocity, and modeling the conditions in a VOF model. Up to this point, the salt plume migration has been modeled almost exclusively as a diffusive process. However, the advective transport developed by the opening of lock gates could drastically affect the overall convection of salt.

If future work encompasses the entire LWSC, it should include longer simulations to model changes throughout the canal over a period greater than 24 hours. Writing a code to simulate the velocity associated with opening the lock gates would allow one to model the velocity “push” that is developed when the gates open. It is possible that this increase in velocity could cause a change in the diffusion of salt upstream.

6.2.1 Model Improvement

The current model is using bathymetric data from a 30 meter resolution bathymetry/topography map obtained from the University of Washington’s School of Oceanography (<http://www.ocean.washington.edu/data/pugetsound/psdem2005.html>). Other data exists that has higher resolution but due to errors in the maps, this data was not able to be used for the project. Increasing the map resolution of the bathymetric data would improve the accuracy of the model. Recently, a new bathymetric survey was done throughout the entire LWSC. Adjusting the model mesh to incorporate more canal bank edge details and using the new 2011 bathymetry data could increase the model geometry detail and possibly improve model results.

6.2.2 Expanding Model Scale

The mesh aspect ratio (squish factor) takes into account the shape of each individual mesh block element. The more stretched an element becomes; the more difficult it is for the model to converge. The aspect ratio increases drastically in shallow water when using a structured mesh because the same number of nodes used in the deep pools and fine detailed sections near the Ballard Locks are used in the shallow areas. Extremely high aspect ratios mean that one or more sides of the box are very small compared to the other sides, thus being “squished.” High aspect ratios can greatly increase the instability of the model. To eliminate the high aspect ratio mesh elements, all shallow areas were removed from the model. The bathymetry of the LWSC encompasses areas with a mean sea level elevation of -30 feet (in Lake Union and by the Ballard Locks) up to areas with a mean sea level elevation of 20 to 22 feet (The entire shoreline of the LWSC). The model only takes into account areas that had an elevation of zero or less. Basically, this means that areas near the shorelines that were shallower than 20 to 22 feet were not included in the model geometry. This was necessary to help the model converge. Developing a model that went all the way out to the bank edges would greatly improve the model fidelity. The most complex geometries of the LWSC are near the banks, because the entire system is surrounded by docks, or concrete walls, the edges become very difficult to model with the many ins and outs of the riverbanks. It is uncertain how pertinent the riverbank edges are to the overall accuracy of the model. However, future models could address this issue.

The USACE Seattle District is directly responsible for salmon moving through the LWSC; understanding the effects surrounding areas, such as Puget Sound or Lake Washington, have on salmon migration would improve the Seattle District’s ability to manage their waterways. Managing the local system successfully can only be accomplished when the surrounding system is understood as well.

REFERENCES

- Berggren, T. J. 1993. An analysis of variables influencing the migration of juvenile salmonids in the columbia river basin. *North American Journal of Fisheries Management* 13 (1): 48.
- Bombardelli, F. A., M. I. Cantero, M. H. Garcia, and G. C. Buscaglia. 2009. Numerical aspects of the simulation of discontinuous saline underflows: The lock-exchange problem. *Journal of Hydraulic Research* 47 (6): 777-789.
- Bombardelli, F. A., M. I. Cantero, G. C. Buscaglia, and M. H. Garcia. 2004b. Comparative study of convergence of CFD commercial codes when simulating dense underflows. *Mecánica Computacional XXIII* (November 2004): 1187-1199.
- Bombardelli, F. A. 2004a. *Turbulence in multiphase models for aeration bubble plumes*.
- Bonnecaze, R. T., H. E. Huppert, and J. R. Lister. 1993. Particle-driven gravity currents. *Journal of Fluid Mechanics* 250 (-1): 339.
- Bournet, P. E., D. Dartus, B. Tassin, and B. Vinçon-Leite. 1999. Numerical investigation of plunging density current. *Journal of Hydraulic Engineering* 125 (6): 584.
- Bradford, S. F., and N. D. Katopodes. 1999. Hydrodynamics of turbid underflows. I: Formulation and numerical analysis. *Journal of Hydraulic Engineering* 125 (10): 1006.
- Cantero, M. I. 2002. *Theoretical and numerical modeling of turbidity currents as two-phase flows*.
- Celedonia, Mark T., Roger A. Tabor, S. Sanders, Daniel W. Lantz, and I. Grettenberger. 2008. Movement and habitat use of juvenile Chinook salmon and two predatory fishes in Lake Washington and the Lake Washington Ship Canal: 2004-05 acoustic tracking studies. U.S. Fish and Wildlife Service, Western Washington Fish and Wildlife Office, Lacey, Washington.
- Celedonia, Mark T., Zhuozhuo Li, Scott T. Sanders, Roger A. Tabor, Terence Lee, Steve Damm, Daniel W. Lantz, and Benjamin E. Price. 2009. Movement and habitat use of chinook salmon smolts in the lake washington ship canal: 2007-2008 acoustic tracking studies. (November 2009).
- Choi, S. U., and M. H. Garcia. 1995. Modeling of one-dimensional turbidity currents with a dissipative-galerkin finite element method. *Journal of Hydraulic Research* 33 (5): 623.
- Crook, N. A., and M. J. Miller. 1985. A numerical and analytical study of atmospheric undular bores. *Quarterly Journal of the Royal Meteorological Society* 111 (463): 225.
- Dallimore, C. J., J. Imberger, and B. R. Hodges. 2004. Modeling a plunging underflow. *Journal of Hydraulic Engineering* 130 (11): 1068.

- Daly, B. J., and W. E. Pracht. 1968. Numerical study of density-□Current surges. *Physics of Fluids* 11 (1): 15.
- De Cesare, G., A. Schleiss, and F. Hermann. 2001. Impact of turbidity currents on reservoir sedimentation. *Journal of Hydraulic Engineering* 127 (1): 6.
- Goodwin, Andrew R., John M. Nestler, SK Ooi, Larry J. Weber, George Constantinescu, Peter Johnson, and David L. Smith. 2007. Ballard locks CFD-NFS project.
- Goodwin, R. A. 2001. Simulating mobile populations in aquatic ecosystems. *Journal of Water Resources Planning and Management* 127 (6): 386.
- Haase, S. P., and R. K. Smith. 1989. The numerical simulation of atmospheric gravity currents. part II. environments with stable layers. *Geophysical and Astrophysical Fluid Dynamics* 46 (1): 35.
- Hodgson, S., and T. P. Quinn. 2002. The timing of adult sockeye salmon migration into fresh water: Adaptations by populations to prevailing thermal regimes. (February 11, 2002).
- Huang, H., J. Imran, and C. Pirmez. 2007. Numerical modeling of poorly sorted depositional turbidity currents. *Journal of Geophysical Research* 112 (c1): C01014.
- Huang, H., J. Imran, and C. Pirmez. 2005. Numerical model of turbidity currents with a deforming bottom boundary. *Journal of Hydraulic Engineering* 131 (4): 283.
- Imran, J., A. Kassem, and S. M. Khan. 2004. Three-dimensional modeling of density current. I. flow in straight confined and unconfined channels. *Journal of Hydraulic Research* 42 (6): 578.
- Kassem, A., and J. Imran. 2004. Three-dimensional modeling of density current. II. flow in sinuous confined and unconfined channels. *Journal of Hydraulic Research* 42 (6): 591.
- Khan, S. M., and J. Imran. 2008. Numerical investigation of turbidity currents flowing through minibasins on the continental slope. *Journal of Sedimentary Research* 78 (4): 245.
- Kramer, D. L. 1987. Dissolved oxygen and fish behavior. *Environmental Biology of Fishes* 18 (2): 81.
- McKillip, Mike, and Scott Wells. 2007. *Lake roosevelt water quality and hydrodynamic model calibration with fish bioenergetics*. EWR-03-06.
- Mitchell, K. E., and J. B. Hovermale. 1977. A numerical investigation of the severe thunderstorm gust front. *Monthly Weather Review* 105 (5): 657.
- Ooi, S. K., S. G. Constantinescu, and L. Weber. 2006. *High resolution numerical simulations of lock-exchange gravity-driven flows*.
- Personal Communication with Frederick Goetz. Seattle ballard locks project meeting. August 10, 2010.

- Personal Communication with Lynne Melder. Seattle ballard locks project meeting. August 10, 2010.
- Rattray, M., G. R. Seckel, and C. A. Barnes. 1954. *Salt budget in the lake washington ship canal system*.
- Rattray, Maurice, and Satish R. Shetye. 1982. *Penetration and dilution of saline water between lake union and lake washington*.
- Simpson, J. E. 1982. Gravity currents in the laboratory, atmosphere, and ocean. *Annual Review of Fluid Mechanics* 14 (1): 213.
- Smith, E. V., and T. G. Thompson. 1927. *Salinity of the lake washington ship canal*. Vol. 41.
- Spotte, Stephen H. 1970. *Fish and invertebrate culture: Water management in closed systems*. 2nd ed. New York; John Wiley & Sons;.
- Straka, J. M., Robert B. Wilhelmson, Louis J. Wicker, John R. Anderson, and Kelvin K. Droegemeier. 1993. Numerical solutions of a non-linear density current: A benchmark solution and comparisons. *International Journal for Numerical Methods in Fluids* 17 (1): 1.
- Timko, M. A., P. A. Nealson, and S. V. Johnston. 2002. Using acoustic tags for monitoring adult chinook salmon behavior at the hiram. M. chittenden locks, summer 2000. (February 22, 2002).
- US Army Corps of Engineers, Seattle Division, and Seattle Public Utilities. 2008. *Synthesis of salmon research and monitoring - investigations conducted in the western lake washington basin*.
- U.S. Government. 1999. U.S. Government Printing Office Pamphlet 1999-791-887: "Lake Washington Ship Canal and Hiram M. Chittenden Locks", p. 3.

APPENDIX

Table A.1 – “Table 9-4. Dissolved Oxygen (mg O₂ l⁻¹) at Saturation in Freshwater, Brackish Water, and Seawater at Different Temperatures. Calculated from Data in Murray and Riley (1969).”

Temperature °C	Chlorinity, %										
	0	2	4	6	8	10	12	14	16	18	20
1	14.24	13.87	13.54	13.22	12.91	12.59	12.29	11.99	11.7	11.42	11.15
2	13.84	13.5	13.18	12.88	12.56	12.26	11.98	11.69	11.4	11.13	10.86
3	13.45	13.14	12.84	12.55	12.25	11.96	11.68	11.39	11.12	10.85	10.59
4	13.09	12.79	12.51	12.22	11.93	11.65	11.38	11.1	10.83	10.59	10.34
5	12.75	12.45	12.18	11.91	11.63	11.36	11.09	10.83	10.57	10.33	10.1
6	12.44	12.15	11.86	11.6	11.33	11.07	10.82	10.56	10.32	10.09	9.86
7	12.13	11.85	11.58	11.32	11.06	10.82	10.56	10.32	10.07	9.84	9.63
8	11.85	11.56	11.29	11.05	10.8	10.56	10.32	10.07	9.84	9.61	9.4
9	11.56	11.29	11.02	10.77	10.54	10.3	10.07	9.84	9.61	9.4	9.2
10	11.29	11.03	10.77	10.53	10.3	10.07	9.84	9.61	9.4	9.2	9
11	11.05	10.77	10.53	10.29	10.07	9.84	9.63	9.41	9.2	9	8.8
12	10.8	10.53	10.29	10.06	9.84	9.63	9.41	9.21	9	8.8	8.61
13	10.56	10.3	10.07	9.84	9.63	9.41	9.21	9.01	8.81	8.61	8.42
14	10.33	10.07	9.86	9.63	9.41	9.21	9.01	8.81	8.62	8.44	8.25
15	10.1	9.86	9.64	9.43	9.23	9.03	8.83	8.64	8.44	8.27	8.09
16	9.89	9.66	9.44	9.24	9.03	8.84	8.64	8.47	8.28	8.11	7.94
17	9.67	9.46	9.26	9.05	8.85	8.65	8.47	8.3	8.11	7.94	7.78
18	9.47	9.27	9.07	8.87	8.67	8.48	8.31	8.14	7.97	7.79	7.64
19	9.28	9.08	8.88	8.68	8.5	8.31	8.15	7.98	7.82*	7.65	7.49
20	9.11	8.9	8.7	8.51	8.32	8.15	7.99	7.84	7.66	7.51	7.36

Table A.1 Continued...

21	8.93	8.72	8.54	8.35	8.17	7.99	7.84	7.69	7.52	7.38	7.23
22	8.75	8.55	8.38	8.19	8.02	7.85	7.69	7.54	7.39	7.25	7.11
23	8.6	8.4	8.22	8.04	7.87	7.71	7.55	7.41	7.26	7.12	6.99
24	8.44	8.25	8.07	7.89	7.72	7.56	7.42	7.28	7.13	6.99	6.86
25	8.27	8.09	7.92	7.75	7.58	7.44	7.29	7.15	7.01	6.88	6.75
26	8.12	7.94	7.78	7.62	7.45	7.31	7.16	7.03	6.89	6.76	6.63
27	7.98	7.79	7.64	7.49	7.32	7.18	7.03	6.91	6.78	6.65	6.52
28	7.84	7.65	7.51	7.36	7.19	7.06	6.92	6.79	6.66	6.53	6.4
29	7.69	7.52	7.38	7.23	7.08	6.95	6.82	6.68	6.55	6.42	6.29
30	7.56	7.39	7.25	7.12	6.96	6.83	6.7	6.58	6.45	6.32	6.19

(Stephen Spotte. "Fish and Invertebrate Culture Water Management In Closed Systems. 2nd Edition." pg. 142.)

*The value at 16% Chlorinity and 19 °C had a typo in Spotte's book, therefore it was interpolated.

Based on Equation A.1 derived by (Wooster W.S., A.J. Lee, and G. Dietrich. 1969.), Table A.1 was converted into a table of

(A.1)

DO values based on temperature and salinity. This table was then graphed and converted into a 6th order polynomial equation

(Equation A.2) that accurately represents the values in Table A.2. This equation was then used in FLUENT to mathematically solve for

the DO level of every cell in the model.

Table A.2 – DO (mg/l) based on varying salinity concentrations (ppt) and water temperature (°C).

Created by Adam Nielsen 9-8-2010

Temperature °C	Salinity, ppt										
	0	2	4	6	8	10	12	14	16	18	20
0	14.56	14.38	14.20	14.02	13.83	13.65	13.47	13.29	13.11	12.93	12.75
1	14.16	13.98	13.81	13.64	13.47	13.30	13.12	12.95	12.78	12.61	12.44
2	13.77	13.61	13.44	13.28	13.11	12.95	12.79	12.62	12.46	12.29	12.13
3	13.40	13.24	13.09	12.93	12.77	12.61	12.46	12.30	12.14	11.98	11.83
4	13.05	12.90	12.75	12.59	12.44	12.29	12.14	11.99	11.84	11.68	11.53
5	12.71	12.57	12.42	12.27	12.13	11.98	11.83	11.69	11.54	11.39	11.24
6	12.39	12.25	12.11	11.96	11.82	11.68	11.54	11.39	11.25	11.11	10.97
7	12.08	11.94	11.81	11.67	11.53	11.39	11.25	11.12	10.98	10.84	10.70
8	11.79	11.65	11.52	11.39	11.25	11.12	10.98	10.85	10.71	10.58	10.45
9	11.51	11.38	11.25	11.11	10.98	10.85	10.72	10.59	10.46	10.33	10.20
10	11.24	11.11	10.98	10.86	10.73	10.60	10.47	10.35	10.22	10.09	9.97
11	10.98	10.85	10.73	10.61	10.48	10.36	10.24	10.11	9.99	9.87	9.74
12	10.73	10.61	10.49	10.37	10.25	10.13	10.01	9.89	9.77	9.65	9.53
13	10.49	10.38	10.26	10.14	10.03	9.91	9.79	9.68	9.56	9.44	9.33
14	10.26	10.15	10.04	9.92	9.81	9.70	9.58	9.47	9.36	9.24	9.13
15	10.05	9.93	9.82	9.71	9.60	9.49	9.38	9.27	9.16	9.05	8.94
16	9.83	9.73	9.62	9.51	9.40	9.30	9.19	9.08	8.98	8.87	8.76
17	9.63	9.53	9.42	9.32	9.21	9.11	9.00	8.90	8.80	8.69	8.59
18	9.43	9.33	9.23	9.13	9.03	8.93	8.83	8.72	8.62	8.52	8.42
19	9.24	9.14	9.05	8.95	8.85	8.75	8.65	8.55	8.46	8.36	8.26
20	9.06	8.96	8.87	8.77	8.68	8.58	8.49	8.39	8.30	8.20	8.10
21	8.88	8.79	8.70	8.60	8.51	8.42	8.32	8.23	8.14	8.05	7.95

Table A.2 Continued...

22	8.71	8.62	8.53	8.44	8.35	8.26	8.17	8.08	7.99	7.90	7.81
23	8.54	8.45	8.37	8.28	8.19	8.10	8.02	7.93	7.84	7.75	7.66
24	8.38	8.30	8.21	8.12	8.04	7.95	7.87	7.78	7.70	7.61	7.53
25	8.23	8.14	8.06	7.98	7.89	7.81	7.72	7.64	7.56	7.47	7.39
26	8.08	7.99	7.91	7.83	7.75	7.67	7.59	7.50	7.42	7.34	7.26
27	7.93	7.85	7.77	7.69	7.61	7.53	7.45	7.37	7.29	7.21	7.13
28	7.79	7.71	7.63	7.56	7.48	7.40	7.32	7.24	7.17	7.09	7.01
29	7.65	7.58	7.50	7.42	7.35	7.27	7.20	7.12	7.04	6.97	6.89
30	7.52	7.45	7.37	7.30	7.22	7.15	7.07	7.00	6.92	6.85	6.77
32	7.28	7.20	7.13	7.06	6.99	6.91	6.84	6.77	6.70	6.63	6.55
34	7.04	6.98	6.91	6.84	6.77	6.70	6.63	6.56	6.49	6.42	6.35
36	6.83	6.76	6.69	6.63	6.56	6.49	6.42	6.35	6.29	6.22	6.15
38	6.62	6.55	6.49	6.42	6.36	6.29	6.22	6.16	6.09	6.02	5.96
40	6.42	6.35	6.28	6.22	6.15	6.08	6.02	5.95	5.88	5.82	5.75

-

(A.2)

DATUM PLANES VICINITY OF LAKE WASHINGTON

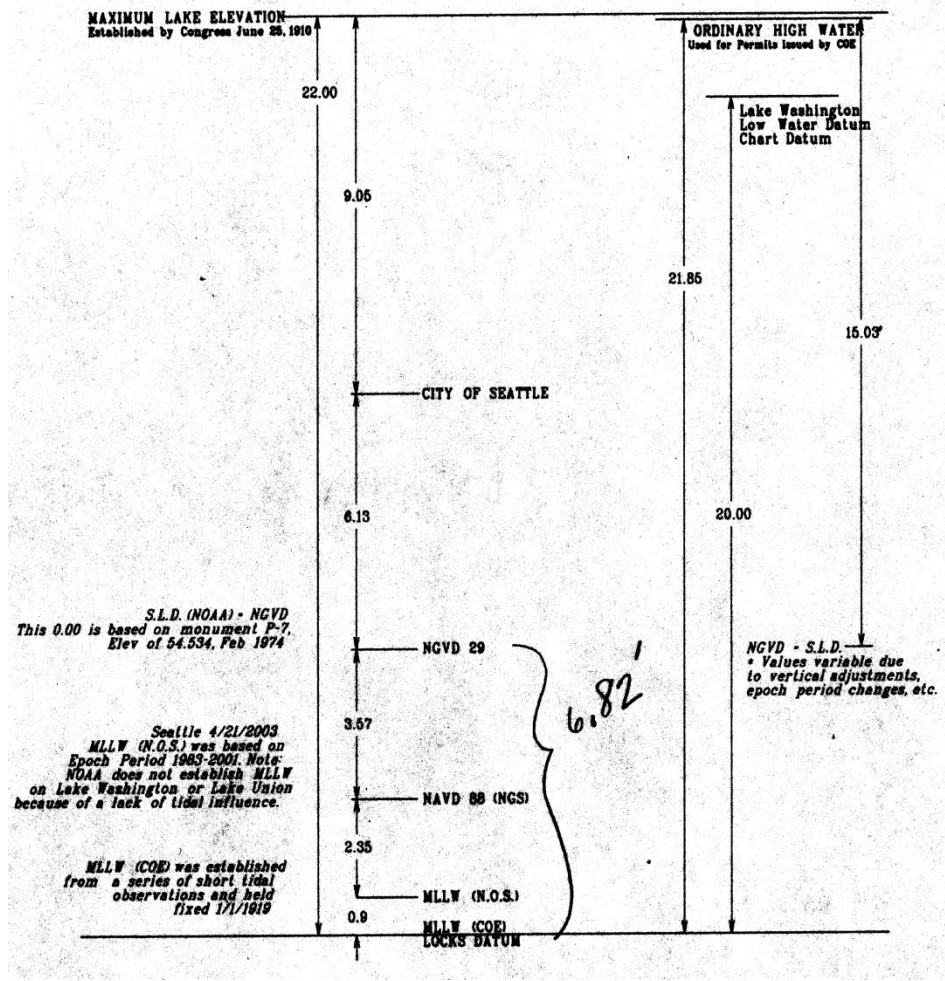


Figure A.1 Datum planes in the vicinity of Lake Washington

Table A.3 Scenario 1 Boundary Conditions in 15 min increments

Average August 2000 Day Set up										
August (15-30) 2000	Lock Operations				Outlet Setup				MassInlet-Flow	Outlet Total
	Small Lock	Large Lock	Small Lock FC	Large Lock FC	SWD	large lock filling culvert	small lock filling culverts	fish ladder		
12:00 AM	Open	Closed	Closed	Closed	0.8959	0.0000	0.0000	0.1041	6258.02	1
12:15 AM	Closed	Closed	Closed	Closed	0.8959	0.0000	0.0000	0.1041	6258.02	1
12:30 AM	Closed	Closed	Closed	Closed	0.8959	0.0000	0.0000	0.1041	6258.02	1
12:45 AM	Closed	Closed	Closed	Closed	0.8959	0.0000	0.0000	0.1041	6258.02	1
1:00 AM	Closed	Closed	Closed	Closed	0.8959	0.0000	0.0000	0.1041	6258.02	1
1:15 AM	Closed	Closed	Closed	Closed	0.8959	0.0000	0.0000	0.1041	6258.02	1
1:30 AM	Closed	Closed	Closed	Closed	0.8959	0.0000	0.0000	0.1041	6258.02	1
1:45 AM	Closed	Closed	Closed	Open	0.2288	0.7446	0.0000	0.0266	24506.64	1
2:00 AM	Closed	Open	Closed	Closed	0.8959	0.0000	0.0000	0.1041	6258.02	1
2:15 AM	Closed	Open	Closed	Closed	0.8959	0.0000	0.0000	0.1041	6258.02	1
2:30 AM	Closed	Open	Closed	Closed	0.8959	0.0000	0.0000	0.1041	6258.02	1
2:45 AM	Closed	Closed	Open	Closed	0.6284	0.0000	0.2986	0.0730	8922.64	1
3:00 AM	Open	Closed	Closed	Closed	0.8959	0.0000	0.0000	0.1041	6258.02	1
3:15 AM	Closed	Closed	Closed	Closed	0.8959	0.0000	0.0000	0.1041	6258.02	1
3:30 AM	Closed	Closed	Closed	Closed	0.8959	0.0000	0.0000	0.1041	6258.02	1
3:45 AM	Closed	Closed	Closed	Closed	0.8959	0.0000	0.0000	0.1041	6258.02	1
4:00 AM	Closed	Closed	Closed	Closed	0.8959	0.0000	0.0000	0.1041	6258.02	1
4:15 AM	Closed	Closed	Closed	Closed	0.8959	0.0000	0.0000	0.1041	6258.02	1
4:30 AM	Closed	Closed	Closed	Closed	0.8959	0.0000	0.0000	0.1041	6258.02	1
4:45 AM	Closed	Closed	Closed	Open	0.2288	0.7446	0.0000	0.0266	24506.64	1
5:00 AM	Closed	Open	Closed	Closed	0.8959	0.0000	0.0000	0.1041	6258.02	1
5:15 AM	Closed	Open	Closed	Closed	0.8959	0.0000	0.0000	0.1041	6258.02	1
5:30 AM	Closed	Open	Closed	Closed	0.8959	0.0000	0.0000	0.1041	6258.02	1
5:45 AM	Closed	Closed	Open	Closed	0.6284	0.0000	0.2986	0.0730	8922.64	1
6:00 AM	Open	Closed	Closed	Closed	0.8959	0.0000	0.0000	0.1041	6258.02	1
6:15 AM	Closed	Closed	Closed	Closed	0.8959	0.0000	0.0000	0.1041	6258.02	1
6:30 AM	Closed	Closed	Open	Closed	0.6284	0.0000	0.2986	0.0730	8922.64	1
6:45 AM	Open	Closed	Closed	Closed	0.8959	0.0000	0.0000	0.1041	6258.02	1
7:00 AM	Closed	Closed	Closed	Closed	0.8959	0.0000	0.0000	0.1041	6258.02	1
7:15 AM	Closed	Closed	Open	Closed	0.6284	0.0000	0.2986	0.0730	8922.64	1
7:30 AM	Open	Closed	Closed	Closed	0.8959	0.0000	0.0000	0.1041	6258.02	1
7:45 AM	Closed	Closed	Closed	Open	0.2288	0.7446	0.0000	0.0266	24506.64	1
8:00 AM	Closed	Open	Open	Closed	0.6284	0.0000	0.2986	0.0730	8922.64	1
8:15 AM	Open	Open	Closed	Closed	0.8959	0.0000	0.0000	0.1041	6258.02	1
8:30 AM	Closed	Open	Closed	Closed	0.8959	0.0000	0.0000	0.1041	6258.02	1
8:45 AM	Closed	Closed	Open	Closed	0.6284	0.0000	0.2986	0.0730	8922.64	1
9:00 AM	Open	Closed	Closed	Closed	0.8959	0.0000	0.0000	0.1041	6258.02	1
9:15 AM	Closed	Closed	Closed	Closed	0.8959	0.0000	0.0000	0.1041	6258.02	1
9:30 AM	Closed	Closed	Open	Closed	0.6284	0.0000	0.2986	0.0730	8922.64	1
9:45 AM	Open	Closed	Closed	Closed	0.8959	0.0000	0.0000	0.1041	6258.02	1
10:00 AM	Closed	Closed	Open	Closed	0.6284	0.0000	0.2986	0.0730	8922.64	1
10:15 AM	Open	Closed	Closed	Closed	0.8959	0.0000	0.0000	0.1041	6258.02	1
10:30 AM	Closed	Closed	Open	Closed	0.6284	0.0000	0.2986	0.0730	8922.64	1
10:45 AM	Open	Closed	Closed	Open	0.2288	0.7446	0.0000	0.0266	24506.64	1
11:00 AM	Closed	Open	Open	Closed	0.6284	0.0000	0.2986	0.0730	8922.64	1
11:15 AM	Open	Open	Closed	Closed	0.8959	0.0000	0.0000	0.1041	6258.02	1
11:30 AM	Closed	Open	Open	Closed	0.6284	0.0000	0.2986	0.0730	8922.64	1
11:45 AM	Open	Closed	Closed	Closed	0.8959	0.0000	0.0000	0.1041	6258.02	1
12:00 PM	Closed	Closed	Closed	Closed	0.8959	0.0000	0.0000	0.1041	6258.02	1

Scenario 1 Boundary Conditions in 15 min increments continued...

12:00 PM	Closed	Closed	Closed	Closed	0.8959	0.0000	0.0000	0.1041	6258.02	1
12:15 PM	Closed	Closed	Open	Closed	0.6284	0.0000	0.2986	0.0730	8922.64	1
12:30 PM	Open	Closed	Closed	Closed	0.8959	0.0000	0.0000	0.1041	6258.02	1
12:45 PM	Closed	Closed	Closed	Open	0.2288	0.7446	0.0000	0.0266	24506.64	1
1:00 PM	Closed	Open	Open	Closed	0.6284	0.0000	0.2986	0.0730	8922.64	1
1:15 PM	Open	Open	Closed	Closed	0.8959	0.0000	0.0000	0.1041	6258.02	1
1:30 PM	Closed	Open	Closed	Closed	0.8959	0.0000	0.0000	0.1041	6258.02	1
1:45 PM	Closed	Closed	Open	Closed	0.6284	0.0000	0.2986	0.0730	8922.64	1
2:00 PM	Open	Closed	Closed	Closed	0.8959	0.0000	0.0000	0.1041	6258.02	1
2:15 PM	Closed	Closed	Closed	Closed	0.8959	0.0000	0.0000	0.1041	6258.02	1
2:30 PM	Closed	Closed	Open	Closed	0.6284	0.0000	0.2986	0.0730	8922.64	1
2:45 PM	Open	Closed	Closed	Open	0.2288	0.7446	0.0000	0.0266	24506.64	1
3:00 PM	Closed	Open	Closed	Closed	0.8959	0.0000	0.0000	0.1041	6258.02	1
3:15 PM	Closed	Open	Open	Closed	0.6284	0.0000	0.2986	0.0730	8922.64	1
3:30 PM	Open	Open	Closed	Closed	0.8959	0.0000	0.0000	0.1041	6258.02	1
3:45 PM	Closed	Closed	Open	Closed	0.6284	0.0000	0.2986	0.0730	8922.64	1
4:00 PM	Open	Closed	Closed	Closed	0.8959	0.0000	0.0000	0.1041	6258.02	1
4:15 PM	Closed	Closed	Open	Closed	0.6284	0.0000	0.2986	0.0730	8922.64	1
4:30 PM	Open	Closed	Closed	Closed	0.8959	0.0000	0.0000	0.1041	6258.02	1
4:45 PM	Closed	Closed	Open	Open	0.2063	0.6716	0.0981	0.0240	27171.26	1
5:00 PM	Open	Open	Closed	Closed	0.8959	0.0000	0.0000	0.1041	6258.02	1
5:15 PM	Closed	Open	Open	Closed	0.6284	0.0000	0.2986	0.0730	8922.64	1
5:30 PM	Open	Open	Closed	Closed	0.8959	0.0000	0.0000	0.1041	6258.02	1
5:45 PM	Closed	Closed	Open	Closed	0.6284	0.0000	0.2986	0.0730	8922.64	1
6:00 PM	Open	Closed	Closed	Closed	0.8959	0.0000	0.0000	0.1041	6258.02	1
6:15 PM	Closed	Closed	Open	Closed	0.6284	0.0000	0.2986	0.0730	8922.64	1
6:30 PM	Open	Closed	Closed	Closed	0.8959	0.0000	0.0000	0.1041	6258.02	1
6:45 PM	Closed	Closed	Open	Open	0.2063	0.6716	0.0981	0.0240	27171.26	1
7:00 PM	Open	Open	Closed	Closed	0.8959	0.0000	0.0000	0.1041	6258.02	1
7:15 PM	Closed	Open	Open	Closed	0.6284	0.0000	0.2986	0.0730	8922.64	1
7:30 PM	Open	Open	Closed	Closed	0.8959	0.0000	0.0000	0.1041	6258.02	1
7:45 PM	Closed	Closed	Open	Closed	0.6284	0.0000	0.2986	0.0730	8922.64	1
8:00 PM	Open	Closed	Closed	Closed	0.8959	0.0000	0.0000	0.1041	6258.02	1
8:15 PM	Closed	Closed	Open	Closed	0.6284	0.0000	0.2986	0.0730	8922.64	1
8:30 PM	Open	Closed	Closed	Closed	0.8959	0.0000	0.0000	0.1041	6258.02	1
8:45 PM	Closed	Closed	Open	Open	0.2063	0.6716	0.0981	0.0240	27171.26	1
9:00 PM	Open	Open	Closed	Closed	0.8959	0.0000	0.0000	0.1041	6258.02	1
9:15 PM	Closed	Open	Closed	Closed	0.8959	0.0000	0.0000	0.1041	6258.02	1
9:30 PM	Closed	Open	Open	Closed	0.6284	0.0000	0.2986	0.0730	8922.64	1
9:45 PM	Open	Closed	Closed	Closed	0.8959	0.0000	0.0000	0.1041	6258.02	1
10:00 PM	Closed	Closed	Closed	Closed	0.8959	0.0000	0.0000	0.1041	6258.02	1
10:15 PM	Closed	Closed	Open	Closed	0.6284	0.0000	0.2986	0.0730	8922.64	1
10:30 PM	Open	Closed	Closed	Closed	0.8959	0.0000	0.0000	0.1041	6258.02	1
10:45 PM	Closed	Closed	Closed	Open	0.2288	0.7446	0.0000	0.0266	24506.64	1
11:00 PM	Closed	Open	Open	Closed	0.6284	0.0000	0.2986	0.0730	8922.64	1
11:15 PM	Open	Open	Closed	Closed	0.8959	0.0000	0.0000	0.1041	6258.02	1
11:30 PM	Closed	Open	Closed	Closed	0.8959	0.0000	0.0000	0.1041	6258.02	1
11:45 PM	Closed	Closed	Open	Closed	0.6284	0.0000	0.2986	0.0730	8922.64	1

Table A.4 Scenario 2 Boundary Conditions in 15 min increments

Average August 2000 (s2) Day Set up										
August (15-30) 2000	Lock Operations				Outlet Setup				Mass Inlet-Flow	Outlet Total
	Small Lock	Large Lock	Small Lock FC	Large Lock FC	SVD	large lock filling culvert	small lock filling culverts	fish ladder		
12:00 AM	Open	Open	Closed	Closed	0.8959	0.0000	0.0000	0.1041	6258.02	1
12:15 AM	Closed	Open	Open	Closed	0.6284	0.0000	0.2986	0.0730	8922.64	1
12:30 AM	Open	Open	Closed	Closed	0.8959	0.0000	0.0000	0.1041	6258.02	1
12:45 AM	Closed	Closed	Open	Closed	0.6284	0.0000	0.2986	0.0730	8922.64	1
1:00 AM	Open	Closed	Closed	Open	0.2288	0.7446	0.0000	0.0266	24506.64	1
1:15 AM	Closed	Open	Open	Closed	0.6284	0.0000	0.2986	0.0730	8922.64	1
1:30 AM	Open	Open	Closed	Closed	0.8959	0.0000	0.0000	0.1041	6258.02	1
1:45 AM	Closed	Open	Open	Closed	0.6284	0.0000	0.2986	0.0730	8922.64	1
2:00 AM	Open	Closed	Closed	Closed	0.8959	0.0000	0.0000	0.1041	6258.02	1
2:15 AM	Closed	Closed	Open	Open	0.2063	0.6716	0.0981	0.0240	27171.26	1
2:30 AM	Open	Open	Closed	Closed	0.8959	0.0000	0.0000	0.1041	6258.02	1
2:45 AM	Closed	Open	Open	Closed	0.6284	0.0000	0.2986	0.0730	8922.64	1
3:00 AM	Open	Open	Closed	Closed	0.8959	0.0000	0.0000	0.1041	6258.02	1
3:15 AM	Closed	Closed	Open	Closed	0.6284	0.0000	0.2986	0.0730	8922.64	1
3:30 AM	Open	Closed	Closed	Open	0.2288	0.7446	0.0000	0.0266	24506.64	1
3:45 AM	Closed	Open	Open	Closed	0.6284	0.0000	0.2986	0.0730	8922.64	1
4:00 AM	Open	Open	Closed	Closed	0.8959	0.0000	0.0000	0.1041	6258.02	1
4:15 AM	Closed	Open	Open	Closed	0.6284	0.0000	0.2986	0.0730	8922.64	1
4:30 AM	Open	Closed	Closed	Closed	0.8959	0.0000	0.0000	0.1041	6258.02	1
4:45 AM	Closed	Closed	Open	Open	0.2063	0.6716	0.0981	0.0240	27171.26	1
5:00 AM	Open	Open	Closed	Closed	0.8959	0.0000	0.0000	0.1041	6258.02	1
5:15 AM	Closed	Open	Open	Closed	0.6284	0.0000	0.2986	0.0730	8922.64	1
5:30 AM	Open	Open	Closed	Closed	0.8959	0.0000	0.0000	0.1041	6258.02	1
5:45 AM	Closed	Closed	Open	Closed	0.6284	0.0000	0.2986	0.0730	8922.64	1
6:00 AM	Open	Closed	Closed	Open	0.2288	0.7446	0.0000	0.0266	24506.64	1
6:15 AM	Closed	Open	Open	Closed	0.6284	0.0000	0.2986	0.0730	8922.64	1
6:30 AM	Open	Open	Closed	Closed	0.8959	0.0000	0.0000	0.1041	6258.02	1
6:45 AM	Closed	Open	Open	Closed	0.6284	0.0000	0.2986	0.0730	8922.64	1
7:00 AM	Open	Closed	Closed	Closed	0.8959	0.0000	0.0000	0.1041	6258.02	1
7:15 AM	Closed	Closed	Open	Open	0.2063	0.6716	0.0981	0.0240	27171.26	1
7:30 AM	Open	Open	Closed	Closed	0.8959	0.0000	0.0000	0.1041	6258.02	1
7:45 AM	Closed	Open	Open	Closed	0.6284	0.0000	0.2986	0.0730	8922.64	1
8:00 AM	Open	Open	Closed	Closed	0.8959	0.0000	0.0000	0.1041	6258.02	1
8:15 AM	Closed	Closed	Open	Closed	0.6284	0.0000	0.2986	0.0730	8922.64	1
8:30 AM	Open	Closed	Closed	Open	0.2288	0.7446	0.0000	0.0266	24506.64	1
8:45 AM	Closed	Open	Open	Closed	0.6284	0.0000	0.2986	0.0730	8922.64	1
9:00 AM	Open	Open	Closed	Closed	0.8959	0.0000	0.0000	0.1041	6258.02	1
9:15 AM	Closed	Open	Open	Closed	0.6284	0.0000	0.2986	0.0730	8922.64	1
9:30 AM	Open	Closed	Closed	Closed	0.8959	0.0000	0.0000	0.1041	6258.02	1
9:45 AM	Closed	Closed	Open	Open	0.2063	0.6716	0.0981	0.0240	27171.26	1
10:00 AM	Open	Open	Closed	Closed	0.8959	0.0000	0.0000	0.1041	6258.02	1
10:15 AM	Closed	Open	Open	Closed	0.6284	0.0000	0.2986	0.0730	8922.64	1
10:30 AM	Open	Open	Closed	Closed	0.8959	0.0000	0.0000	0.1041	6258.02	1
10:45 AM	Closed	Closed	Open	Closed	0.6284	0.0000	0.2986	0.0730	8922.64	1
11:00 AM	Open	Closed	Closed	Open	0.2288	0.7446	0.0000	0.0266	24506.64	1
11:15 AM	Closed	Open	Open	Closed	0.6284	0.0000	0.2986	0.0730	8922.64	1
11:30 AM	Open	Open	Closed	Closed	0.8959	0.0000	0.0000	0.1041	6258.02	1
11:45 AM	Closed	Open	Open	Closed	0.6284	0.0000	0.2986	0.0730	8922.64	1
12:00 PM	Open	Closed	Closed	Closed	0.8959	0.0000	0.0000	0.1041	6258.02	1

Scenario 2 Boundary Conditions in 15 min increments continued...

12:00 PM	Open	Closed	Closed	Closed	0.8959	0.0000	0.0000	0.1041	6258.02	1
12:15 PM	Closed	Closed	Open	Open	0.2063	0.6716	0.0981	0.0240	27171.26	1
12:30 PM	Open	Open	Closed	Closed	0.8959	0.0000	0.0000	0.1041	6258.02	1
12:45 PM	Closed	Open	Open	Closed	0.6284	0.0000	0.2986	0.0730	8922.64	1
1:00 PM	Open	Open	Closed	Closed	0.8959	0.0000	0.0000	0.1041	6258.02	1
1:15 PM	Closed	Closed	Open	Closed	0.6284	0.0000	0.2986	0.0730	8922.64	1
1:30 PM	Open	Closed	Closed	Open	0.2288	0.7446	0.0000	0.0266	24506.64	1
1:45 PM	Closed	Open	Open	Closed	0.6284	0.0000	0.2986	0.0730	8922.64	1
2:00 PM	Open	Open	Open	Closed	0.6284	0.0000	0.2986	0.0730	8922.64	1
2:15 PM	Open	Open	Open	Closed	0.6284	0.0000	0.2986	0.0730	8922.64	1
2:30 PM	Open	Closed	Open	Closed	0.6284	0.0000	0.2986	0.0730	8922.64	1
2:45 PM	Open	Closed	Open	Open	0.2063	0.6716	0.0981	0.0240	27171.26	1
3:00 PM	Open	Open	Open	Closed	0.6284	0.0000	0.2986	0.0730	8922.64	1
3:15 PM	Open	Open	Open	Closed	0.6284	0.0000	0.2986	0.0730	8922.64	1
3:30 PM	Open	Open	Open	Closed	0.6284	0.0000	0.2986	0.0730	8922.64	1
3:45 PM	Open	Closed	Open	Open	0.2063	0.6716	0.0981	0.0240	27171.26	1
4:00 PM	Open	Open	Open	Closed	0.6284	0.0000	0.2986	0.0730	8922.64	1
4:15 PM	Open	Open	Open	Closed	0.6284	0.0000	0.2986	0.0730	8922.64	1
4:30 PM	Open	Open	Open	Closed	0.6284	0.0000	0.2986	0.0730	8922.64	1
4:45 PM	Open	Closed	Open	Open	0.2063	0.6716	0.0981	0.0240	27171.26	1
5:00 PM	Open	Open	Open	Closed	0.6284	0.0000	0.2986	0.0730	8922.64	1
5:15 PM	Open	Open	Open	Closed	0.6284	0.0000	0.2986	0.0730	8922.64	1
5:30 PM	Open	Open	Open	Closed	0.6284	0.0000	0.2986	0.0730	8922.64	1
5:45 PM	Open	Closed	Open	Open	0.2063	0.6716	0.0981	0.0240	27171.26	1
6:00 PM	Open	Open	Open	Closed	0.6284	0.0000	0.2986	0.0730	8922.64	1
6:15 PM	Open	Open	Open	Closed	0.6284	0.0000	0.2986	0.0730	8922.64	1
6:30 PM	Open	Open	Open	Closed	0.6284	0.0000	0.2986	0.0730	8922.64	1
6:45 PM	Open	Closed	Open	Open	0.2063	0.6716	0.0981	0.0240	27171.26	1
7:00 PM	Open	Open	Open	Closed	0.6284	0.0000	0.2986	0.0730	8922.64	1
7:15 PM	Open	Open	Open	Closed	0.6284	0.0000	0.2986	0.0730	8922.64	1
7:30 PM	Open	Open	Open	Closed	0.6284	0.0000	0.2986	0.0730	8922.64	1
7:45 PM	Open	Closed	Open	Open	0.2063	0.6716	0.0981	0.0240	27171.26	1
8:00 PM	Open	Open	Open	Closed	0.6284	0.0000	0.2986	0.0730	8922.64	1
8:15 PM	Open	Open	Open	Closed	0.6284	0.0000	0.2986	0.0730	8922.64	1
8:30 PM	Open	Open	Open	Closed	0.6284	0.0000	0.2986	0.0730	8922.64	1
8:45 PM	Open	Closed	Open	Closed	0.6284	0.0000	0.2986	0.0730	8922.64	1
9:00 PM	Open	Closed	Closed	Open	0.2288	0.7446	0.0000	0.0266	24506.64	1
9:15 PM	Closed	Open	Open	Closed	0.6284	0.0000	0.2986	0.0730	8922.64	1
9:30 PM	Open	Open	Closed	Closed	0.8959	0.0000	0.0000	0.1041	6258.02	1
9:45 PM	Closed	Open	Open	Closed	0.6284	0.0000	0.2986	0.0730	8922.64	1
10:00 PM	Open	Closed	Closed	Closed	0.8959	0.0000	0.0000	0.1041	6258.02	1
10:15 PM	Closed	Closed	Open	Open	0.2063	0.6716	0.0981	0.0240	27171.26	1
10:30 PM	Open	Open	Closed	Closed	0.8959	0.0000	0.0000	0.1041	6258.02	1
10:45 PM	Closed	Open	Open	Closed	0.6284	0.0000	0.2986	0.0730	8922.64	1
11:00 PM	Open	Open	Closed	Closed	0.8959	0.0000	0.0000	0.1041	6258.02	1
11:15 PM	Closed	Closed	Open	Closed	0.6284	0.0000	0.2986	0.0730	8922.64	1
11:30 PM	Open	Closed	Closed	Closed	0.8959	0.0000	0.0000	0.1041	6258.02	1
11:45 PM	Closed	Closed	Open	Open	0.2063	0.6716	0.0981	0.0240	27171.26	1

Table A.5 Scenario 3 and 4 Boundary Conditions in 15 min increments

Specific Day Set up											
June (10-25) 2007	Small Lock	Large Lock	Small Lock fe	Large Lock fe	SVD	large lock filling culvert	small lock filling culverts	fish ladder	Massinlet-Flow	Spillway	total
12:00 AM	Closed	Closed	Closed	Closed	0.4708	0.0000	0.00000	0.0722	902146	0.4570	10000
12:15 AM	Closed	Closed	Closed	Closed	0.4708	0.0000	0.00000	0.0722	902146	0.4570	10000
12:30 AM	Closed	Closed	Closed	Closed	0.4708	0.0000	0.00000	0.0722	902146	0.4570	10000
12:45 AM	Closed	Closed	Closed	Closed	0.4708	0.0000	0.00000	0.0722	902146	0.4570	10000
1:00 AM	Closed	Closed	Closed	Closed	0.4708	0.0000	0.00000	0.0722	902146	0.4570	10000
1:15 AM	Closed	Closed	Closed	Closed	0.4708	0.0000	0.00000	0.0722	902146	0.4570	10000
1:30 AM	Closed	Closed	Closed	Closed	0.4708	0.0000	0.00000	0.0722	902146	0.4570	10000
1:45 AM	Closed	Closed	Closed	Closed	0.4708	0.0000	0.00000	0.0722	902146	0.4570	10000
2:00 AM	Closed	Closed	Closed	Closed	0.4708	0.0000	0.00000	0.0722	902146	0.4570	10000
2:15 AM	Closed	Closed	Closed	Closed	0.4708	0.0000	0.00000	0.0722	902146	0.4570	10000
2:30 AM	Closed	Closed	Closed	Closed	0.4708	0.0000	0.00000	0.0722	902146	0.4570	10000
2:45 AM	Closed	Closed	Closed	Open	0.1858	0.6692	0.00000	0.0239	27270.09	0.1511	10000
3:00 AM	Closed	Open	Closed	Closed	0.4708	0.0000	0.00000	0.0722	902146	0.4570	10000
3:15 AM	Closed	Open	Closed	Closed	0.4708	0.0000	0.00000	0.0722	902146	0.4570	10000
3:30 AM	Closed	Open	Closed	Closed	0.4708	0.0000	0.00000	0.0722	902146	0.4570	10000
3:45 AM	Closed	Closed	Closed	Closed	0.4708	0.0000	0.00000	0.0722	902146	0.4570	10000
4:00 AM	Closed	Closed	Closed	Closed	0.4708	0.0000	0.00000	0.0722	902146	0.4570	10000
4:15 AM	Closed	Closed	Closed	Closed	0.4708	0.0000	0.00000	0.0722	902146	0.4570	10000
4:30 AM	Closed	Closed	Closed	Closed	0.4708	0.0000	0.00000	0.0722	902146	0.4570	10000
4:45 AM	Closed	Closed	Open	Closed	0.3331	0.0000	0.16510	0.0603	10805.43	0.3815	10000
5:00 AM	Open	Closed	Closed	Closed	0.4708	0.0000	0.00000	0.0722	902146	0.4570	10000
5:15 AM	Closed	Closed	Closed	Closed	0.4708	0.0000	0.00000	0.0722	902146	0.4570	10000
5:30 AM	Closed	Closed	Closed	Closed	0.4708	0.0000	0.00000	0.0722	902146	0.4570	10000
5:45 AM	Closed	Closed	Open	Closed	0.3331	0.0000	0.16510	0.0603	10805.43	0.3815	10000
6:00 AM	Open	Closed	Closed	Closed	0.4708	0.0000	0.00000	0.0722	902146	0.4570	10000
6:15 AM	Closed	Closed	Closed	Closed	0.4708	0.0000	0.00000	0.0722	902146	0.4570	10000
6:30 AM	Closed	Closed	Closed	Closed	0.4708	0.0000	0.00000	0.0722	902146	0.4570	10000
6:45 AM	Closed	Closed	Open	Closed	0.3331	0.0000	0.16510	0.0603	10805.43	0.3815	10000
7:00 AM	Open	Closed	Closed	Closed	0.4708	0.0000	0.00000	0.0722	902146	0.4570	10000
7:15 AM	Closed	Closed	Closed	Closed	0.4708	0.0000	0.00000	0.0722	902146	0.4570	10000
7:30 AM	Closed	Closed	Closed	Closed	0.4708	0.0000	0.00000	0.0722	902146	0.4570	10000
7:45 AM	Closed	Closed	Open	Closed	0.3331	0.0000	0.16510	0.0603	10805.43	0.3815	10000
8:00 AM	Open	Closed	Closed	Closed	0.4708	0.0000	0.00000	0.0722	902146	0.4570	10000
8:15 AM	Closed	Closed	Closed	Closed	0.4708	0.0000	0.00000	0.0722	902146	0.4570	10000
8:30 AM	Closed	Closed	Closed	Closed	0.4708	0.0000	0.00000	0.0722	902146	0.4570	10000
8:45 AM	Closed	Closed	Open	Open	0.1462	0.6281	0.06140	0.0224	29054.05	0.1419	10000
9:00 AM	Open	Open	Closed	Closed	0.4708	0.0000	0.00000	0.0722	902146	0.4570	10000
9:15 AM	Closed	Open	Closed	Closed	0.4708	0.0000	0.00000	0.0722	902146	0.4570	10000
9:30 AM	Closed	Open	Open	Closed	0.3331	0.0000	0.16510	0.0603	10805.43	0.3815	10000
9:45 AM	Open	Closed	Closed	Closed	0.4708	0.0000	0.00000	0.0722	902146	0.4570	10000
10:00 AM	Closed	Closed	Closed	Closed	0.4708	0.0000	0.00000	0.0722	902146	0.4570	10000
10:15 AM	Closed	Closed	Open	Closed	0.3331	0.0000	0.16510	0.0603	10805.43	0.3815	10000
10:30 AM	Open	Closed	Closed	Closed	0.4708	0.0000	0.00000	0.0722	902146	0.4570	10000
10:45 AM	Closed	Closed	Closed	Closed	0.4708	0.0000	0.00000	0.0722	902146	0.4570	10000
11:00 AM	Closed	Closed	Open	Closed	0.3331	0.0000	0.16510	0.0603	10805.43	0.3815	10000
11:15 AM	Open	Closed	Closed	Closed	0.4708	0.0000	0.00000	0.0722	902146	0.4570	10000
11:30 AM	Closed	Closed	Closed	Closed	0.4708	0.0000	0.00000	0.0722	902146	0.4570	10000
11:45 AM	Closed	Closed	Open	Open	0.1462	0.6281	0.06140	0.0224	29054.05	0.1419	10000
12:00 PM	Open	Open	Closed	Closed	0.4708	0.0000	0.00000	0.0722	902146	0.4570	10000

Scenario 3 and 4 Boundary Conditions in 15 min increments continued...

12:00 PM	Open	Open	Closed	Closed	0.4708	0.0000	0.00000	0.0722	902146	0.4570	10000
12:15 PM	Closed	Open	Closed	Closed	0.4708	0.0000	0.00000	0.0722	902146	0.4570	10000
12:30 PM	Closed	Open	Open	Closed	0.3931	0.0000	0.16510	0.0603	10805.43	0.3815	10000
12:45 PM	Open	Closed	Closed	Closed	0.4708	0.0000	0.00000	0.0722	902146	0.4570	10000
1:00 PM	Closed	Closed	Closed	Closed	0.4708	0.0000	0.00000	0.0722	902146	0.4570	10000
1:15 PM	Closed	Closed	Open	Closed	0.3931	0.0000	0.16510	0.0603	10805.43	0.3815	10000
1:30 PM	Open	Closed	Closed	Closed	0.4708	0.0000	0.00000	0.0722	902146	0.4570	10000
1:45 PM	Closed	Closed	Closed	Closed	0.4708	0.0000	0.00000	0.0722	902146	0.4570	10000
2:00 PM	Closed	Closed	Open	Closed	0.3931	0.0000	0.16510	0.0603	10805.43	0.3815	10000
2:15 PM	Open	Closed	Closed	Closed	0.4708	0.0000	0.00000	0.0722	902146	0.4570	10000
2:30 PM	Closed	Closed	Closed	Closed	0.4708	0.0000	0.00000	0.0722	902146	0.4570	10000
2:45 PM	Closed	Closed	Open	Open	0.1462	0.6281	0.06140	0.0224	29054.05	0.1419	10000
3:00 PM	Open	Open	Closed	Closed	0.4708	0.0000	0.00000	0.0722	902146	0.4570	10000
3:15 PM	Closed	Open	Closed	Closed	0.4708	0.0000	0.00000	0.0722	902146	0.4570	10000
3:30 PM	Closed	Open	Open	Closed	0.3931	0.0000	0.16510	0.0603	10805.43	0.3815	10000
3:45 PM	Open	Closed	Closed	Closed	0.4708	0.0000	0.00000	0.0722	902146	0.4570	10000
4:00 PM	Closed	Closed	Closed	Closed	0.4708	0.0000	0.00000	0.0722	902146	0.4570	10000
4:15 PM	Closed	Closed	Open	Closed	0.3931	0.0000	0.16510	0.0603	10805.43	0.3815	10000
4:30 PM	Open	Closed	Closed	Closed	0.4708	0.0000	0.00000	0.0722	902146	0.4570	10000
4:45 PM	Closed	Closed	Open	Open	0.1462	0.6281	0.06140	0.0224	29054.05	0.1419	10000
5:00 PM	Open	Open	Closed	Closed	0.4708	0.0000	0.00000	0.0722	902146	0.4570	10000
5:15 PM	Closed	Open	Open	Closed	0.3931	0.0000	0.16510	0.0603	10805.43	0.3815	10000
5:30 PM	Open	Open	Closed	Closed	0.4708	0.0000	0.00000	0.0722	902146	0.4570	10000
5:45 PM	Closed	Closed	Open	Closed	0.3931	0.0000	0.16510	0.0603	10805.43	0.3815	10000
6:00 PM	Open	Closed	Closed	Closed	0.4708	0.0000	0.00000	0.0722	902146	0.4570	10000
6:15 PM	Closed	Closed	Open	Closed	0.3931	0.0000	0.16510	0.0603	10805.43	0.3815	10000
6:30 PM	Open	Closed	Closed	Closed	0.4708	0.0000	0.00000	0.0722	902146	0.4570	10000
6:45 PM	Closed	Closed	Open	Closed	0.3931	0.0000	0.16510	0.0603	10805.43	0.3815	10000
7:00 PM	Open	Closed	Closed	Closed	0.4708	0.0000	0.00000	0.0722	902146	0.4570	10000
7:15 PM	Closed	Closed	Open	Closed	0.3931	0.0000	0.16510	0.0603	10805.43	0.3815	10000
7:30 PM	Open	Closed	Closed	Closed	0.4708	0.0000	0.00000	0.0722	902146	0.4570	10000
7:45 PM	Closed	Closed	Closed	Open	0.1558	0.6692	0.00000	0.0239	27270.09	0.1512	10001
8:00 PM	Closed	Open	Open	Closed	0.3931	0.0000	0.16510	0.0603	10805.43	0.3815	10000
8:15 PM	Open	Open	Closed	Closed	0.4708	0.0000	0.00000	0.0722	902146	0.4570	10000
8:30 PM	Closed	Open	Closed	Closed	0.4708	0.0000	0.00000	0.0722	902146	0.4570	10000
8:45 PM	Closed	Closed	Open	Closed	0.3931	0.0000	0.16510	0.0603	10805.43	0.3815	10000
9:00 PM	Open	Closed	Closed	Closed	0.4708	0.0000	0.00000	0.0722	902146	0.4570	10000
9:15 PM	Closed	Closed	Closed	Closed	0.4708	0.0000	0.00000	0.0722	902146	0.4570	10000
9:30 PM	Closed	Closed	Closed	Closed	0.4708	0.0000	0.00000	0.0722	902146	0.4570	10000
9:45 PM	Closed	Closed	Closed	Closed	0.4708	0.0000	0.00000	0.0722	902146	0.4570	10000
10:00 PM	Closed	Closed	Closed	Closed	0.4708	0.0000	0.00000	0.0722	902146	0.4570	10000
10:15 PM	Closed	Closed	Open	Closed	0.3931	0.0000	0.16510	0.0603	10805.43	0.3815	10000
10:30 PM	Open	Closed	Closed	Closed	0.4708	0.0000	0.00000	0.0722	902146	0.4570	10000
10:45 PM	Closed	Closed	Closed	Open	0.1558	0.6692	0.00000	0.0239	27270.09	0.1512	10001
11:00 PM	Closed	Open	Closed	Closed	0.4708	0.0000	0.00000	0.0722	902146	0.4570	10000
11:15 PM	Closed	Open	Closed	Closed	0.4708	0.0000	0.00000	0.0722	902146	0.4570	10000
11:30 PM	Closed	Open	Closed	Closed	0.4708	0.0000	0.00000	0.0722	902146	0.4570	10000
11:45 PM	Closed	Closed	Closed	Closed	0.4708	0.0000	0.00000	0.0722	902146	0.4570	10000

Key Words

Fish Passage, Computational Fluid Dynamics (CFD), Lock-Exchange Flows,
Density Current Flows, Navier-Stokes Equations, Migratory Fish, Salmon